REACTOR MATERIALS

A Quarterly Technical Progress Review

Prepared for DIVISION OF TECHNICAL INFORMATION, USAEC, by
R. W. DAYTON, E. M. SIMONS, and ASSOCIATES, BATTELLE MEMORIAL INSTITUTE

Spring 1965

● VOLUME 8

● NUMBER 1

TECHNICAL PROGRESS REVIEWS

To meet the needs of industry for concise summaries of current atomic developments, the Atomic Energy Commission is publishing this series, Technical Progress Reviews. Issued quarterly, each of the reviews digests and evaluates the latest findings in a specific area of nuclear technology and science.

The five journals published in this series are:

Isotopes and Radiation Technology, P. S. Baker, A. F. Rupp, and associates, Oak Ridge National Laboratory

Nuclear Safety, Wm. B. Cottrell, W. H. Jordan, and associates, Oak Ridge National Laboratory

Power Reactor Technology, W. H. Zinn and J. R. Dietrich, Combustion Engineering, Inc., Nuclear Division

Reactor Fuel Processing, Stephen Lawroski and associates, Chemical Engineering Division, Argonne National Laboratory

Reactor Materials, R. W. Dayton, E. M. Simons, and associates, Battelle Memorial Institute

Each journal may be purchased from the Superintendent of Documents, U. S. Government Printing Office, Washington, D. C., 20402. *Isotopes and Radiation Technology* at $2.00 per year for subscription or $0.55 for individual issues; the other four journals at $2.50 per year and $0.70 per issue. See back cover for remittance instructions and foreign postage requirements.

The views expressed in this publication do not necessarily represent those of the United States Atomic Energy Commission, its divisions or offices, or of any Commission advisory committee or contractor.

Availability of Reports Cited in This Review

Unclassified AEC reports are available for inspection at AEC depository libraries and are sold by the Clearinghouse for Federal Scientific and Technical Information, National Bureau of Standards, U. S. Department of Commerce, 5285 Port Royal Road, Springfield, Va., 22151. Some of the reports cited are not available owing to their preliminary nature; however, the information contained in them will eventually be made available in formal progress or topical reports.

Unclassified reports issued by other Government agencies or private organizations should be requested from the originator.

Unclassified British and Canadian reports may be inspected at AEC depository libraries. British reports are sold by the British Information Service, 45 Rockefeller Plaza, New York, N. Y.; Canadian reports (AECL series) are sold by the Scientific Document Distribution Office, Atomic Energy of Canada, Ltd., Chalk River, Ontario, Canada.

Classified U. S. and foreign reports identified in this journal as Classified may be purchased by properly cleared Access Permit Holders from the Division of Technical Information Extension, U. S. Atomic Energy Commission, P. O. Box 1001, Oak Ridge, Tenn., 37831. Such reports may be inspected at classified AEC depository libraries.

REACTOR MATERIALS

A REVIEW OF RECENT DEVELOPMENTS

Prepared for DIVISION OF TECHNICAL INFORMATION, USAEC,
by R. W. DAYTON, E. M. SIMONS, and ASSOCIATES,
BATTELLE MEMORIAL INSTITUTE

SPRING 1965

VOLUME 8

NUMBER 1

Foreword

Reactor Materials is one of a series of quarterly technical progress reviews broadly covering the field of nuclear science and technology. Under the auspices of the USAEC Division of Technical Information, *Reactor Materials* is prepared by Battelle personnel from worldwide literature. It covers properties, behavior, and fabrication processes of materials applicable to nuclear reactor components and associated equipment.

The reader will recognize that the scope of this Review is too broad to permit detailed coverage of every topic. Rather, the authors and editors attempt to combine the highlights of significant new developments into an information summary of current research for both management and the technical specialist. As a rule, enough of the results are presented to define the research and summarize the findings. For readers desiring more information on any particular topic, a complete set of references is provided at the end of each section.

Each quarter, a number of bibliographies, monographs, and books appear on subjects within the scope of *Reactor Materials*. Although the main purpose of this Review is to call attention to findings that are new and significant, such publications are noted in the text because they often represent excellent compilations of available information on important materials topics.

R. W. DAYTON
E. M. SIMONS
R. W. ENDEBROCK
Battelle Memorial Institute

DEPOSITED BY THE
UNITED STATES OF AMERICA

Contents

I Fuel and Fertile Materials 1
Uranium Metal and Alloys 1
Plutonium 3
Thorium 5
Metal-Ceramic Fuels 6
Coated-Particle Fuel Materials 7
Uranium Oxides 9
Carbide and Nitride Fuels 10
Mechanism of Corrosion of Fuel Alloys 13
Fuel-Water Reactions 13
Basic Studies of Irradiation Effects in Fuel Materials 14
References 15

II Moderator Materials 18
Graphite 18
Beryllium Metal and Alloys 18
Beryllium Oxide 20
Beryllium Intermetallic Compounds . . . 21
Solid Hydrides 21
References 23

III Nuclear Poisons 24
Metallic Poison Materials 24
Dispersion and Nonmetallic Poison Materials 25
References 25

IV Cladding and Structural Materials . . 27
Corrosion 27
Metal-Water Reactions 31
Radiation Effects in Nonfuel Materials . . 33
Selected Mechanical Properties of Cladding and Structural Materials . . . 34
Selected Metallurgical Aspects of Cladding and Structural Materials 35
Diffusion Studies 39
Ceramic Technology 40
References 41

V Special Fabrication Techniques 45
Melting, Casting, and Fabrication 45
Cladding 46
Metals Joining 48
Nondestructive Testing 48
References 50

VI Materials Information Presented at the Third Geneva Conference . . . 52

Issued quarterly by the U. S. Atomic Energy Commission. Use of funds for printing this publication approved by the Director of the Bureau of the Budget on October 14, 1963.

Section

I

Reactor Materials

Fuel and Fertile Materials

Uranium Metal and Alloys

Unalloyed Uranium

The French[1] determined the activation energies for creep in monocrystalline and polycrystalline uranium as a function of temperature. For polycrystals between 325 and 415°C and for monocrystals between 325 and 480°C, the activation energies were constant and nearly identical (31,200 and 31,500 cal/mole, respectively), and thus a single mechanism of deformation is implied for both forms of uranium. Plateaus of activation energy were also observed between 520 and 660°C; but the values for the polycrystalline and monocrystalline forms were 42,000 and 65,000 cal/mole, respectively.

To prepare specimens for a study of the effect of annealing temperature on the ductility and fracture of uranium, the British[2] subjected commercial-purity uranium (total impurities <500 ppm) to a rolling and annealing schedule to produce a fine, uniform grain structure. Samples were rolled 28% at 300°C, annealed for 24 hr at temperatures between 240 and 750°C, and then tensile tested. The tensile properties together with hardness measurements were correlated with the metallography of fracture. A hypothesis for the two ductility peaks is presented in terms of the change in fracture characteristics.

Workers at Hanford[3] studied the extraction of hydrogen from uranium in a vacuum at temperatures between 600 and 750°C. They found that the amount of hydrogen added to uranium during the beta-heat-treatment procedure is small compared with the volume contained in as-rolled metal. It was determined, however, that the added hydrogen stays in the outer 0.20 in. of the slug. The location of this gas is perhaps more important than the actual amount present. The investigations revealed that the hydrogen content of uranium powder-metallurgy compacts is generally lower than that of standard production pieces.

Alpha-Phase Uranium Alloys

The kinetics of the beta-alpha phase transformation in a uranium–0.5 at.% chromium alloy also were studied by the British.[4] Resistivity studies revealed the various mechanisms for the beta-alpha transformation. These can be summarized as conventional diffusion, controlled nucleation and growth at high temperature, a mixed reaction involving both shear and diffusion at intermediate temperatures, and a process involving shear alone at low temperatures.

The French[5] conducted a systematic study of the annealing of the beta phase retained by water-quenching uranium-chromium alloys containing between 0.37 and 4 at.% chromium. They demonstrated that alloys containing less than 1 at.% chromium are transformed between room temperature and 250°C according to a bainitic process involving activation energies of the order of 14,500 cal/mole. Alloys containing more than 1 at.% chromium are transformed at a temperature between 400 and 650°C by way of a germination-and-growth process involving an activation energy of the order of 33,000 cal/mole. The limit of solubility of chromium in beta-phase uranium plays a fundamental part in the transformations of the alloys.

The British[6] have studied very dilute uranium-iron-aluminum alloys by means of electrical resistivity and metallography. Their conclusions are:

1. Iron dissolves rapidly in beta-phase uranium, and some UAl_2 precipitates dissolve.

2. At beta-phase temperatures, where the solubility limit is exceeded, the UAl_2 precipitates that do not dissolve become coarser.
3. Only a brief excursion into the beta phase is sufficient to remove the very fine precipitates thought to be responsible for the good swelling resistance of adjusted uranium (dilute uranium-iron-aluminum alloy).
4. Both iron and aluminum dissolve rapidly in gamma uranium.
5. The gamma phase exists in equilibrium down to 710°C in adjusted uranium.
6. Grain refinement could be due to:
   a. Iron in solution depressing the beta-to-alpha transformation temperature
   b. Gamma uranium at beta boundaries and polygon boundaries limiting alpha grain size
   c. Undissolved UAl_2 particles inhibiting beta grain growth and acting as nucleation sites for future alpha formation

The solid solubility of aluminum in uranium and iron in uranium and the ternary solubility of aluminum-plus-iron in uranium were determined by Nuclear Metals workers.[7] The results are shown in Table I-1.

The effect of cooling rate on the decomposition of the gamma phase in uranium-zirconium alloys was studied by the British.[8] Uranium-zirconium rods containing from 2.5 to 50 at.% zirconium were end quenched. The phases formed and their distribution and hardness were then examined as functions of composition and cooling rate. The omega phase, or metastable nonstoichiometric disordered epsilon phase, plays a large part in the decomposition of the alloys containing 30 to 50 at.% zirconium. The omega phase is also very important in decomposition of alloys containing from 10 to 30 at.% zirconium, although, in those alloys examined in this range, the omega phase could not be retained to room temperature. In the more dilute alloys, there is no sign of its appearance.

Gamma-Phase Uranium Alloys

Investigators at the Lawrence Radiation Laboratory[9] have studied the properties of a metastable gamma-phase alloy, uranium–7.5 wt.% niobium–2.5 wt.% zirconium. The relation of transformation characteristics of the alloy to its physical and mechanical properties has been determined. Tensile yield strengths of 100,000 to 200,000 psi are possible, with elongations of 12 to 4%, respectively, depending on heat-treatment. The alloy can be welded by TIG or electron-beam fusion methods.

Dilute Uranium Alloys

The palladium-uranium phase diagram has been solved[10] for alloys containing up to 25 at.% uranium. High-purity palladium-uranium alloys were examined by means of metallography and X-ray diffraction. The terminal face-centered cubic phase undergoes two eutectoid transformations: the first, at 13.5 at.% uranium and 694°C, gives the compounds $Pd_{17}U_2$ and $Pd_{11}U_2$; and the second, at 15.5 at.% uranium and 1015°C, gives $Pd_{11}U_2$ and Pd_5U. The Pd_3U forms by peritectic reaction at 18.5 at.% uranium and 1440°C and exists over a small solu-

Table I-1 SOLID SOLUBILITY OF ALUMINUM AND IRON IN URANIUM[7]

System	Temp., °C	Solubility of alloying element in gamma uranium, ppm	Temp., °C	Solubility of alloying element in beta uranium, ppm	Temp., °C	Solubility of alloying element in alpha uranium, ppm
U-Al	1000	5000/2000	750/700	263/162	635/550	44/34
	925	~2500				
	~800	~2500				
	790	1550				
U-Fe	1100	1220				
	1000	2250	750	790		
	~900	~3085	725	680	635	59/12
	~825	~3100	700	425		
	~750	~1800				
U-Al-Fe	1000	~[(Al + Fe) = 2000] Up to 1550 Al and 1800 Fe, same as that at 1000°C	750	(500 Al + 900 Fe)	635	(40 Al + 20 Fe)
	700					

bility range. The nominal compound Pd_4U forms by peritectic reaction at 21 at.% uranium and 1525°C; this also has a small solubility range. The compounds $Pd_{17}U_2$, $Pd_{11}U_2$, and Pd_5U have noncubic structures; Pd_4U has an ordered structure of the Cu_3Au type. The variation of electrical resistivity with composition is given for alloys containing up to 15.5 at.% uranium.

(M. S. Farkas)

Plutonium

Plutonium Metal and Alloys

The beta-to-alpha and alpha-to-beta transformation kinetics of high-purity electrorefined plutonium have been found to be comparable to the kinetics of high-purity, as-reduced and vacuum-cast plutonium. The only noticeable difference is that, for beta-to-alpha transformation at isothermal temperatures above 75°C, the incubation time for the electrorefined metal is shorter and the transformation rate is faster. TTT curves of the transformations of the electrorefined metal are shown in Fig. I-1 (Ref. 11).

Further studies of the plutonium-copper system are being conducted. The crystal structure of $PuCu_4$ is reported to be orthorhombic, with unit cell parameters of $a = 10.06$ A, $b = 8.16$ A, $c = 5.14$ A. $PuCu_2$ is isomorphous with $CeCu_2$.

Los Alamos[12] studies of plutonium-scandium alloys in the range between 40 and 60 at.% scandium have revealed evidence of a nonstoichiometric intermetallic phase, which has a hexagonal alpha-lanthanum type structure. A small homogeneity range for this phase is indicated by lattice-parameter differences between plutonium-rich and scandium-rich compositions. The tentative lattice parameters are, for the plutonium-rich compositions,

$$a = 3.310 \text{ A}, c = 10.717 \text{ A}, c/a = 3.238$$

and, for the scandium-rich compositions,

$$a = 3.308 \text{ A}, c = 10.709 \text{ A}, c/a = 3.237$$

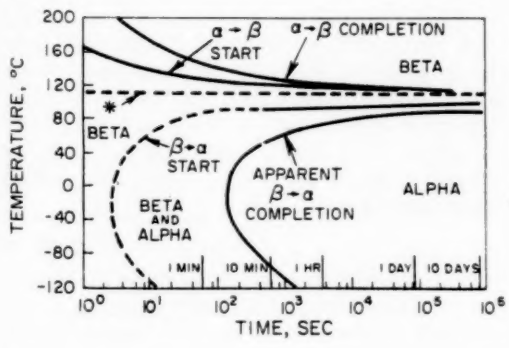

Fig. I-1 TTT curves of the β → α and α → β transformations of electrorefined plutonium.[11] The asterisk denotes β ⇌ α equilibrium transformation temperature (112°C).

The tensile properties of various uranium-plutonium-molybdenum alloys have been measured by the British[13] between room temperature and 800°C. Results are presented in Table I-2.

Table I-2 TENSILE PROPERTIES OF URANIUM-PLUTONIUM-MOLYBDENUM ALLOYS[13]

Composition (balance uranium), at.%	Temp., °C	Ultimate tensile strength, tsi	0.2% proof stress, tsi	Elongation, %
12 Mo–12 Pu	20	53.5	52	2.5
	800	1.5	1.5	22
15 Mo–15 Pu	20	55.5	52	1
	600	4.8	4.5	2
	800	2.0	1.8	18
13.5 Mo–10 Pu	20	51	51	2
	600	2	2	
	800	1.5	1.5	16 to 88
20 Mo–20 Pu	600	3.5	3.5	2
	800	0.8	0.8	20

Argonne[14] is investigating various uranium-plutonium-base alloys for possible fuel applications in zero-power criticality experiments. In studies of the effects of ternary alloying on the ignition temperatures of uranium-plutonium alloys, uranium–20 at.% plutonium–6 at.% molybdenum and uranium–30 at.% plutonium–6 at.% molybdenum alloys were found to be nearly as resistant to ignition as is unalloyed uranium. Decreasing the molybdenum content to 3 or 4.5 at.% uranium–20 at.% plutonium alloys lowered the resistance to ignition. However, ignition-resistance characteristics were still superior to those of a binary uranium–20 at.% plutonium alloy. Other alloying elements that improved ignition resistance at certain compositions were aluminum, carbon, copper, iron, titanium, vanadium, and zirconium.

The thermal-expansion coefficients for a uranium–20 wt.% plutonium–2.5 wt.% molybdenum alloy at various temperature ranges are presented in Table I-3. Compressive proper-

Table I-3 EXPANSION BEHAVIOR OF A CAST URANIUM–20 WT.% PLUTONIUM–2.5 WT.% MOLYBDENUM ALLOY[14]

Temp. range, °C	Average thermal-expansion coefficient, $°C^{-1}$	Total linear unit expansion
30 to 220	15.3×10^{-6}	
220 to 380	23.7×10^{-6}	
380 to 545	24.8×10^{-6}	
545 to 617	Transformation	3.95×10^{-3}
617 to 700	23.4×10^{-6}	

ties of uranium-plutonium-molybdenum alloys at temperatures up to 480°C are shown in Table I-4.

In studies of the compatibility of a uranium–10 wt.% plutonium–10 wt.% fizzium alloy with various potential cladding materials for fast reactor fuels, a vanadium–20 wt.% titanium alloy appears promising.[15] Diffusion couples annealed from 550 to 700°C for 7 to 104 days showed the penetration into the cladding to be given by $X = (Kt)^{1/3.5}$ cm, where t is time in seconds and K is penetration coefficient in $cm^{3.5}/sec$, given by $K = 0.17 \exp(-74{,}300/RT)$.

(V. W. Storhok)

Plutonium Compounds

Investigators at United Nuclear[16,17] have further characterized the $(U_{0.95}Pu_{0.05})C_{0.98}$ solid solution as having a solidus at 2520 ± 25°C and liquidus at 2535 ± 20°C. No niobium cladding-fuel reaction was noted after irradiation of this material to 7.9×10^{20} fissions/cm^3 at 795°C for 3270 hr. Type 316 stainless-steel cladding will carburize at 850°C if sesquicarbide is present[13] and a reaction product is observed within the fuel. The vapor pressures of uranium and plutonium over this $(U_{0.95}Pu_{0.05})C$ fuel in vacuum at 1995°C are 3×10^{-6} and (1 to 2) $\times$ 10^{-5} atm, respectively. Argonne[14,15] agrees that a preferential plutonium loss occurs in vacuum, where a mixed-carbide pellet containing 19.1 wt.% plutonium before heating was analyzed at 17.2 wt.% after 40 min at 2000°C. However, no loss was detected after sintering 2 hr at 2000°C under an argon atmosphere.

The results of an argon-atmosphere transpiration study[13] of the vapor pressure of PuC are presented in Table I-5.

The British have developed two techniques for the preparation of dense (U,Pu)C pellets, either by reaction-sintering the elemental constituents[18] or by sintering very fine particle-size mixed carbides in a dry argon atmosphere.[19] The PuC powder prepared by arc melting and crushing is reported[13] to sinter to 96% of theoretical density at the relatively low temperature of 1350°C. However, sintered density will decrease linearly with increased oxygen content. A recent publication[20] presents detailed data on the heat capacity of PuC, as well as enthalpy change and entropy up to the melting point of the compound.

Table I-4 COMPRESSIVE PROPERTIES OF URANIUM-PLUTONIUM-MOLYBDENUM ALLOYS[14]

Nominal composition, wt.%			Temp., °C	Maximum compressive strength		Compression, %	Elastic modulus	
U	Pu	Mo		Kg/mm^2	10^3 psi		10^3 kg/mm^2	10^6 psi
77.5	20	2.5	23	134	190	0	10.5	14.9
77.5	20	2.5	280	81	115	0		
76	22	2	376	49.8	70.8	0	5	7
76	22	2	405	56.2	80.0	5		
77.5	20	2.5	480	28.8	41.0	>50	3	4

X-ray diffraction studies[21] of 50 wt.% BeO–50 wt.% PuO_2 pellets fused by a plasma showed only small BeO and PuO_2 crystallites and indicated no solid solubility or compound formation. Nuclear Materials[22] reports a thermal-expansion coefficient for PuO_2 of 8.41×10^{-6}/°C from 20 to 1200°C, as compared with the earlier value of 9.0×10^{-6}/°C cited by several other investigators.

Table I-5 VAPOR PRESSURE OF PLUTONIUM MONOCARBIDE[13]

Temperature, °C	Vapor pressure, atm
1500	$(3.8 \pm 0.6) \times 10^{-7}$
1533	$(8.0 \pm 1.1) \times 10^{-7}$
1550	$(2.4 \pm 0.4) \times 10^{-6}$
1565	$(4.1 \pm 0.6) \times 10^{-6}$

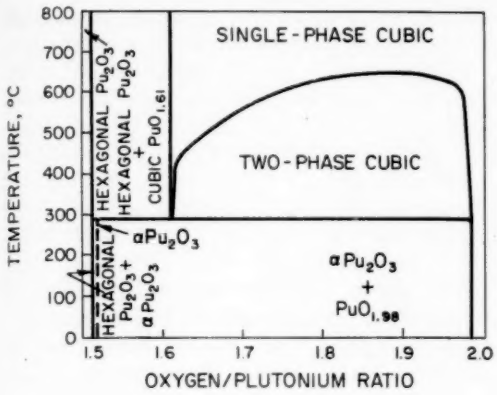

Fig. I-2 Plutonium-oxygen phase diagram.[25]

Several studies of plutonium-oxygen phase equilibria continue. Los Alamos[23] found Pu_4O_7 in all cases after firing mixes of PuO_2 and PuH_2 in vacuum at 1600°C, followed by heating at 500 or 800°C and cooling. The same report shows that self-irradiation lattice damage increases rapidly with increased ^{238}Pu content in the oxide. Solid solutions of Pu(O,C) have been prepared by carbon reduction of PuO_2 and appear to be fairly oxidation resistant but are generally more volatile than Pu_2O_3 (Ref. 24). The lattice parameter[23] of $Pu(C_{1-x}O_x)$ in equilibrium with Pu_2C_3 at 1400°C is 4.972 A and possibly increases to a maximum as the oxygen content is increased to the solubility limit at approximately $x = 0.4$.

High-temperature X-ray diffraction has been used to establish that portion[25] of the plutonium-oxygen phase diagram shown in Fig. I-2 which discounts the previously accepted eutectoid reaction at $PuO_{1.71}$. Other British results[13] show that the PuO_2-Fe_2O_3 system contains a monotectic with two eutectics at 90 wt.% PuO_2 (melting point = 1570 ± 10°C) and 10 wt.% PuO_2 (melting point = 1500 ± 10°C). Interdiffusion studies of ^{233}U-^{242}Pu oxide couples indicate comparable diffusion rates of plutonium and uranium in this system.[26]

Hanford has found PuN, UN, and (Pu,U)N materials to be volatile at 1800°C in a 10^{-5} mm Hg vacuum and no solid solubility of PuN with TiN, ThN, or ZrN after a 4-hr heat-treatment[27,28] at 2000°C. No reaction between PuO_{2-x} and PuN at 1500°C in nitrogen was detected by X-ray methods, nor was a liquid phase observed[29] in PuN–15 vol.% plutonium at 2200°C. A similar hypostoichiometric PuN specimen irradiated to an estimated burnup of 35×10^{20} fissions/cm^3 showed a partial conversion to an unidentified powder.[30] Battelle is currently preparing and evaluating Pu(N,C) alloys.[31]

(W. M. Pardue)

Thorium

The mean coefficient of expansion for the rolled and swaged alloy thorium–30 wt.% plutonium, over the temperature ranges from 25 to 300°C and from 25 to 900°C, has been found by Argonne workers[32] to be 11.4×10^{-6} and 12.1×10^{-6}/°C, respectively. The electrical resistivity of this alloy is shown in Fig. I-3.

Hanford workers have reported[33] on the melting of a thorium–2.5 wt.% uranium (93.2% enriched)–1.0 wt.% zirconium alloy into ingots of good quality by the vacuum consumable-electrode arc process. This alloy was successfully coextruded with Zircaloy-2 cladding on the inside and outside of a tube. The 1.0 wt.% zirconium lowers the hardness from 95 to 73 BHN but improves the castability of the alloy and the homogeneity of the ingot. Fusing of pure zirconium into a weld joint of pure thorium eliminates weld-joint cracking.

The brazing of end caps in Zircaloy-2-clad thorium-uranium fuel elements has proved dif-

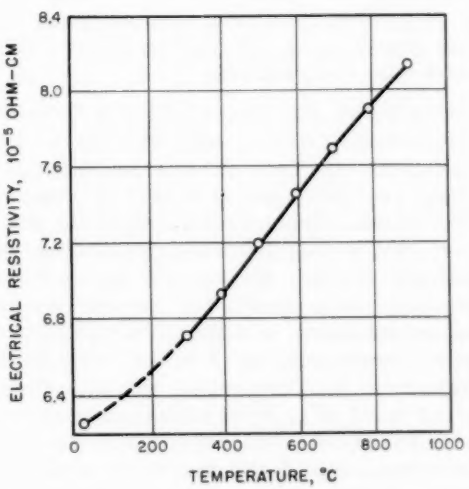

Fig. I-3 Electrical resistivity of thorium–30 wt.% plutonium.[32]

ficult in the past because of the difficulty in wetting the core. Hanford workers have demonstrated a technique for assuring wetting of thorium-uranium by the Zircaloy-2–5 wt.% beryllium brazing alloy. Zircaloy-2 brushes were fabricated and used to remove the oxide from the core ends. As a result the core is cleaned of oxide and coated with a smeared film of Zircaloy-2. This film is bright, prevents further oxidation, and permits the production of sound, nonporous, fully bonded vacuum-brazed joints. Brazing is followed by an electron-beam seal weld. (R. L. Martin)

Metal-Ceramic Fuels

Dispersion Fuels

A new method[34] for preparing a fuel dispersion in which PuO_2 or UO_2 is dispersed in an iron matrix has been developed in England. Briefly, a mixture of iron oxide and PuO_2 or UO_2 is heated to melt a substantial proportion of the mixture. The resultant mass is crushed to powder, green compacted, and sintered in a reducing atmosphere to produce a compact of PuO_2 or UO_2 particles contained in an iron matrix. Another technique[35] yields a dispersion of UN in an iron matrix by casting. The preferred composition of this fuel dispersion is 12 to 18 at.% uranium, 12 to 17 at.% nitrogen, and the balance iron, with the nitrogen-to-uranium ratio being at least 0.8. Replacing 50 wt.% of the UN with an equivalent amount of PuN results in a fuel that is believed to be suitable for fast reactors.

Sample fuel plates manufactured by Sylvania[36] were prepared from cores containing 48 wt.% −100-mesh U_3Si particles dispersed in an 1100 aluminum matrix and clad with an aluminum alloy (APM). Strips were cut from the fabricated fuel plates, sealed in glass tubes, and annealed for 24, 90, and 163 hr at 600°C. Metallographic examination showed that the larger fuel particles contained a dark central portion surrounded by a lighter gray region adjacent to the U_3Si-aluminum interface, whereas all the fine U_3Si particles appeared light gray. Microprobe analysis and X-ray diffraction tests indicated that the lighter gray area contained UAl_3 plus an unidentified phase (or phases). The altered fuel particle appeared stable since the extended time at 600°C did not convert the UAl_3 to UAl_4 or cause uranium and silicon to diffuse into the 1100 aluminum matrix.

At Los Alamos recent improvements in devices and operating conditions have been instrumental in the successful powder rolling, sintering, and hot rolling of 45 vol.% UO_2–tungsten strips with uniform thicknesses. The UO_2 and tungsten powders were blended in a twin-shell blender for 2 hr, hydrogen fired at 700°C for 1 hr to remove surface oxides from the tungsten and reduce the UO_2, and stored in a chamber at 35% relative humidity before powder rolling to ensure consistent flow characteristics from the feed hopper and reproducible rolling behavior. The rolls were roughened with SiC paper to increase the friction between the rolls and the UO_2-tungsten powders, and the rolling speed was adjusted to produce 0.057-in.-thick (±4%) strip with 75% of theoretical density. The 3½-in.-wide green strip was sintered in hydrogen at 2250°C for 1 hr to 85 to 90% of theoretical density, then hot rolled and simultaneously clad with tungsten foil at 2250°C. Creep specimens were prepared from the finished strip, and test results indicated that the 45 vol.% UO_2–tungsten dispersion can withstand between 30 and 90% of the stress supported by commercial tungsten rods at identical temperatures and creep rates. Examination of the specimens revealed that the lower values can be attributed to edge defects incurred during machining.[37]

Workers at Battelle[31] have prepared fuel plates containing 37 wt.% UO_2–type 347 stainless-steel cores clad with type 347 stainless steel. Three blending techniques were used to mix the powders, and the cores were green pressed at 7030 kg/cm² (50 tsi), sintered in hydrogen at 1225°C for 75 min, and recoined at 7030 kg/cm² (50 tsi). After coining, the cores were loaded in the type 347 stainless-steel packs, electron-beam welded, and hot rolled from the hydrogen muffle at 1200°C.

UO_2-tungsten dispersions, ranging from pure tungsten to 50 vol.% fused UO_2 loadings, were prepared at Hanford[38] by pneumatic impaction at 1200°C. The room-temperature tensile fracture stress of densified, machined specimens decreased from 22,000 to 14,000 psi as the composition varied from pure tungsten to 50 vol.% UO_2–tungsten. The 20 vol.% UO_2–tungsten body showed an average modulus of rupture of 45,690 psi, whereas the ordinary tensile test gave a fracture stress of 18,400 psi.

(D. L. Stoltz)

Cermet Fuels

Workers at Brookhaven[39] have evaluated 80 vol.% (UO_2-PuO_2)–stainless steel, molybdenum, tungsten, zirconium, niobium, or chromium cermet fuels for the settled-bed concept. Compared to a UC-PuC core and UC blanket, cermets containing 80 vol.% (UO_2-PuO_2) dispersed in either stainless steel or molybdenum appear promising on the basis of core and blanket breeding ratio and critical mass. Initial specimens to be fabricated will substitute enriched UO_2 for the UO_2-PuO_2 mixture.

(D. E. Kizer)

Coated-Particle Fuel Materials

Particle Coating

Recently published reports indicate that the improvement of pyrolytic carbon (PyC) coatings is the subject being most intensively studied in the coated-particle field. Workers at Oak Ridge[40] are continuing a study of the deposition of PyC and have fluidized-bed equipment in operation for the deposition of PyC at temperatures of <1000°C to at least 1800°C. It has been found that the PyC deposition rate is unaffected, at constant hydrocarbon feed rate and degree of fluidization, by changing from a helium fluidized bed to a bed fluidized at reduced pressure. However, the use of hydrogen greatly retards carbon deposition. Porous carbon coatings of promising quality were prepared at 900°C with acetylene at a partial pressure of 670 torrs. Coating experiments,[41] performed over a wide range of deposition rates at 1300 and 1400°C with methane, indicated that, at any given deposition rate, the density of the PyC coatings deposited at 1300°C was higher than the density of coatings deposited at 1400°C.

At Battelle work is being continued on a relatively new approach to limiting fission-product diffusion through PyC coatings.[31] Since barium is one of the more undesirable fission products, its control is being investigated first. The approach is to include a material in the PyC coating that will react with fission products to form a compound that will diffuse slowly, if at all, through the PyC coating. The concept is being evaluated with SiO_2-doped PyC. It is postulated that barium, a fission product, will react with the SiO_2 to form barium oxide, which would be expected to diffuse slowly. Preliminary irradiation results indicate some promise. (N. D. Veigel)

Irradiation and Evaluation of Coated-Particle Fuels

Oxide-Base Fuel. Studies of the irradiation behavior of oxide fuel particles coated with PyC are in progress at Oak Ridge[41] and at Battelle. Particles of $(Th,U)O_2$ prepared by the sol-gel process and coated with a duplex type of PyC coating are being irradiated at 1200°C at Oak Ridge. After a burnup of 0.4 at.% of the heavy metal, the coatings are still intact, fission-gas-release fractions being on the order of 10^{-6}.

The benefits of using porous UO_2 particles with PyC coatings are being evaluated in the Battelle program.[31,42,43] A specimen of 200-μ, 78% dense UO_2 particles coated with 73 μ of columnar PyC has been irradiated to about 6 at.% burnup at 815°C. The fission-gas-release fractions increased from 10^{-8} to 10^{-6} after approximately 3 at.% burnup and have remained at this level. This represents failure of less than 0.1% of the coatings. A similar specimen having a columnar coating only 51 μ thick began to exhibit failure after 0.5 at.% burnup at 815°C, and the failure continued until an estimated 2% of the coatings were cracked at 1.5 at.% burnup. The fission-gas-release fractions were in the order of 10^{-5}. Both these materials resisted failure in irradiations at 100°C to 1 at.% burnup. The performance of these thin, monolithic coatings is much improved over similar coatings deposited on dense UC_2 particles.

Carbide-Base Fuel. Very good in-pile performance has been found by workers at Oak Ridge for duplex and triplex PyC coatings on UC_2 and $(Th,U)C_2$ particles.[40,44] One specimen with a triplex coating was irradiated to 15 at.% burnup at 1120°C and another to 24 at.% burnup at 1370°C. A duplex-PyC-coated specimen was irradiated to 16.2 at.% burnup at 1370°C. In all these cases the fission-gas-release fractions were in the range of 10^{-6} to 10^{-5}.

A collection of papers that were presented at a coated-particle symposium held in association with the American Nuclear Society meeting in November 1963 has been published in *Nuclear Science and Engineering*. These papers[45–50]

represent a good review of the state of the art as of that time. (C. W. Townley)

Coated-Particle Fuel-Materials Compatibility

Workers at Oak Ridge[40] have completed compatibility studies involving PyC coatings on Eu_2O_3, UO_2, and ThO_2 substrate particles prepared by the sol-gel process. Vacuum thermogravimetric studies using mixtures of the uncoated oxides with graphite flour indicate that the initial ThO_2-graphite reaction begins at approximately 1360°C. However, after 2 hr at 1750°C the reaction is only 52% complete. The initial UO_2-graphite reaction begins at 1260°C, but it is 97% complete after 2 hr at 1750°C. Spherical ThO_2 particles (40 to 160 μ) coated with 35 to 160 μ of PyC and spherical UO_2 particles (150 to 250 μ) coated with 100 μ of PyC were vacuum (10^{-5} torr) heat-treated for 1000 hr at 1100°C and for 200 hr at 1400°C. Surface examination, radiography, and metallography showed that no chemical reaction or fuel migration had occurred during the annealing experiment. In addition, there was no observable decrease in the crushing strength of the particles. PyC-coated Eu_2O_3 particles, of the same size as the UO_2 particles, gave similar results after annealing at 1100°C. However, after the 1400°C anneal a few particles exhibited migration into coating delaminations.

To study the diffusion of actinides in PyC, workers[40] prepare diffusion couples by embedding the actinides on carbon surfaces using ion bombardment. After vacuum annealing is completed, grinding, sectioning, and counting operations are used to determine the diffusion profile. Although there is an unusually high degree of scatter in the results, the data, shown in Fig. I-4, indicate that the diffusion characteristics of all actinides in PyC are similar and follow the equations

$$D_{\text{parallel}} = 1.2 \times 10^{-2} \exp(-60.8/RT)$$

$$D_{\text{perpendicular}} = 3.2 \times 10^{-5} \exp(-60.8/RT)$$

where D is in square centimeters per second, parallel or perpendicular to the deposition planes, and RT is in kilocalories per mole.

Additional experiments were performed in PyC, deposited at 2000°C, both in the as-prepared condition and after a 3-hr heat-treatment at 2650°C. Structural studies utilizing electron microscopy have shown that PyC, in the as-deposited condition, possesses a high fraction of defective areas in the basal surfaces. Although annealing at 2650°C pro-

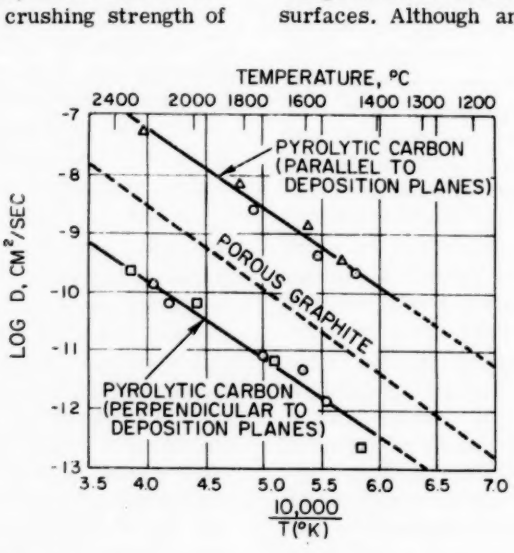

Fig. I-4 Arrhenius plot summarizing the actinide diffusion results with as-deposited PyC.[40] △, ^{235}U (as F.P.); ○, ^{233}Pu (with thorium); □, ^{232}Th.

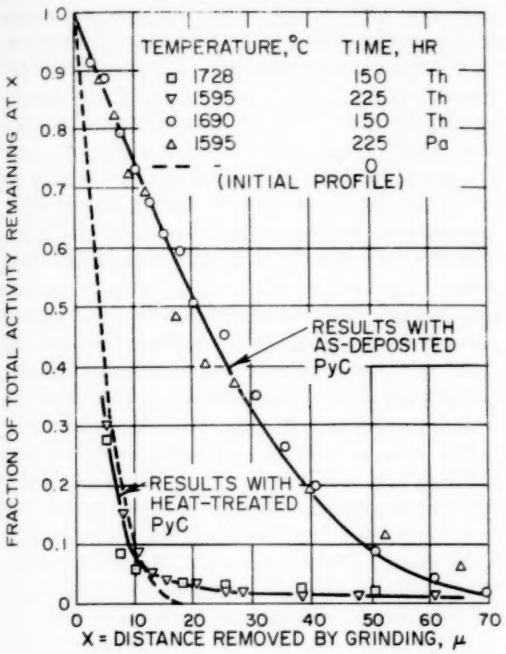

Fig. I-5 Effect of structural improvement on the diffusion of actinides in high-density carbon.[40] In all cases diffusion was perpendicular to the average basal surface.

duced only a slight increase, from 2.19 to 2.25 g/cm^3, in the density of the PyC, it induced grain growth in both the lateral and vertical directions and formed graphitic platelets. Defective material at grain boundaries of as-deposited PyC was consumed during the growth process and was replaced by more perfect material. A comparison of the diffusion profiles in the annealed and the as-deposited structures is shown in Fig. I-5. Diffusion across basal surfaces in annealed PyC was suppressed to values below the limits of detection. (W. H. Pfeifer)

Uranium Oxides

Properties and Behavior of Uranium Oxide Fuels

The formation of metallic uranium in UO_2 irradiated at high temperatures in a variety of fuel-element systems has been studied at Hanford.[52] Metallic uranium was observed in all cases where central temperatures in the fuel were high enough to produce extensive grain growth. The minimum temperature for formation of the metal appears to be about 1500°C. The uranium, which appeared in the beta phase, was in the form of small inclusions with diameters ranging up to 25 μ. Fission products were found to be more concentrated near the uranium inclusions.

Recent fission-gas-release studies at Oak Ridge are of interest.[40,53,54] Measurements of fission-gas release from UO_2 single crystals during irradiation indicated that burnup and fission rate affect the release rate. Increased fission rate was observed to retard gas release, and the release rate decreased with burnup. The latter effect was attributed to irradiation smoothing of the specimen surface. Fission-gas release was independent of temperature below 600°C and increased exponentially with increasing temperature. A recoil process is thought to be the controlling factor at low temperatures, whereas the high-temperature release that was often attributed to diffusion is now postulated to be controlled by a trapping mechanism. Fission gases trapped at defects are thought to be released from the UO_2 at a rate controlled by escape from the traps rather than by diffusion. Trapping sites such as pores, grain boundaries, impurities, point defects, and point-defect clusters are considered to play important roles in the high-temperature release process.

The thermal expansion of well-characterized single-crystal UO_2 with an oxygen-to-uranium ratio of 2.00 and a theoretical density of greater than 99% was measured at Hanford.[30] Between 300 and 1600°C the expansion coefficient was 12.1×10^{-6}/°C. It also appears that there may be a discontinuity in the expansion coefficient at about 1400°C.

Rufeh[55] has measured the solubility of helium in UO_2 powder. At 1200 and 1300°C the solubility was 6.71×10^{-4} and 3.23×10^{-4} cm^3 (STP)/(g of UO_2)(atm), respectively. The heat of solution was about 34 kcal/gram mole. A diffusion coefficient for helium in UO_2 was estimated to be about 1.5×10^{-13} cm^2/sec at 1200°C.

Roellig[56] has reported information on the reaction between UO_2 and aluminum. The reaction follows the equation

$$3UO_2 + 16Al = 3UAl_4 + 2Al_2O_3$$

Oxide-free aluminum is more reactive than aluminum with oxide. The reaction rate for aluminum follows an activation energy of 61 kcal/gram mole for temperatures between 570 and 620°C. (R. H. Barnes)

Preparation of Uranium Oxide Fuel Bodies

A British patent[57] has been issued on the preparation of granular uranium dioxide, suitable for vibratory compacting, by arc-melting the starting powder. In the process the fine powder is applied to a support and the surface layer is melted in an electric arc. The granules are formed upon solidification. The process utilizes tungsten electrodes, a hydrogen atmosphere, and a water-cooled copper support plate.

Fabrication techniques for aluminum-base fuels for use in the 250-Mw Advanced Test Reactor have been investigated at Oak Ridge.[58] Fabrication is complicated because the 40 fuel elements are in a serpentine arrangement requiring each fuel-element cross section to be wedge shaped and each of the 19 plates, in each element, to have its own specific radius of curvature. Each plate contains 34 wt.% U_3O_8 and 0.2 wt.% B_4C, and the remainder is aluminum. Conventional powder-metallurgical dry-blending techniques produce fuel compacts exhibiting a homogeneous mixture of the three phases. The plates are clad with type 6061 aluminum by hot roll bonding and then shaped to the required radii of curvature by a modified marforming process.

FIAT investigators[59] have fabricated both stainless-steel and Zircaloy-2-clad uranium dioxide fuel rods by a 4-min pneumatic vibration, followed by two swages without intermediate annealing. The rods had an average density of 92.5% of theoretical. Lengths were 125 to 190 cm, and the variation in density along the rods was −0.5 to +1.5% of the average.

Fuel rods having densities of 90% of theoretical have been fabricated from UO_2-ThO_2 mixtures for the Kilorod Facility by Oak Ridge.[60] The results have proved the feasibility of a bulk-oxide vibratory-compaction method for fuel-element fabrication.

Mattys and Hauser[61] have fabricated UO_2-ThO_2 mixtures having densities greater than 96% of theoretical by sintering in air at 1600°C. The extent to which the sintering process was a success depended on the choice of the source material. Mixed ThO_2-U_3O_8 precipitates yielded quite satisfactory results, and the addition of CaO permitted the sintering temperature to be lowered to 1400°C with no apparent change in density.

British investigators[62] have fabricated 0.5-in.-diameter UO_2 disks having a thickness of 0.005 in. and a density of 96% of theoretical. Granules (−44 +100 mesh) were formed using a paraffin wax binder. These granules were pressed at 15 tsi, debonded in CO_2 at 800°C, and sintered in cracked ammonia at 1580°C. During sintering the UO_2 disks were stacked between either alumina or molybdenum disks and supported by a molybdenum sleeve.

Battelle investigators[63] have recently completed a study of the fabrication procedures, physical properties, and phase relations in the UO_2-ZrO_2 system. Particular emphasis was placed on the 50 mole % UO_2 − 50 mole % ZrO_2 composition. Homogeneous fuel pellets with densities in excess of 97% of theoretical were prepared from ball-milled powders compacted at 50 tsi and heat-treated in a single 20-hr treatment at 1700°C in hydrogen.

(T. R. Wright)

Carbide and Nitride Fuels

Properties

Two reviews of carbide technology have been published recently. One review[64] deals with carbides in general, both as structural materials and as fuels for nuclear devices operating at high temperatures. The other[65] is a more detailed review of data on only the uranium carbides.

Further studies of the uranium-carbon-molybdenum system at low carbon contents have disclosed that the pseudobinary tie line between UC and molybdenum exists only up to about 1800°C. Chubb and Keller report[66] that, at a temperature between 1800 and 1900°C, UC and molybdenum react peritectically to form uranium liquid and a low-carbon form of $UMoC_2$. The latter contains only 46 at.% carbon and is characterized by a twinned microstructure and by an X-ray pattern distinctly different from the orthorhombic pattern of stoichiometric $UMoC_2$.

The as-cast microstructures of uranium-carbon-tantalum alloys containing 5 at.% tantalum and 45 to 65 at.% carbon suggest that the

minimum in the liquidus between UC and UC_2 develops into a eutectic-like trough that passes through a minimum temperature at a point containing negligible tantalum and 57 to 59 at.% carbon. The trough proceeds on through a point near 65 at.% carbon, 2 to 3 at.% tantalum, and the balance uranium.[67]

A topical report summarizing the results of extensive studies of the compatibility of uranium carbides with stainless steel and other metals has been issued by Atomics International.[68] At temperatures below 980°C, no significant amount of uranium or carbon is transferred by sodium from hypostoichiometric UC to type 304 stainless steel, Nb–1 Zr alloy, or a zirconium-base alloy (3Z1). Some reaction potential does exist, however, since it is stated that reactions would be expected between the materials in direct contact over long periods of time.

In-pile thermal conductivity of $(U_{0.8}Pu_{0.2})C_{0.95}$ was estimated[16] to be 0.046 cal/(sec)(cm)(°C) in the temperature range from 700 to 1000°C. This estimate was obtained by measurements of fuel temperature and from heat-generation rates.

The mean linear-thermal-expansion coefficient of U_2C_3 from 20 to 1600°C is approximately 12.2×10^{-6}/°C, according to Mendez-Penalosa and Taylor.[69]

The minimum creep rates of hyperstoichiometric uranium carbide were determined[13] by compressive creep tests at 1200, 1300, and 1400°C. An Arrhenius plot of the data gave an apparent activation energy of 49 ± 8 kcal/mole. The minimum creep rate at 1300°C and 6000 psi was 1.5×10^{-4}/hr. The rate decreased with stress to about 2.5×10^{-5}/hr at 2000 psi.

A cylindrical, cast specimen of slightly hypostoichiometric UC was annealed[70] for 5 hr at 1700°C, electropolished to produce a mirror-smooth surface, and then irradiated at 200°C for 8.5×10^5 sec in a thermal flux of 8.2×10^{12} neutrons/cm^2. It was then electropolished again and annealed for various times at temperatures from 1000 to 1500°C. The ^{133}Xe released during these annealing treatments was monitored and the diffusion rate of xenon in uranium carbide was determined to obey the Arrhenius type relation: $D = 1.26 \times 10^{-10} \exp(-42{,}400/RT)$.

A 6-in.-long fuel rod 0.87 in. in diameter, consisting of hypostoichiometric UC (4.6 wt.% carbon) clad in type 304 stainless steel, was subjected to a series of power pulses in TREAT.[71] A final power pulse of 0.4-sec duration raised the central temperature of the UC to 2000°C for several seconds. The fuel rod was recovered intact and, from its external appearance, apparently undamaged. Sectioning of the fuel rod revealed internal cracks that were attributed to thermal shock produced by the temperature transient.

The UN-ZrN pseudobinary system involves solid solution to at least 10 wt.% zirconium. On the other hand, the UN-TiN pseudobinary system is a eutectic type system with the eutectic near 10 wt.% titanium. The solubility of TiN in UN is small at the solidus.[72]

The decomposition pressure of uranium mononitride, from 10^{-7} to 2.5 atm, may be expressed by the formula:[73]

$$\log P\,(\text{atm}) = 35.1854 - 18.571 \times 10^4 \left(\frac{1}{T}\right) + 2.98 \times 10^8 \left(\frac{1}{T}\right)^2 - 18.14 \times 10^{10} \left(\frac{1}{T}\right)^3$$

where T is in degrees Kelvin. (W. Chubb)

Fabrication of Ceramic Fuels Other Than Uranium Oxides

As a simple, versatile procedure for preparing ceramic fuel materials, the sol-gel process developed at Oak Ridge[74] looks quite promising. The process starts with the nitrate solutions of thorium, uranium, or plutonium and produces either oxides or carbides. The advantages of the process are its simplicity, the ability to produce desired product shapes and sizes as part of the process, the relatively low calcination temperatures required to obtain densification, and, particularly in fast breeder systems where "hot" fuel must be recycled, its adaptability to remote operation in a shielded facility.

Preparation of thorium oxide by the sol-gel process is accomplished in four steps: (1) drying and denitration of thorium nitrate to obtain a reactive oxide; (2) dispersion of this thorium oxide to form a hydrosol; (3) gelation by either evaporation or solvent extraction of water from the sol; and (4) calcination to obtain the final ceramic form desired.

The sol-gel process followed by vibratory compaction to make fuel elements of oxide in metal tubes has been tested[74] on a pilot-plant scale in the Kilorod Program. At Hanford,[27] ThO_2 gel particles that were dried at 90°C and

dry pressed at 0.689×10^9 to 3.45×10^9 dynes/cm^2 (10,000 to 50,000 psi) before firing at 1150°C for 90 min showed pellet densities ranging from 86.1 to 93.0% of the theoretical ThO_2 density. Up to 2.76×10^9 dynes/cm^2 (40,000 psi), the sintered bulk density increased as the pressing pressure increased. Weight-loss data indicated that all volatile material was not removed during firing, suggesting that higher sintered densities might have been obtained if the firing temperature had been higher or the time longer.

The sol-gel process is being adapted to the preparation of microspheres of the oxide or carbide of thorium or mixed thorium-uranium.[74] Particle diameters can be closely controlled and varied between 50 and 2000 μ. The formation of microspheres of oxide or carbide is accomplished by dispersing the sol into an immiscible organic solvent, such as carbon tetrachloride, in a spray column. Microspheres of ThO_2 and ThO_2-UO_2 prepared by the sol-gel process show excellent size uniformity, surface smoothness, and sphericity. The spheres can be coated with PyC with no detectable reaction between the oxide and coating. Oak Ridge workers expect that alterations being made to the distillation system[41] will permit sustained operation to produce thoria microspheres at about 100 g/hr.

Some amount of well-distributed porosity may be desirable in fuel particles to provide fission-gas traps and possibly to increase the rate of fuel dissolution in recycling processes by increasing the surface area accessible to the solvent. Two modifications[41] to the basic sol-gel process have resulted in thoria preparations having about 3 vol.% of well-distributed and open porosity: (1) adding carbon at the sol stage and subsequently removing it by firing during the calcination step, and (2) reducing the calcination temperature.

Attempts are being made to use the sol-gel process to prepare dense thorium nitride (ThN) by firing thoria-carbon gels in nitrogen. A carbon-to-thorium ratio of 2 gave the "highest" percentage of nitride with the "least" amount of oxide and carbide impurities. An atom ratio of 1 led to residual oxide in the nitride product and to a "little" Th_2N_3. An atom ratio of 3 led to a "large" amount of thorium carbide. The optimum reaction temperature seemed to be about 1800°C. British workers at Harwell[75] have been trying to develop the same basic process, i.e., carbothermic reduction of the oxide in a stream of nitrogen, as a way for preparing uranium mononitride from UO_2 rather than from the metal. Two applications of the reaction

$$UO_2 + (2 + x)C \xrightarrow[1450°C]{N_2} U(C_xN_{1-x}) + 2CO$$

were studied with the use of fluidized beds. In one the oxide was heated in a stream of nitrogen gas mixed with a hydrocarbon vapor (benzene), and in the other the oxide powder and carbon were mixed intimately and heated in a stream of nitrogen. Neither technique produced pure UN. The particles were fluidized in graphite vessels heated by induction. With the hydrocarbon method, 99 to 100% conversion of the oxide to carbonitride $[U(C_xN_{1-x})]$ could be achieved. However, the process was complicated by a number of side effects such as (1) sintering of the bed at temperatures above 1500°C, (2) coating of the particles with a layer of impervious PyC at high benzene feed rates or temperatures below 1450°C, and (3) adhering of the product to the reaction-vessel walls. The UN contents higher than 70 wt.% could be obtained only if the reaction was stopped before complete conversion of the UO_2. The method involving mixing of the powders was somewhat more flexible in that, by control of the relative amounts of reactants, carbonitrides ranging from "pure" UC to 96 wt.% UN could be prepared.

Because of the "excellent" pressing and sintering properties of the uranium carbide powder that is prepared by adding carbon to a zinc-magnesium solution of uranium that precipitates UC at 750 to 800°C, the process has been scaled up at Argonne[76] to produce 0.5 to 1 kg of UC per batch for fuel-element fabrication and irradiation tests. The magnesium and zinc are removed from the carbide by siphoning and distillation. Refinement of the process has reduced the oxygen content of the product to below 0.2 wt.%, but the carbon content is still running higher than the 5.2 wt.% desired for fuel-element fabrication. The lower limit on the oxygen content is now governed by the oxygen content of the carbon used in the process. The best material produced to date contained 0.14 wt.% oxygen and 5.6 wt.% carbon.

Two summary reports[77,78] have been issued describing the results of studies on the stoi-

chiometry control and oxygen levels obtainable in a potential large-scale production process for uranium carbide, that of melting and casting of prereacted UO_2-carbon feed stock.

(E. O. Speidel)

Mechanism of Corrosion of Fuel Alloys

The contact potential difference between ultrahigh-vacuum-deposited films of gold and uranium has been measured during the admission of oxygen in studies conducted at Harwell.[79] The surface potential of uranium was found to be positive with respect to clean metal at all oxygen pressures investigated. Surface-potential changes were related to penetration of atomic oxygen at interstitial sites in the uranium; this penetration was followed by the appearance of uranium dioxide and then higher oxides of uranium. (W. E. Berry)

Fuel-Water Reactions

Studies of the reaction of water with UO_2-core Zircaloy-2-clad fuel pins were made in the TREAT reactor[14] to obtain kinetic data under circumstances that simulate a power excursion or a runaway incident. The data of particular importance to the analysis of reactor safeguards are the rate and extent of reaction between molten metals at high temperature and water. Information on the degree of subdivision that a fuel pin undergoes during the course of a transient is important to the understanding of the metal-water reaction.

In the experiments a single fuel pin is submerged in water contained in a stainless-steel capsule or autoclave. During the power excursion the pressure in the autoclave is measured by means of a strain-gauge transducer. After the irradiation has been completed, a sample of the gas phase in the autoclave is taken. From the amount of hydrogen present in the gas phase and the known weight of zirconium in the fuel pin, the amount of zirconium that reacted with water can be computed. Finally, particle-size determinations of the fragmented fuel are made.

The results of the experiments are given in Fig. I-6, where each datum is located by its extent of reaction (percent) and by its fission energy input (calories per gram of core). Figure I-6 also gives the data obtained in previous experiments with mixed-oxide*-core Zircaloy-2-clad fuel pins. Two energy scales and one temperature scale are used in the figure to place the two sets of data on the same basis. It should be noted that the two energy scales have been placed so as to give correspondence with the single temperature scale by choosing a melting point of 2700°C as the fixed point of comparison.

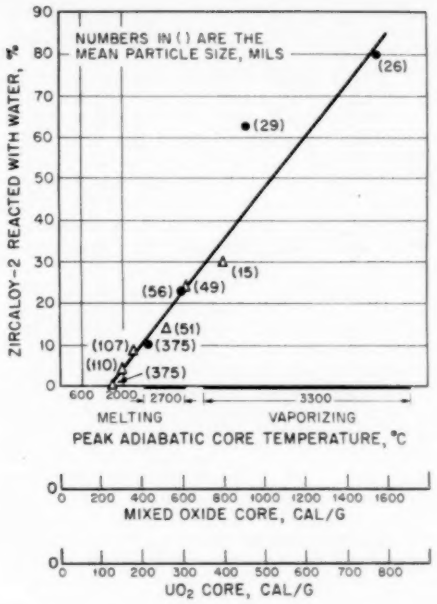

Fig. I-6 Results of meltdown experiments in TREAT on UO_2-core and mixed-oxide-core Zircaloy-2-clad fuel pins submerged in water.[14] △, mixed-oxide core; ●, UO_2 core.

Also reported by Argonne[80] were the results of experiments performed to determine the rate of reaction of steam with uranium metal in the form of a cube supported by a quartz tube containing a thermocouple.

The parabolic-rate-law constants obtained from this and an earlier series of experiments are plotted in Fig. I-7 as a function of reciprocal temperature. Shown on the figure are the values of k in the equation $V^2 = kt$ for the two

*Mixed oxide is 81.5 wt.% ZrO_2–9.06 wt.% CaO–0.74 wt.% Al_2O_3–8.69 wt.% UO_2 (93% enriched).

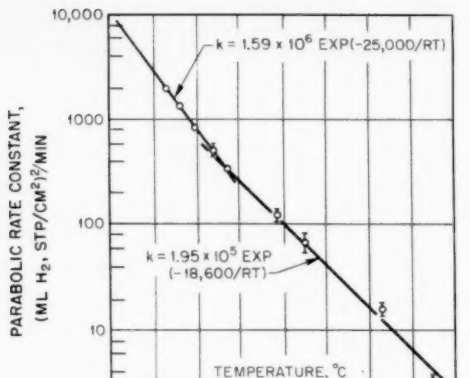

Fig. I-7 Effect of temperature on the rate of hydrogen evolution for the reaction of steam with uranium.[80]

temperature ranges, 600 to 1200°C and 1200 to 1600°C. In these expressions

V = volume of hydrogen evolved, ml (STP)/cm^2
t = time, min
R = ideal gas constant
T = absolute temperature, °K

For some runs the steam flow rate was varied by a factor of 10 with no observed change in the rate of reaction, although it took longer to reach the temperature at high steam flow rates.

Optical pyrometer measurements of the outer oxide surface during the course of several runs showed that the surface temperature was 100 to 400°C below the metal temperature as indicated by the central thermocouple. This resulted from the relatively poor thermal conductivity of the oxide and the very thick films developed during the oxidations.

Metal-gas reactions that follow the parabolic rate law are usually considered to be controlled by the diffusion of an ionic species through the oxide film. The existence of a significant temperature gradient through the oxide film, therefore, suggests that the rate law observed may not be representative of truly isothermal conditions. In particular, one would expect that the rate data developed in this study would give low results if extrapolated to very short reaction times when the temperature drop across the oxide film would be small. It does appear, however, that the parabolic rate law would apply and that only a minor change in the parabolic law constants would be required to describe the reaction at short times.

The change in reaction mechanism implied by the change of slope of the Arrhenius plot may be due to the melting of the metal at 1133°C. The state of the oxide is presumably the controlling factor in the parabolic oxidation, and there is no change in the oxide at this temperature. This accounts for the fact that the change in rate caused by melting of the metal is relatively minor. (A. W. Lemmon, Jr.)

Basic Studies of Irradiation Effects in Fuel Materials

Metals

The applicability of the Harwell model for swelling,[81] discussed last quarter, to the behavior of fission-product gases in uranium and uranium dioxide is discussed briefly in another paper.[82] In uranium the tendency to swell has been reduced by introducing precipitates that are believed to anchor the bubbles. The bubbles are thus prevented from migrating, so they do not coalesce and increase their total volume due to the fall in pressure as the bubble size increases. In uranium dioxide the behavior of the inert-gas bubbles differs from that in uranium, and the large temperature gradients influence the migration and complicate the overall behavior. It is suggested that it may be possible to reduce the release of gas in UO_2 by limiting the migration of gas bubbles in a manner analogous to that in uranium or by reducing the temperature gradients that are believed to be the cause of their migration.

At Harwell[83] the mechanisms involved in the mass transport of uranium by fission fragments have been studied by electron microscopy and alpha-particle spectroscopy. It is shown that displacement spikes involving about 10,000 atoms are probably responsible for the ejection of particles from a uranium-metal surface. When these particles are collected on a surface near the uranium surface, they are vaporized when ionization occurs due to the passage of a fission fragment.

A simplified empirical model developed at Hanford[84] predicts the swelling in irradiated uranium with good reliability.

Ceramics

A recent paper from the University of California[85] emphasizes the need to account for vaporization in high-temperature fission-gas-release experiments where vaporization is appreciable. Equations are given which permit analysis of the fractional release where vaporization occurs.

A final report issued by the Hahn-Meitner Institut[86] gives data on rare-gas diffusion in a number of materials. Included are data for xenon diffusion in UO_2, UC, and ThO_2; argon diffusion in CaF_2 and KCl; and helium diffusion in AgLi.

A report from West Germany[87] reviews the possible causes of the nonideal gas-release kinetics often observed in postactivation diffusion experiments. It is pointed out that, in the calculation of diffusion coefficients from the corresponding release curves, the D values may vary by orders of magnitude and will depend on how the experimental curve is interpreted. This fact may contribute to the broad scattering of the values of diffusion coefficients found in the literature and shows that a deeper insight of the underlying physical processes is needed in order to evaluate the experimental data correctly. In the discussion of present experimental results, different assumptions regarding the nature of these processes are made, and the consequences for the experimentally observed release patterns are considered. Recommendations are given for the evaluation of complicated release curves.

At the Hahn-Meitner Institut[88] the activation energy for xenon diffusion in UO_2 single crystals (Hanford) in experiments under an atmosphere of helium with 5% hydrogen was found to be 66 kcal/mole between 1000 and 1800°C, if the strong evaporation above 1700°C is taken into account. (F. A. Rough)

References

1. P. Grenier, J. P. Andre, and P. Lacombe, Activation Energies for Creep of Monocrystalline and Polycrystalline Uranium Between 120 and 650°C, *Compt. Rend.*, 258: 3485-3487 (April 1964).
2. D. N. R. Taplin and J. W. Martin, The Effect of Annealing Temperature on the Ductility and Fracture of Uranium, *J. Less-Common Metals*, 6: 430-433 (June 1964).
3. W. E. Ray and H. C. Bowen, The Hydrogen Content of Fabricated Uranium, USAEC Report HW-30116, Hanford Atomic Products Operation, Nov. 30, 1953.
4. P. H. Dixon and J. Burke, Kinetics of the $\beta \rightarrow \alpha$ Phase Transformation in a Uranium–0.5 Atomic Percent Chromium Alloy, British Report AERE-R-4431, March 1964.
5. M. Degois, Studies on Tempering at Different Temperatures of the Beta Phase Retained by Water Quenching in Uranium-Chromium Alloys Containing from 0.37 to 4 Atomic Percent Chromium, French Report CEA-R-2340, 1963.
6. P. H. Dixon, F. H. Fern, and B. R. Butcher, The Solution of Precipitates in Very Dilute U-Fe-Al Alloys, British Report AERE-R-4636, May 1964.
7. R. B. Russell, The Uranium-Aluminum-Iron Constitution Diagram, Summary Report, USAEC Report NMI-2813, Nuclear Metals Division of Textron Inc., June 30, 1964.
8. R. F. Hills, B. R. Butcher, B. W. Howlett, and D. Stewart, The Effect of Cooling Rate on the Decomposition of the γ-Phase in Uranium-Zirconium Alloys, British Report AERE-R-4557, April 1964.
9. C. A. W. Peterson and R. R. Vandervoort, The Properties of a Metastable Gamma-Phase Uranium-Base Alloy: U–7.5 Nb–2.5 Zr, USAEC Report UCRL-7869, University of California, Lawrence Radiation Laboratory, May 13, 1964.
10. G. P. Pells, The Palladium-Uranium Phase Diagram Up to 25 at.% Uranium, *J. Inst. Metals*, 92: 416-418 (August 1964).
11. Hanford Atomic Products Operation, Metallurgy Research Operation. Quarterly Progress Report, January–March 1964, USAEC Report HW-81269, Apr. 15, 1964.
12. Los Alamos Scientific Laboratory, Plutonium Reactor Fuel Development, Quarterly Status Report for Period Ending May 20, 1964, USAEC Report LAMS-3096, June 24, 1964.
13. Metallurgy Division, AERE, Unpublished information, January 1964.
14. Argonne National Laboratory, Reactor Development Program Progress Report, June 1964, USAEC Report ANL-6912, July 21, 1964.
15. Argonne National Laboratory, Reactor Development Program Progress Report, May 1964, USAEC Report ANL-6904, June 15, 1964.
16. United Nuclear Corp. and The Carborundum Company, June 30, 1964. (Unpublished)
17. United Nuclear Corp., Sept. 9, 1964. (Unpublished)
18. J. W. Isaacs and M. Polfreyman, Improvements in or Relating to Process for the Preparation of Carbide, British Patent 954,821, Apr. 8, 1964.
19. L. E. Russell and J. D. Lawrence, Improvements in or Relating to Reactor Fuels, British Patent 954,720, Apr. 8, 1964.
20. D. L. Kruger and H. Savage, Heat Capacity of Plutonium Monocarbide from 400 to 1300°K, *J. Chem. Phys.*, 40: 3324-3328 (June 1964).
21. L. J. Wittenberg and G. R. Grove, Reactor Fuels and Materials Development Plutonium Research, January–March 1964, USAEC Report MLM-1199, Mound Laboratory, Mar. 31, 1964.
22. Nuclear Materials & Equipment Corp., Development of Plutonium-Bearing Fuel Materials. Prog-

ress Report, October 1–December 31, 1963, USAEC Report NUMEC-2389-1.

23. J. A. Leary, W. J. Maraman, W. N. Miner, and F. W. Schonfeld, Quarterly Status Report on Solid-Plutonium Fuels Program for Period January 1–March 31, 1964, USAEC Report LAMS-3107, Los Alamos Scientific Laboratory, July 17, 1964.
24. R. E. Skavdahl, The Reactions Between PuO_2 and Carbon, USAEC Report HW-77906, Hanford Atomic Products Operation, May 1964.
25. E. R. Gardner, T. L. Markin, and R. S. Street, The Plutonium-Oxygen Phase Diagram, British Report AERE-R-4602, May 1964.
26. General Electric Company, Atomic Power Equipment Department, Sodium Cooled Reactors Program, Fast Ceramic Reactor Development Program, Ninth Quarterly Report, October–December 1963, USAEC Report GEAP-4480, January 1964.
27. Hanford Atomic Products Operation, Ceramics Research and Development Operation. Quarterly Report, January–March 1964, USAEC Report HW-81600. (Classified)
28. F. W. Albaugh, Reactor and Fuels Laboratory Monthly Report, May 1964, USAEC Report HW-82428A, Hanford Atomic Products Operation, June 15, 1964. (Classified)
29. F. W. Albaugh, Reactor and Fuels Laboratory Monthly Report, July 1964, USAEC Report HW-83445A, Hanford Atomic Products Operation, Aug. 14, 1964. (Classified)
30. F. W. Albaugh, Reactor and Fuels Laboratory Monthly Report, August 1964, USAEC Report HW-83820A, Hanford Atomic Products Operation, Sept. 15, 1964. (Classified)
31. R. W. Dayton and R. F. Dickerson, Progress Relating to Civilian Applications During August 1964, USAEC Report BMI-1691(Del.), Battelle Memorial Institute, Sept. 1, 1964.
32. Argonne National Laboratory, Reactor Development Program. Progress Report, July 1964, USAEC Report ANL-6923, Aug. 20, 1964.
33. R. S. Kemper, R. N. Johnson, J. E. Minor, and R. G. Nelson, Fabrication of Zircaloy-2 Clad Thorium-Uranium Alloy Fuel Elements, USAEC Report HW-79843, Hanford Atomic Products Operation, March 1964.
34. L. E. Russell and B. Riley, Improvements in or Relating to Nuclear Fuel Compositions, British Patent 945,726, Jan. 8, 1964.
35. H. J. Hedger and J. Williams, Improvements in or Relating to Nuclear Fuels, British Patent 954,939, Apr. 8, 1964.
36. Phillips Petroleum Company, Materials Testing Reactor–Engineering Test Reactor Technical Branches, Quarterly Report, October 1–December 31, 1963, USAEC Report IDO-16977, May 1964.
37. T. J. Ready, W. V. Green, and H. D. Lewis, Fabrication and Evaluation of Powder-Rolled Tungsten-Uranium Dioxide Dispersions, USAEC Report LA-2485, Los Alamos Scientific Laboratory, Apr. 6, 1964.
38. E. A. Snajdr, Fracture Stresses of UO_2-Tungsten Cermets Evaluated by the Diametral Tensile Test, Interim Report No. 1, USAEC Report HW-79676, Hanford Atomic Products Operation, January 1964.
39. Brookhaven National Laboratory, Progress Report, Nuclear Engineering Department September 1–December 31, 1963, USAEC Report BNL-841.
40. Oak Ridge National Laboratory, Gas-Cooled Reactor Program, Semiannual Progress Report for Period Ending March 31, 1964, USAEC Report ORNL-3619, July 1964.
41. Oak Ridge National Laboratory, Aug. 6, 1964. (Unpublished)
42. R. W. Dayton and R. F. Dickerson, Progress Relating to Civilian Applications During June 1964, USAEC Report BMI-1674(Del.), Battelle Memorial Institute, July 1, 1964.
43. R. W. Dayton and R. F. Dickerson, Progress Relating to Civilian Applications During July 1964, USAEC Report BMI-1681(Del.), Battelle Memorial Institute, Aug. 1, 1964.
44. Oak Ridge National Laboratory, July 7, 1964. (Unpublished)
45. J. M. Blocher, Jr., M. F. Browning, W. J. Wilson, V. M. Secrest, R. B. Landrigan, and J. H. Oxley, Properties of Ceramic-Coated Nuclear-Fuel Particles, *Nucl. Sci. Eng.*, 20(2): 153–170 (October 1964).
46. C. W. Townley, N. E. Miller, R. L. Ritzman, and R. J. Burian, Irradiation Studies of Ceramic-Coated Nuclear-Fuel Particles, *Nucl. Sci. Eng.*, 20(2): 171–179 (October 1964).
47. F. L. Carlsen, Jr., E. S. Bomar, and W. O. Harms, Development of Fueled Graphite Containing Pyrolytic-Carbon-Coated Carbide Particles for Nonpurged, Gas-Cooled Reactor Systems, *Nucl. Sci. Eng.*, 20(2): 180–200 (October 1964).
48. W. V. Goeddel, Development and Utilization of Pyrolytic-Carbon-Coated Carbide Fuel for the High-Temperature Gas-Cooled Reactor, *Nucl. Sci. Eng.*, 20(2): 201–218 (October 1964).
49. R. A. Reuter, Duplex Carbon-Coated Fuel Particles, *Nucl. Sci. Eng.*, 20(2): 219–226 (October 1964).
50. H. G. Sowman, R. L. Surver, and J. R. Johnson, The Development of Spherical Pyrolytic-Carbon-Coated UC_2 and $UThC_2$ Fuel Particles, *Nucl. Sci. Eng.*, 20(2): 227–234 (October 1964).
51. Reference deleted.
52. J. L. Bates, Metallic Uranium in Irradiated UO_2, USAEC Report HW-82263, Hanford Atomic Products Operation, May 1964.
53. R. M. Carroll and O. Sisman, In-Pile Fission-Gas Release from Single-Crystal UO_2, USAEC Report TID-20672, Oak Ridge National Laboratory, July 1964.
54. R. M. Carroll, R. B. Perez, and O. Sisman, Release of Fission Gas During Fissioning of UO_2, USAEC Report TID-20671, Oak Ridge National Laboratory, July 1964.
55. F. Rufeh, Solubility of Helium in Uranium Dioxide (Thesis), USAEC Report UCRL-11043, University of California, Lawrence Radiation Laboratory, Mar. 19, 1964.
56. H. E. Roellig, On the Compatibility of Uranium Dioxide and Aluminum. 1. Communication: Studies on the Kinetics of the UO_2-Al Reaction in Powder Briquets, USAEC Translation ANL-TRANS-17 [translated from *Kernenergie*, 6: 685–691 (December 1963)].

57. Process and Apparatus for Obtaining Granular Uranium Dioxide, British Patent 954,868, Apr. 8, 1964.
58. R. J. Beaver, G. M. Adamson, and P. Patriarca, Procedures for Fabricating Aluminum-Base ATR Fuel Elements, USAEC Report ORNL-3632, Oak Ridge National Laboratory, June 1964.
59. G. Frigerio, Swaging of Uranium Dioxide, Italian Report EUR-117.e, 1962.
60. J. E. Van Cleve, Jr., and A. L. Lotts, Experience in the Fabrication of Uranium-233 Bearing ThO_2-UO_2 Rods in a Lightly Shielded Facility at ORNL, USAEC Report ORNL-P-123, Oak Ridge National Laboratory, November 1963.
61. M. Mattys and R. Hauser, Fabrication of Mixed UO_2-ThO_2 Pellets by Sintering in Air, French Report EUR-8.f, March 1962.
62. L. E. J. Roberts and P. Murray, United Kingdom Atomic Energy Authority, February 1964. (Unpublished)
63. T. R. Wright, D. E. Kizer, and D. L. Keller, Studies in the UO_2-ZrO_2 System, USAEC Report BMI-1689, Battelle Memorial Institute, Aug. 27, 1964.
64. S. Langer, Physicochemical Properties of Carbides for Nuclear Applications, in *Materials and Fuels for High Temperature Nuclear Energy Applications*, Chap. 12, pp. 242-286, MIT Press, Cambridge, Mass., 1964.
65. B. R. T. Frost, The Carbides of Uranium, *J. Nucl. Mater.*, 10: 265-300 (1963).
66. W. Chubb and D. L. Keller, Constitution of the Systems of Uranium and Carbon with Molybdenum, Niobium, Rhenium, Tungsten, and Yttrium, USAEC Report BMI-1685, Battelle Memorial Institute, Aug. 11, 1964.
67. W. Chubb and D. L. Keller, Effect of 5 At.% Tantalum on the UC-UC_2 System, USAEC Report BMI-1673, Battelle Memorial Institute, July 13, 1964.
68. P. E. Elkins, Compatibility of Uranium Carbide Fuels with Cladding Materials, USAEC Report NAA-SR-7502, Atomics International, Aug. 1, 1964.
69. R. Mendez-Penalosa and R. E. Taylor, Thermal Expansion of Uranium Sesquicarbide, *J. Am. Ceram. Soc.*, 47: 416-417 (August 1964).
70. K. R. Montgomery and I. H. Scobey, The Diffusion of Xenon-133 in Uranium Carbide, British Report TRG-Report-747, Mar. 24, 1964.
71. S. J. Stachura, M. Silberberg, and R. N. Cordy, Uranium Carbide Transient Heating Experiments. Phase I, USAEC Report NAA-SR-9508, Atomics International, Aug. 1, 1964.
72. D. L. Keller, Development of Uranium Mononitride, Quarterly Progress Report, October-December 1963, USAEC-Euratom Report BMI-X-10073 (EURAEC-957), Battelle Memorial Institute, Jan. 1, 1964.
73. D. L. Keller, Development of Uranium Mononitride, Quarterly Progress Report, January-March 1964, USAEC-Euratom Report BMI-X-10083 (EURAEC-1033), Battelle Memorial Institute, Apr. 1, 1964.
74. D. E. Ferguson and J. A. Lane, Technical Status of the ORNL Thorium Utilization Program, USAEC Report ORNL-TM-859, Oak Ridge National Laboratory, May 6, 1964.
75. K. R. Hyde, D. A. Landsman, J. B. Morris, W. F. Seddon, and H. J. C. Tulloch, The Preparation of Uranium Nitride and Carbonitrides from Uranium Oxide in a Fluidized Bed, British Report AERE-R-4650, June 1964.
76. Argonne National Laboratory, Chemical Engineering Division Research Highlights, May 1963-April 1964, USAEC Report ANL-6875.
77. W. Draganchuk, UC Fuel Element Design and Fabrication, USAEC Report NAA-SR-9988, Atomics International, Aug. 1, 1964.
78. J. Crane and E. Gordon, The Development of Uranium Carbide as a Nuclear Fuel, Final Report, USAEC Report UNC-5080, United Nuclear Corp., Feb. 29, 1964.
79. J. C. Riviere, The Surface Potential of Oxygen on Uranium, British Report AERE-R-4631, May 1964.
80. Argonne National Laboratory, Chemical Engineering Division Semiannual Report, July-December, 1963, USAEC Report ANL-6800, May 1964.
81. R. S. Barnes, A Theory of Swelling and Gas Release for Reactor Materials, *J. Nucl. Mater.*, 11: 135-148 (February-March 1964).
82. R. D. Barnes, R. G. Bellamy, B. T. Bradbury, J. B. Sayers, and A. D. Whapham, The Behavior of Fission-Product Gases in Uranium and Uranium Dioxide, *Trans. Am. Nucl. Soc.*, 7: 89 (June 1964).
83. M. D. Rogers, Mass Transport of Uranium by Fission Fragments, British Report AERE-R-4639, May 1964.
84. Hanford Atomic Products Operation, Metallurgy Development Operation Quarterly Progress Report, October-December 1963, USAEC Report HW-80112, Jan. 20, 1964. (Classified)
85. S. D. Lowe, R. L. Chambers, and T. H. Pigford, Release of Fission Gas by Simultaneous Diffusion and Evaporation, *Trans. Am. Nucl. Soc.*, 7: 95-96 (June 1964).
86. A. Brenner, F. Felix, T. Lagerwall, H. Migge, A. Richter, P. Schmeling, and K. E. Zimen, Rare Gas Diffusion in Solids, Final Report No. 3, September 1, 1962-December 12, 1963, USAEC-Euratom Report EURAEC-1006, Hahn-Meitner-Institut für Kernforschung, March 1964.
87. T. Lagerwall and P. Schmeling, Interpretation and Evaluation of Non-Ideal Gas Release in Post-activation Measurements, USAEC-Euratom Report EURAEC-806, Hahn-Meitner-Institut für Kernforschung, October 1963.
88. Hahn-Meitner-Institut für Kernforschung, Diffusion of Rare Gases in Solids, Quarterly Report, January-March 1964, USAEC-Euratom Report EURAEC-1043, April 1964.

Section

II

Reactor Materials

Moderator Materials

Graphite

Published work has revealed much disagreement on the nature of irradiation-induced defects in graphite. A recent British study[1] has utilized detailed analyses of defect-loop contrasts to characterize such defects more precisely. This electron-microscopic examination of neutron damage in graphite single crystals irradiated at 900 and 1200°C revealed two types of defects. Large interstitial loops with a radius of 350 A were surrounded by small vacancy loops that appeared to form in their stress fields. Annealing at 1820°C caused some of the interstitial loops to shear to a configuration of lower stacking-fault energy.

Researchers at Oak Ridge have reported an electron-optical study[2] of the structural features of pyrolytic carbons applied to uranium carbide fuel particles. Of particular interest is the nature of microporosity as related to bulk carbon density. Both columnar and laminar type carbons, with densities ranging from 1.4 to 2.08 g/cm^3, were studied. Transmission-electron micrographs showed that, as bulk density decreased, pore density increased. The size of the microvoids ranged from 50 to 100 A. Changes in crystallite size did not appear to correlate with physical density. In supporting work annealing studies were conducted on massive pyrolytic carbon (PyC) deposits. For the massive PyC, it was demonstrated that, in 3 hr at 2650°C, crystallites grow to a few tenths of a micron in diameter and approximately 100 A in thickness and that microvoids are eliminated.

In the continuing search for oxidation inhibitors, the inhibitive effects of carbon tetrachloride, thionyl chloride, chlorine, sulfur dioxide, trimethyl phosphate, and phosphorus oxychloride upon the oxidation of graphite in air or in oxygen have been reported by British investigators.[3] Of these materials, only phosphorus oxychloride showed a potential for application in a reactor. It gave the highest degree of inhibition, and its effects persisted for some time after its addition to the reacting system had ceased. The mechanism of inhibition was not established conclusively, but it was proposed that the phosphorus oxychloride decomposed to produce phosphorus oxide, P_4O_{10}, on the graphite surface. No interplanar penetration of any decomposition products was observed.

The successful performance of cemented graphite joints following irradiation was achieved by Hanford.[4] The tensile strength (1173 psi) of a cemented graphite joint after exposure to 7.9×10^{20} neutrons/cm^2 ($E > 0.18$ Mev) at 600°C was higher than that of an unirradiated control specimen (697 psi). In previous irradiation of cemented joints, failures during irradiation were traced to the $\frac{1}{16}$-in.-wide cement layer in which cracks developed. Also, previous joints were not heat-treated prior to irradiation. The above successful data were for a thin, approximately 0.05-in., joint that was graphitized prior to irradiation.

(M. C. Brockway)

Beryllium Metal and Alloys

Physical Metallurgy

Kaufman and Aronin at Nuclear Metals[5] studied the deformation characteristics of beryllium single crystals and examined the influence of iron and silicon additions on deformation. Extremely high purity levels (12 zone-refining passes on distilled beryllium) gave improved mechanical properties in basal slip, where glide strains up to 175% were noted. Crystals made by six zone-refining passes on

SR material and tested in c-axis compression at 400 to 700°C showed no new modes of deformation. In these tests failure occurred by gross basal slip and shear, as contrasted to brittle cleavages in materials of commercial purity. The addition of 1000 ppm of iron to six-pass SR material increased the critical resolved shear stress for basal slip to a level obtained in commercial-purity materials. The high glide capacity, however, was comparable to that of the zone-refined crystals. Silicon did not change the deformation behavior.

Jacobsen at Lockheed[6] determined the tensile properties from −195 to 200°C on beryllium extrusions of various grain sizes. Tensile specimens were oriented both longitudinally and at 45° to the extrusion direction to induce prism and basal slip, respectively. At less than −100°C, properties on as-extruded beryllium were better in the 45° direction (basal slip) than in the longitudinal direction. Solution-treating the extrusions 6 hr at 900°C, followed by a 48-hr 700°C precipitation anneal, improved the tensile properties for both types of specimens without affecting the elongation. The heat-treatment apparently removed impurity elements, especially iron and aluminum, from solid solution and thus permitted more uniform deformation. At temperatures below ambient the ultimate tensile strength of the heat-treated specimens oriented for prism slip (longitudinal direction) decreased with decreasing temperature. This was attributed to twinning, which caused premature failure.

Corrosion

Ervin and Mackay at Atomics International[7] studied the corrosion of beryllium by high-temperature air to investigate potential problems in the SNAP-8 ground-test reactor. Oxidation in the range of 500 to 900°C proceeded slowly during an initial period but catastrophically during a subsequent period. The rate during the protective period was parabolic and decreased in proportion to the $^1/_5$ power of oxygen pressure, indicating that the rate was controlled by beryllium-ion vacancies in the BeO film. Moisture shortened the protective period, but a 1 wt.% calcium alloy had improved corrosion resistance. Failure of the protective BeO film was attributed to small pits that developed in the metal surface under the oxide film.

Koch, Riskevics, and Ritchie at Babcock & Wilcox[8] studied the corrosion resistance of beryllium in 100 and 120°C water as an evaluation of materials for application in the Advanced Test Reactor (ATR). Beryllium is to be used as a moderator and will operate in a thermal-neutron flux of 1.5×10^{15} neutrons/(cm^2)(sec). Corrosion rates were found to be sensitive to environmental changes. For example, decreasing the coolant temperature from 120 to 100°C decreased the corrosion rate by 50%. An increased coolant flow or oxygen content increased the corrosion rate, whereas an increased pH decreased the corrosion rate. Beryllium was not sensitive to stress corrosion.

Thompson Ramo Wooldridge Inc. workers[9] studied the reactions of beryllium with nitrogen, air, oxygen, and carbon monoxide in the range of 1000 to 1500°C. Beryllium reacted with carbon monoxide below the melting point of beryllium approximately 40 times as rapidly as it did with oxygen or nitrogen. On the other hand, above its melting point, beryllium reacted faster with oxygen than with nitrogen, air, or carbon monoxide. Above its melting point beryllium reacted at approximately the same rate with dry air as with nitrogen. Combustion particles of less than 10 μ diameter were formed and were capable of being airborne.

Melting and Casting

The Beryllium Corporation[10,11] is investigating casting and hot-working of large diameter beryllium ingots. Sound ingots 6 in. dia. by 12 - 13 in. long were produced from AEC-grade beryllium melting stock. High purity stock (UKAEA specifications) was more susceptible to cracking than the AEC-grade stock, limiting the usable length of the ingots produced to 6 to 12 in. Equations were developed for predicting heat-transfer conditions needed to produce sound ingots.

Berylco forced directional solidification using a composite graphite and aluminum mold with its bottom chilled with a water-cooled copper plug, and top heated by an induction coil. Radial grain growth was thus minimized during solidification where normally excessive thermal stresses cause subsequent cracking. Also, the molten reservoir of metal at the top of the ingot minimized the length of centerline pipe; in a 4 7/8 in. dia. ingot, pipe depth required is

2 1/2 in., whereas it is approximately 4 in. in a 6 in. dia. ingot. Bottom pouring of the molten metal is preferred over tilt pouring; tilt pouring apparently upsets the heat balance of the ingot, producing an unsatisfactory thermal gradient in the mold and consequent stress cracking.

Fabrication

Investigators at Nuclear Metals[12] studied warm drawing as a technique for dimensionally stabilizing beryllium extrusions of complex cross sections. A U-channel was chosen as a typical structure. Reductions up to 16% per pass were made on extrusions up to 10 ft in length. Large increases in longitudinal and transverse strength levels were noted at ambient temperature and −73°C (−100°F) after warm drawing at 427°C (800°F). Yield strength was increased approximately 2500 psi per 1% drawing reduction. The strain-to-fracture values were reduced from 6 to 2%. Annealing after drawing reduced the strength to approximately the as-extruded level but did not restore the directional ductility. The preferred orientation of the extrusion was basically unchanged by the warm drawing.

Beryllium-clad stainless steel and niobium-liner tubing were fabricated at Beryllium Corporation[13] to test the resistance of beryllium to simulated meteoroid collisions. Four approaches were investigated: (1) direct casting of beryllium around the liner, (2) coextrusion, (3) silver brazing, and (4) solid-state diffusion bonding. Direct casting was successful in producing composite tubes. Brazing and diffusion bonding with silver as the intermediate material were moderately successful.

Similar studies were conducted at Battelle[14] on the fabrication of duplex tubes by gas-pressure bonding. Hot isostatic pressing was used to densify beryllium powder around the liner tubes and simultaneously effect a solid-state bond between these components. Composite tubes were also fabricated by solid-state bonding extruded-beryllium tubes to the liners. Both techniques successfully produced composite tubes.

Miscellaneous

Proceedings of the first meeting of the Materials Advisory Board Committee on Beryllium Metallurgy[15] have been published. This report includes a description of all government-sponsored contracts and selected industrial research efforts on beryllium. Basic AEC beryllium activities as reported by J. G. Conner include purification studies at Lawrence Radiation Laboratory and Nuclear Metals, irradiation-damage studies at the National Reactor Testing Station (Phillips Petroleum Company), and gamma-activation analysis studies at Texas Nuclear Corp. No effort is currently being expended toward the use of beryllium as a cladding material. (H. D. Hanes)

Beryllium Oxide

General Electric workers have previously reported data on radiation-induced expansion of BeO which appeared to follow first-order kinetics, but the data were incomplete at low temperatures. They have now reported supplementary low-flux low-temperature data.[16] The composite data indicate that the expansion of BeO deviates somewhat from the theoretical case of first-order kinetics. However, the overall expansion can be described empirically by the following type of equation:

For temperatures greater than 600°C,

$$\frac{\Delta V}{V} = \frac{K}{A}\left[1 - \exp\left(-At\right)\right]$$

where $K = 3.3 \times 10^{-23}\ \phi$

$A = 6.1 \times 10^{-5} \exp\left(-10{,}300/RT\right)$

ϕ = neutron flux ($\geq$ 1 Mev)

R = molar gas constant 1.987 kcal/(mole) (°K)

T = absolute temperature, °K

In the reported test data, specimen volume changes ranged from 0.5 to 2.4% for exposures of 1.8 to 2.3 × 10^{20} neutrons/cm^2 ($\geq$ 1 Mev) at irradiation temperatures of 140 to 360°C. The data show that irradiation at temperatures up to 360°C has a small effect on expansion. The expansion of samples irradiated in the temperature range 440 to 490°C to about 2 to 3 × 10^{20} neutrons/cm^2 ($\geq$ 1 Mev) ranged from approximately 0.6% in the 5-μ grain size to 1.2% in the 50-μ AOX-grade BeO material. Apparent density measurements indicated that microcracking occurred in AOX specimens with grain sizes of 10 μ or larger but were not conclusive for (UOX + MgO)-grade BeO.

For both irradiation conditions given above, the expansion of the Experimental Beryllium Oxide Reactor samples (1 wt.% bentonite in UOX-grade BeO) appeared comparable to that of the UOX + MgO and somewhat better than that of the AOX specimen of 20-μ grain size.

Oak Ridge investigations[17] have revealed an appreciable difference in self-diffusion rates in low-density vs. high-density BeO, as shown in Fig. II-1. It is believed that rapid diffusion

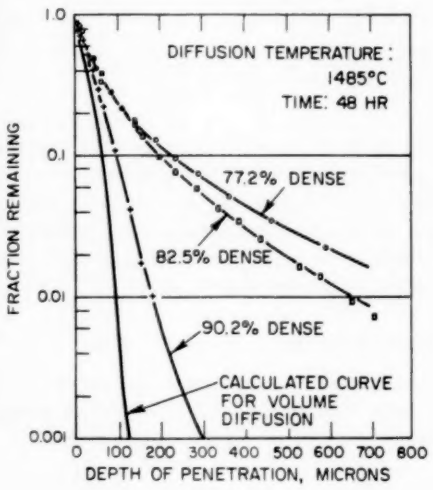

Fig. II-1 Effect of density on self-diffusion in low-density polycrystalline-BeO compacts.[17]

along grain-boundary surfaces of the low-density BeO, as contrasted to slower bulk diffusion through grains in dense BeO, accounts for the differences in self-diffusion rates. A theoretical analysis based on simultaneous grain-boundary and volume diffusion indicates a diffusion coefficient for surface diffusion that is three orders of magnitude greater than the volume-diffusion coefficient. (M. C. Brockway)

Beryllium Intermetallic Compounds

Brush Beryllium[18] has continued its research on intermediate-temperature oxidation of zirconium and niobium beryllides. Ternary additions of nickel, silicon, tantalum, and aluminum were tried in an effort to improve the oxidation resistance. Nickel was ineffective because of its high solubility in the beryllides; silicon was effective, but the alloys were found to possess inferior mechanical properties at temperatures of 2000°F and above. Tantalum-alloy additions of 3 wt.% as $TaAl_3$ did not improve the oxidation resistance. Aluminum was most effective, particularly in single-phase beryllides. For example, 0.35 wt.% in $ZrBe_{13}$, 1.4 wt.% in Zr_2Be_{17}, 0.75 wt.% in $NbBe_{12}$, or 1.25 wt.% in Nb_2Be_{17} enhances oxidation resistance at temperatures (to 1900°F) at which the unmodified compounds would oxidize catastrophically in short order.

It was shown that the improvement in intermediate-temperature oxidation resistance of the beryllides through the addition of aluminum depends upon the presence of free aluminum at the temperatures in question. This ties in with a hypothesis that the protection actually results from the relief of microstresses at the grain boundaries. (R. W. Getz)

Solid Hydrides

A patent[19] on moderator compounds for high-temperature applications has been issued to the UKAEA. These moderator materials are hydrides of zirconium, titanium, or rare-earth metals, with at least 1 atom of hydrogen for every 4 atoms of metal. In addition, they contain nitrogen, carbon, or oxygen because the moderator compounds are prepared by heating a metal hydride having a dissociation pressure of < 1 atm at 800°C with the refractory-metal oxide, nitride, or carbide in hydrogen at high temperature. The neutron-absorbing properties of the product may be modified by small additions of calcium, lithium, or plutonium.

Zirconium Hydride

A bibliographic survey of zirconium hydride and zirconium-uranium hydride publications has been issued by Atomics International.[20,21] The first volume contains 384 abstracts of unclassified reports and papers, and the second volume covers 170 classified reports on zirconium hydride materials. Both volumes contain author, subject, and report-number indexes. The effects of hydrogen on Zircaloy-2 have been covered in a similar survey[22] made at Savannah River. Abstracts of all reports issued on this subject from January 1955 to June 1962 are included.

A somewhat different approach for the preparation of zirconium hydride has been reported by Meerson and Roi.[23] By reducing ZrO_2 with magnesium in an atmosphere of hydrogen at 1100°C, they obtained hydride containing 2.0 wt.% hydrogen. Another innovation was the use of a CaO crucible to getter the system while it served to contain the reaction mixture.

Studies of the delta- and epsilon-phase regions of the zirconium-hydrogen system have continued at Atomics International.[24] Equilibrium dissociation pressures in these regions have been represented by an equation involving both temperature and composition

$$\log P\ (\text{atm}) = K_1 + \frac{10^3\ K_2}{T(^\circ\text{K})}$$

where

$$K_1 = -3.8415 + 38.6433X - 34.2639X^2 + 9.2821X^3$$

$$K_2 = 31.2982 + 23.5741X - 6.0280X^2$$

and X is the hydrogen-to-zirconium atom ratio. On the basis of the results of this investigation, together with previously known facts about the delta-epsilon transformation, a modification of the phase diagram is proposed, as shown in Fig. II-2. The dotted line, extending upward from the composition $ZrH_{1.59}$ and bending toward the ZrH_2 line with increasing temperature, represents the boundary at which the cubic-to-tetragonal transformation begins. The partial molal heat of solution of hydrogen in the delta and epsilon hydride phases decreases continuously with increasing solute concentration, with no discontinuity at the transformation point. Its value drops from −46.3 kcal/mole for the composition $ZrH_{1.4}$ to −37.7 kcal/mole at $ZrH_{1.9}$.

Zirconium hydride is unusual in being a neutron moderator with well-separated energy levels rather than having a large overlapping continuum of energy-exchange mechanisms. Since the hydrogen atom is bound within a tetrahedron of zirconium atoms, in the first approximation the hydrogen is a harmonic oscillator, and the cross sections for neutron scattering from the first level vary with scattering angle as predicted for such an oscillator. However, it has been found at General Atomic[25] that angular variation in scattering from the second excited level is quite different from that predicted for a harmonic oscillator. The cross section for purely elastic scattering by hydrogen atoms bound in $ZrH_{0.5}$ varies linearly with momentum transfer as required for harmonic motion. For $ZrH_{2.0}$, the variation deviates from linearity for large momentum transfers and indicates that the binding of hydrogen atoms is significantly different in this composition.

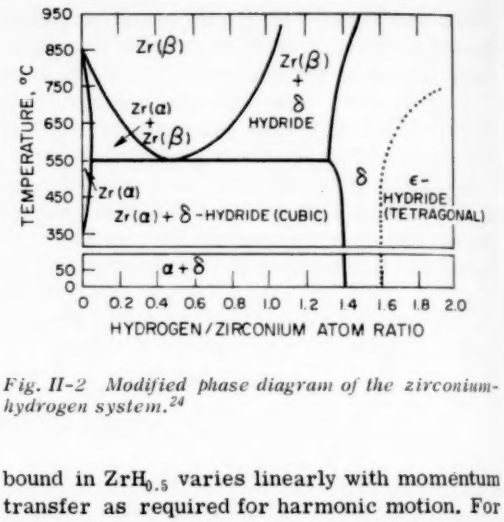

Fig. II-2 Modified phase diagram of the zirconium-hydrogen system.[24]

Yttrium Hydride

The dissociation pressure of yttrium hydride has been determined at the United Kingdom Atomic Weapons Research Establishment:[26]

$$\log P\ (\text{mm}) = 10.31 - \frac{11{,}830}{T(^\circ\text{K})}$$

where the composition is YH_2. The heat of formation of YH_2 was reported to be −54.1 kcal/mole.

Niobium Hydride

A series of niobium-hydrogen alloys with compositions in the two-phase and single-phase fields has been examined at room temperature by X-ray diffraction at the National Physical Laboratory in the U.K.[27] The unit cells were found to be slightly tetragonal, with a small departure from 90° of the angle opposite the c axis.

Hydrided Zirconium-Uranium Alloys

The release of fission products from hydrided zirconium−10 wt.% uranium fuel used in the SNAP-10A/2 reactor has been studied at Atomics International.[28] After irradiation in the Materials Testing Reactor, simulating 1 year of operation at 60 kw, samples were heated in a closed induction furnace to temperatures in

the range 2000 to 3000°F. This temperature was maintained for 10 min in the case of melts and for 8 hr when melting did not occur. Dehydriding occurred rapidly at the start. Fission-product release was high for melts but quite low at 2000°F, where melting did not occur, especially in samples clad with Hastelloy N. It was concluded that, unless a reactor core is completely vaporized during an excursion of temperature, there definitely is not a great instantaneous release of fission products. Rather, they are released at steadily decreasing rates for periods of several hours during the tests.

(H. H. Krause)

References

1. P. A. Thrower, Interstitial and Vacancy Loops in Graphite Irradiated at High Temperatures, British Report AERE-R-4612, April 1964.
2. J. O. Stiegler, C. K. H. DuBose, and J. L. Cook, An Electron Optical Study of Structural Features of Pyrolytic Carbons, USAEC Report ORNL-TM-863, Oak Ridge National Laboratory, July 1964.
3. W. J. Dodds and D. Raeburn, British Report, March 1964, Unpublished.
4. F. W. Albaugh, Reactor and Fuels Laboratory Monthly Report, July 1964, USAEC Report HW-83445A, Hanford Atomic Products Operation, Aug. 14, 1964. (Classified)
5. D. F. Kaufman and L. R. Aronin, Fundamentals of Single-Crystal Deformation in Zone-Refined Beryllium, USAEC Report NMI-1257, Nuclear Metals Division of Textron Inc., May 8, 1964.
6. M. I. Jacobsen, Tensile Properties of Extruded Beryllium from −195 to 200°C, *Trans. Am. Soc. Metals*, 57 (2): 482-493 (June 1964).
7. G. Ervin, Jr., and T. L. Mackay, Beryllium Oxidation Research Relative to the SNAP-8 Reactor, USAEC Report NAA-SR-9672, Atomics International, July 24, 1964.
8. D. W. Koch, K. F. Riskevics, and E. E. Ritchie, Advanced Test Reactor, Investigation of the Corrosion Behavior of Materials of Construction, USAEC Report IDO-24460, Babcock & Wilcox Co., Aug. 1, 1963.
9. J. L. Blumenthal and M. Santy, Beryllium Study Program, Second Quarterly Progress Report for Period January 1−March 31, 1964, USAEC Report SC-DC-64-864, Thompson Ramo Wooldridge Space Technology Laboratories, Apr. 14, 1964.
10. C. J. Patenaude, Casting and Hot Working of Sound Large-Diameter Beryllium Ingots. Phase I, Final Report, Report NP-13847, Beryllium Corp., Jan. 1, 1964.
11. C. J. Patenaude, Casting and Hot Working of Sound Large-Diameter Beryllium Ingots. Phase II, Final Report, Report NP-14025, Beryllium Corp., Apr. 1, 1964.
12. R. G. Jenkins, J. M. Siergiej, A. K. Wolff, and J. L. Klein, Development of Improved Fabrication Methods, Processes, and Techniques for Producing Typical Aircraft Shapes from Beryllium, Report ML-TDR-64-108, Nuclear Metals Division of Textron Inc., May 29, 1964.
13. C. J. Patenaude and W. H. Santschi, Casting of Beryllium−Stainless Steel and Beryllium−Columbium Impact Target Specimens, Report NASA-CR-54144, Beryllium Corp., June 9, 1964.
14. R. J. Diersing, H. D. Hanes, and E. S. Hodge, Fabrication of Beryllium-Clad Tubular Hypervelocity Impact Targets by Gas-Pressure Bonding, Report NASA-CR-54058, Battelle Memorial Institute, Nov. 6, 1963.
15. National Research Council, First Progress Report by the Committee on Beryllium Metallurgy of the Materials Advisory Board, Report MAB-199-M(1), June 16, 1964.
16. General Electric Company, Advanced Technology Services, High-Temperature Materials Program Progress Report No. 36, Part A, USAEC Report GEMP-36A, June 19, 1964.
17. Oak Ridge National Laboratory, Gas-Cooled Reactor Program, Semiannual Progress Report for Period Ending March 31, 1964, USAEC Report ORNL-3619, July 1964.
18. R. M. Paine, A. J. Stonehouse, and W. W. Beaver, Research on Modified Beryllides as High-Temperature Nuclear Materials, USAEC Report BBC-120, Brush Beryllium Co., Oct. 15, 1963.
19. W. J. Kramers, W. Bradshaw, J. R. Smith, R. P. Sinden, and P. S. Rogers, Refractory Metal Compounds, British Patent 960,720, June 17, 1964.
20. A. W. Barsell, L. D. Montgomery, and J. T. Roberts, Bibliographical Survey of SNAP Fuel Materials. Vol. I, Zirconium−Uranium Hydride and Related Zirconium and Uranium Systems, USAEC Report NAA-SR-9525 (Vol. I), Atomics International, July 15, 1964.
21. A. W. Barsell, L. D. Montgomery, and J. T. Roberts, Bibliographical Survey of SNAP Fuel Materials. Vol. II, Zirconium−Uranium Hydride and Related Zirconium and Uranium Systems, USAEC Report NAA-SR-9525 (Vol. II), Atomics International, June 26, 1964. (Classified)
22. M. S. Feldman, Hydriding of Zircaloy-2, A Literature Search, USAEC Report DP-803 (Del.), Savannah River Laboratory, May 1963.
23. G. A. Meerson and S. Roi, Preparation of Zirconium Nitride and Hydride Directly from the Dioxide, *Poroshkovaya Met. Akad. Nauk Ukr. SSR*, 3 (6): 71-77 (1963).
24. J. W. Raymond, Equilibrium Dissociation Pressures of the Delta and Epsilon Phases in the Zirconium−Hydrogen System, USAEC Report NAA-SR-9374, Atomics International, May 31, 1964.
25. W. L. Whittemore, Neutron Interactions in Zirconium Hydride, USAEC Report GA-4490 (Rev.), General Atomic Division, General Dynamics Corp., Jan. 6, 1964.
26. P. M. S. Jones, J. Southall, and K. Goodhead, The Thermal Stability of Metal Hydrides. Part I. Rare Earth and Yttrium Hydrides and Deuterides, British Report AWRE-O-22/64, June 1964.
27. C. Wainsright, A. J. Cook, and B. E. Hopkins, The Structures of Niobium Hydride Alloys, *J. Less-Common Metals*, 6 (5): 363-374 (May 1964).
28. W. M. Cegelski, Fission Product Release from Irradiated Uranium−Zirconium Hydride SNAP Fuel, USAEC Report NAA-SR-9673, Atomics International, July 15, 1964. (Classified)

Section

III

Reactor Materials

Nuclear Poisons

Metallic Poison Materials

Investigation of the iron-chromium-gadolinium system by the Bureau of Mines[1,2] has shown that the best alloy for control-rod material would be one containing 10 to 30 wt.% chromium with about 3 wt.% gadolinium. The two phases present in this composition range are $(Fe,Cr)_9Gd$ and the body-centered cubic iron-chromium solid solution. The melting point of this alloy is about 1200°C.

Tensile tests have shown that increasing the gadolinium content up to 4 wt.% increases the tensile strength but that further gadolinium additions cause a slight decrease in tensile strength. Also the addition of gadolinium seriously impairs the ductility, as shown below.

Gadolinium, wt.%	Elongation,* %
0	25 to 29
1	17 to 29
2	12 to 25
3	10 to 15
4	5 to 6
5	1 to 2

*Range in elongation stems from variations in chromium content of the alloy.

Five-week corrosion tests in water at 354°C showed that the gadolinium content did not affect the corrosion rate. However, as expected, specimens containing more chromium showed better corrosion resistance.

The scandium-gadolinium system was found[3] by thermal and X-ray methods to be characterized by complete solid solubility in the low-temperature hexagonal form and in the high-temperature body-centered cubic form. In other work with rare-earth intermetallics, the crystal structures of Gd_3Al_2, Dy_3Al_2, Gd_5Ge_3, Dy_5Ge_3, and $DyAl_3$ have been determined.[4]

German workers[5] have investigated the effect of boron additions to stainless steels on mechanical properties and corrosion resistance. Tensile characteristics were investigated at 20 to 1200°C, notch-impact strength at 20 to 300°C, and corrosion resistance to boiling HNO_3 of 18-11 chromium-nickel steels containing 0.7 to 1.3 wt.% boron.

Workers at Westinghouse Astronuclear Laboratory[6] have improved the fabrication procedures for aluminum–20 wt.% boron plates for control rods in the NERVA reactor. Plates are fabricated by sintering aluminum and boron powders to densities up to 98% of theoretical, and the bodies thus yielded have the following typical tensile properties:

Testing temp., °C	Yield strength, 1000 psi	Ultimate tensile strength, 1000 psi	Elongation, %
80	15	19	9
150	13	17	11
400	12	12	6

At Harwell[7] corrosion tests of hafnium in steam at 500°C have shown that after the first day the corrosion rate at 1 atm pressure is 30 times that at 1000 psi.

Nickel alloys containing 0.1 to 10 wt.% hafnium have been patented in Germany.[8] These alloys have very high recrystallization temperatures and good mechanical properties at high temperatures.

Solubility of tin in hafnium was found[9] to be 9.9 wt.% at 1680°C and 6.2 wt.% at 800°C. This high solubility rules out the possibility that hafnium-Zircaloy butt-weld cracking is caused

by the presence of brittle hafnium-tin intermetallic compounds. (M. Kangilaski)

Dispersion and Nonmetallic Poison Materials

Three capsules containing B_4C-graphite specimens were exposed by General Atomic workers[10] to a reactor environment simulating the Peach Bottom High-Temperature Gas-Cooled Reactor (HTGR). The samples contained 30 wt.% boron dispersed as B_4C powder in a graphite matrix. In two of the capsules the samples were extruded, and in the third the samples were hot pressed. After irradiation, samples from each capsule were evaluated as to dimensional changes, microstructure, fission-gas release, and boron depletion. The extruded B_4C-graphite samples expanded when irradiated at 300 to 340°C for six cycles, whereas the hot-pressed samples exhibited both expansion and contraction. The stability of the compacts appeared to be more dependent on thermal-neutron damage than on fast-neutron damage to the graphite matrix.

According to Hanford workers,[11] pneumatically impacted Sm_2O_3 melts at 2250 ± 50°C and 2260 ± 50°C in 8 vol.% hydrogen–argon and pure-argon atmospheres, respectively. The corresponding value for Nd_2O_3 was 2260 ± 30°C for both atmospheres. The Knoop hardness numbers (KHN) of Sm_2O_3 and Nd_2O_3 were 448 and 317, respectively.

Procedures for the fabrication of ceramic control-rod elements for the Molten-Salt Reactor were worked out by Oak Ridge.[12] The elements are made up of stacked thick-walled bushings of 75 wt.% Gd_2O_3–25 wt.% Al_2O_3. These bushings are made from prereacted powders that are crushed, pressed, and sintered. The use of prereacted powders eliminates excessive shrinkage stemming from reactions between the two oxides during sintering. After being heated to 1500°F to drive off absorbed moisture, the sintered bushings are sealed into the annulus between two concentric Inconel tubes by welding Inconel end closures into both ends.

The oxidation kinetics of dispersions of ZrB_2 in iron, cobalt, or nickel at 500 to 1000°C were examined by the Soviets.[13] The rate of oxidation was found to increase with increasing metal content and increasing temperature. These zirconium boride-base systems are considerably more stable than systems with a titanium boride base.

Working with single crystals, Wang et al.[14] determined that the crystal structure of Gd_6Mn_{23} is face-centered cubic, in agreement with previous work. The density of the compound was found to be 7.39 g/cm^3.

Workers at Southern Research Institute[15] recently studied the tensile properties of composites made from 86 wt.% ZrB_2–13 wt.% $MoSi_2$–1 wt.% BN over the temperature range 70 to 3500°F. The tensile tests were made on hot-pressed and pressed-and-sintered material with average densities of 5.5 and 4.9 g/cm^3, respectively. Up to 2000°F the ultimate tensile strength agreed well with values obtained from modulus-of-rupture (bend) tests. However, at 2000°F the tensile strength of the hot-pressed material decreased rapidly, whereas the corresponding modulus-of-rupture values remained higher for another 1000°F. Young's modulus of the hot-pressed material also decreased sharply at about 2000°F. The anomaly between the results from the tensile and bend tests was attributed to the presence of silica and the fairly high creep rate of the material during testing, although strain rate differences for the two tests may also have some influence.

Studies of the oxidation kinetics of ZrB_2 at 945 to 1256°C and of ZrC at 554 to 652°C were carried out at the University of Wisconsin.[16] The ZrB_2-O_2 reaction was parabolic throughout the temperature range studied, whereas the ZrC-O_2 reaction was linear. In the former case, ZrO_2, together with a molten layer of boron oxide, was formed and protected the ZrB_2 base against further direct reaction with oxygen. During the oxidation of ZrC, a porous film of ZrO_2 was formed which did not protect against further oxidation.

A recent book by Weidenbaum et al.[17] contains a chapter devoted to control-rod materials for high-temperature applications. Particular attention is given to transition-metal borides, rare-earth borides, and rare-earth oxides and their properties. (E. G. Smith, Jr.)

References

1. Bureau of Mines, Albany Metallurgy Research Center, Quarterly Metallurgical Progress Report No. 22 for the Period of January 1–March 31, 1964, USAEC Report USBM-U-1109.

2. Bureau of Mines, Albany Metallurgy Research Center, Quarterly Metallurgical Progress Report No. 23, April 1–June 30, 1964, USAEC Report USBM-RC-1122.
3. B. J. Beaudry and A. H. Daane, The Sc-Gd System, *J. Less-Common Metals*, 6: 322-325 (April 1964).
4. N. C. Baenziger and J. J. Hegenbarth, Gadolinium and Dysprosium Intermetallic Phases, *Acta Cryst.*, 17: 620-621 (May 10, 1964).
5. K. Bungardt and R. Oppenheim, Properties of Boron-Stainless Steels for Nuclear Reactors, *Dow Tech. Ver.* (in German), 4: 9-12 (1964).
6. J. B. McAndrew, Aluminum-Boron Control Plates for the NERVA Reactors; Fabrication and Properties, Report WANL-TME-654, Westinghouse Electric Corp., Astronuclear Laboratory, Jan. 13, 1964.
7. Metallurgy Division, AERE, Unpublished information, January 1964.
8. R. Reinbach, Nickel-Hafnium Alloy, German Patent 1,168,649, June 29, 1959.
9. G. E. Wasielewski, Phase Relations in the Hafnium-Rich Hafnium-Tin System, USAEC Report KAPL-3019, Knolls Atomic Power Laboratory, June 15, 1964.
10. G. B. Engle, Irradiation of B_4C-Graphite Capsules (GA-032-1A1 and -2A2), USAEC Report GA-4557, General Atomic Division, General Dynamics Corp., Apr. 30, 1964.
11. F. W. Albaugh, Reactor and Fuels Laboratory Monthly Report, April 1964, USAEC Report HW-82001A, Hanford Atomics Products Operation, May 15, 1964. (Classified; material cited is unclassified.)
12. Oak Ridge National Laboratory, Molten-Salt Reactor Program, Semiannual Progress Report for Period Ending January 31, 1964, USAEC Report ORNL-3626, July 1964.
13. V. F. Funke and S. I. Yudkovskii, High-Temperature Oxidation of Zirconium Borides Containing Iron-Group Metals, *Zh. Fiz. Khim.* (in Russian), 38: 1280-1283 (May 1964).
14. F. E. Wang, J. V. Gilfrich, D. W. Ernst, and W. M. Hubbard, Report on the Crystal Structure of Gd_5Mn_{23}, *Acta Cryst.*, 17: 931-932 (July 10, 1964).
15. F. J. Digesu and C. D. Pears, The Tensile Stress-Strain Properties of a Composition of Zirconium Diboride–Molybdenum Disilicide and Its Anomalous Strain Behavior, USAEC Report CONF-553-1, paper presented at American Ceramic Society 66th Annual Meeting, Chicago, April 1964.
16. A. K. Kuriakose and J. L. Margrave, The Oxidation Kinetics of ZrB_2 and ZrC at High Temperatures, *J. Electrochem. Soc.*, 111: 827-831 (July 1964).
17. B. Weidenbaum et al., Properties of Some High-Temperature Control Materials, in *Materials and Fuels for High-Temperature Nuclear Energy Application*, 344 pp., 1964.

Section

IV

Reactor Materials

Cladding and Structural Materials

Corrosion

Zirconium Corrosion

Long-term corrosion studies at Bettis[1] revealed that alpha-annealed and beta slowly cooled Zircaloy-2 exhibit similar corrosion behavior in 680°F water and steam, whereas the beta slowly cooled treatment causes accelerated attack in 750°C steam. Bettis workers also compared the corrosion behavior of PWR core 1 blanket fuel rods with that of unirradiated Zircaloy-2 exposed to similar water conditions. They concluded that the processes of corrosion of Zircaloy-2 cladding in an operating reactor for times of the order of five years and to exposures beyond transition can be predicted from data on unirradiated material.

Zircaloy-2 was supercharged with hydrogen in excess of the terminal solubility by thermal cycling between 25 and 400°C, in experiments reported by Hanford.[2] The supercharging was explained in two ways: one involved thermodynamic principles, and the other involved kinetic principles. Neither of these was believed to produce sufficient supercharging to account for the very high hydrogen concentrations observed in some aqueous corrosion specimens.

The hot hardness of modified zirconium oxides has been studied at Vallecitos[3] to determine oxide plasticity and relate it to corrosion behavior. Iron, nickel, or chromium additions to the oxide resulted in softer (more plastic) structures; aluminum had no effect; and yttrium produced a harder structure. Anion-deficient oxides appeared to be more plastic than stoichiometric oxides. Tensile tests of thick oxides indicated considerable plasticity at 500°C but brittleness at 23°C. (W. E. Berry)

Aluminum Corrosion

The corrosion behavior of 1100 aluminum in low-temperature (<100°C) reactor water was reviewed by Savannah River.[4] Recommendations for minimizing corrosion include (1) the use of high-purity water, maintained at 0.1 to 0.2 μmho/cm conductivity by ion-exchange resins; (2) in the absence of ion exchange, the use of inhibitors including 0.3 M solutions of $MgCrO_4$, $CaCrO_4$, or Na_2CrO_4-$MgCrO_4$; and (3) the avoidance of galvanic couples between aluminum and dissimilar metals.

Bent-beam stressed specimens of 7075 aluminum and B120VCA titanium alloys were exposed to PuF_6 at Argonne.[5] The four aluminum samples did not rupture after 30 days at 65°C plus an additional 14 days at 25°C. The two titanium samples failed by stress-corrosion cracking after 3 and 5¾ days, respectively, at 65°C. (W. E. Berry)

Stainless-Steel Corrosion

The effect of surface treatment on the corrosion of steels in 300°C water and 400°C steam is being studied in Belgium.[6,7] Results for low-alloy steels were the same in static water and steam, with corrosion rates on electrolytically polished specimens being one-half those for ground or mechanically polished specimens. With 18-8 stainless steel the corrosion rates in static water for the electrolytic polish were one-third to one-fourth those for mechanical treatments, whereas the rate in static steam for the electrolytic polish was 50% higher. Preliminary tests in flowing water at 300°C indicate that the electrolytic polish on stainless steel is superior to mechanical treatments but not to so great an extent as in static tests.

The tenacity and film release under thermal shock of deposited oxides (crud) were studied

by Hanford[8] by noting changes in the surface radioactivity levels of various alloys exposed in a bypass loop to contaminated neutral or high-*p*H reactor cooling water. The results indicate that components made of stainless steel should be less prone to "crud-burst" problems than components of aluminum, Zircaloy-2, or carbon steel. Crud burst refers to the sudden increase in reactor-water contamination following a departure from steady-state flow conditions.

The effect of *p*H on the stress-corrosion behavior of type 304 stainless-steel U-bend specimens in 90°C water containing 10 and 100 ppm NaCl has been studied at Savannah River.[9] Sensitized-and-pickled specimens exhibited mostly transgranular cracking at *p*H 4 to 7, only intergranular cracking at *p*H 3 to 3.5, no attack at *p*H 2.5, and some slight general intergranular attack at *p*H 0 and 1. Cracking was less severe in nonsensitized material. Transgranular cracking occurred at *p*H 3.5 to 7, and no cracks were detected below *p*H 3.

Long-term corrosion tests in flowing borated water (0.89 wt.% H_3BO_3) at 600°F have been conducted by Westinghouse.[10] Corrosion rates of austenitic stainless steels ranged from 1.6 to 4.0 mg/(dm^2)(month), with metal release rates to the water running about one-half the corrosion rates. Corrosion rates for 440°C stainless steel and 17-4 PH steel were 23.6 and 10.8 mg/(dm^2)(month), respectively. Other metals that were studied included Inconel, Inconel X, Zircaloy-2, zirconium-beryllium braze, Nicrobraze, and 80 wt.% silver – 15 wt.% indium – 5 wt.% cadmium braze.

In support of the water-boiler reactor program at Los Alamos, 300-series austenitic stainless steels have been exposed three years at 95°C to 0.05*M* uranyl solutions containing 0.10*M* HNO_3 or 0.75*M* H_3PO_4 (Ref. 11). Average corrosion rates were 0.11 and 0.6 mil/year in the HNO_3 and H_3PO_4 solutions, respectively. Grain-boundary attack, 1 to 2 grains deep, was observed in the HNO_3 solutions.

Examination of a stainless-steel-clad fuel element from the Organic-Moderated Reactor Experiment (OMRE) after 282-Mwd irradiation revealed thin-film deposits which followed the burnup profile.[12] These ranged in thickness from ~0.2 μ at the inlet end to 3.5 to 3.6 μ at the high-flux area and ~0.9 μ at the outlet end. The film deposits were made up of particles 0.5 to 2 μ in diameter containing a magnetite center surrounded by an organic matrix.

(W. E. Berry)

Corrosion of Iron- and Nickel-Base Alloys

EXPOSURE TO GASES

Nitrogen gas at 1100 and 1200°C is being used at Hanford[13] to evaluate alloys for structural and cladding service in the HTLTR (High-Temperature Lattice Test Reactor). After 200 hr the samples containing chromium and supported by or near graphite tended to become embrittled as a result of carburization. Hastelloy B, nickel, and TD nickel (thoria dispersion nickel), on the other hand, retained room-temperature ductility, even though there is a high mobility of carbon in these nickel-base materials.

In support of the gas-cooled reactor, metals are being studied[2] in helium plus 15 torrs H_2O at 1700°F (920°C), 1900°F (1030°C), and 2100°F (1150°C). Hastelloy N, Hastelloy X, Hastelloy 280, Hastelloy C, and Inconel 600 all showed less than 0.75 mg/cm^2 weight gain after 300 hr of exposure.

Saclay[14] is studying the compatibility of chromium-aluminum-molybdenum steels in dry, oxygen-free CO_2 at 25 atm pressure and temperatures from 450 to 550°C. The alloy APS 10M4 (0.002 wt.% chromium, 0.035 wt.% aluminum, 0.035 wt.% molybdenum) is expected to find application in heat-exchange service. Adding water vapor increased the rate of attack in some alloys.

Iron has been exposed to fast neutrons at the Massachusetts Institute of Technology[15] to study the effect of irradiation on the chemical reactivity in dry oxygen. In the parabolic range between 220 and 275°C, radiation increased the oxidation rate. It was believed that irradiation may increase the work function of oxide or decrease that of metal at the oxide-metal interface and thus facilitate electron transfer.

EXPOSURE TO WATER AND STEAM

Incoloy 800 fuel-cladding performance is being investigated in a boiling-water-reactor superheated-steam loop at Vallecitos.[16] Good corrosion resistance is obtained under heat-transfer conditions after a 4000-hr exposure to 1300°F (705°C) steam. For three years of

service, the maximum penetration at a 95% confidence level is calculated to be 0.0033 in., and the oxide layer, 0.0017 in.

Hanford[17] finds a corrosion rate for mild steel of 0.15 mil/year after 2500 hr of exposure in ammoniated water (*p*H 10) at 300°C. At the end of this period, the rate of corrosion-product deposition was higher than the rate of iron loss to the system. (F. W. Fink)

Corrosion of Refractory Metals

Union Carbide has been granted a patent[18] for corrosion-resistant vanadium-base alloys. One of the alloy compositions, vanadium–40 wt.% niobium–10 wt.% titanium, was reported to have the following properties:

(*a*) Corrosion in boiling acids
18 mils/year for 65% HNO_3
46 mils/year for 10% HCl
56 mils/year for 20% H_2SO_4
(*b*) Weight gain during 10 hr of oxidation in oxygen
95 mg/cm^2 at 700°C
155 mg/cm^2 at 800°C
280 mg/cm^2 at 900°C

Russian investigators[19] have shown that rhenium alloying additions to tungsten increase the rate of oxidation in the 500 to 900°C temperature range, as would be predicted by the Wagner theory of oxidation. For example, a tungsten–5 wt.% rhenium alloy oxidized almost five times as fast as pure tungsten at 800°C. Larger additions of rhenium, up to 20 wt.%, had less of an effect on the oxidation rate.

Basic kinetic data on the effects of dissociation of molecular oxygen on the oxidation rates of molybdenum and tungsten are being obtained by Aerochem.[20] The investigators found that oxidation probabilities for atomic oxygen are one to two orders of magnitude higher than for molecular oxygen, and the corresponding activation energy is considerably lower—about 4 kcal/atom, compared to about 30 kcal/molecule. (The authors define oxidation probability as the ratio of the flux of oxidized metal atoms away from the surface to the flux of oxygen atoms or molecules colliding with the surface.)

Studies of the corrosion of niobium-base alloys in steam at 540 and 650°C resulted in the development of several promising cladding materials for nuclear superheat applications.[21] Two of the more promising alloys, niobium–21 wt.% titanium–12 wt.% vanadium–9 wt.% chromium and niobium–24 wt.% titanium–12 wt.% vanadium–12 wt.% chromium, were reported to be about as oxidation resistant as austenitic stainless steel. The alloys have thermal-neutron absorption cross sections lower than those of austenitic stainless steel and much better high-temperature strengths. No long-lived radioisotopes are contained in the corrosion products of the niobium alloys.

Hafnium-tantalum alloys are showing promise as potential oxidation-resistant coating materials for the refractory metals. In studies conducted at Marquardt,[22] a hafnium–27 wt.% tantalum alloy developed a smooth, crack-free, adherent oxide at temperatures as high as 4000°F. Oxidation at 4000°F for 10 min resulted in the formation of a 20-mil-thick oxide with an inner 6-mil oxygen-affected zone. These hafnium-tantalum alloys have high emissivity (~0.85), low thermal conductivity of the oxide [~0.9 Btu/(hr)(ft)(°R)], and a good thermal-expansion match with the refractory metals, making them attractive coating materials. Marquardt is currently evaluating various techniques for coating the refractory metals with hafnium-tantalum. Vapor deposition, slurry coating, cladding, and plasma-arc spraying are being examined as possible coating processes. (J. J. English)

Corrosion by Liquid Metals and Organics

Proceedings of the Fourth Joint NASA-AEC Liquid Metals Corrosion Meeting held at the Lewis Research Center on Oct. 2 and 3, 1963, have been documented in two volumes.[23,24] The first volume presents unclassified material covering corrosion mechanisms, compatibility experiments in approximately 10 laboratories, and certain aspects of heat transfer and fluid flow. The second volume presents classified information from investigations at Pratt & Whitney and Oak Ridge.

A summary report[25] issued by MSA Research Corp. covers that segment of their research in which the effect of 1100°F sodium on the physical properties of 2¼ wt.% chromium–1 wt.% molybdenum steel has been investigated. Comparisons among results for sodium, air, and helium exposures have led to conclusions such as the following:

Fatigue. In cyclic constant-strain experiments, the number of cycles to failure for sodium exposures was (1) 5 to 16 times greater than for air exposures and (2) approximately equivalent to that for helium exposures. The results for sodium with 30 ppm oxygen and for sodium with 300 ppm oxygen were substantially the same.

Rupture. Sodium exposure, whether during the period that the stress was applied or as a presoak, tended to reduce rupture strength slightly.

Creep. Minimum creep rates were accelerated by sodium exposure. Third-stage creep was attained relatively early in the sodium and helium environments.

Strength and Ductility. Tensile and yield strengths were reduced and ductility was increased by exposure to sodium for 4000 hr without stress prior to testing in air or helium.

Decarburization. The experimental material decarburized in both high- and low-oxygen sodium; the rate was higher in the high-oxygen case.

Nejedlik and Vargo of Thompson Ramo Wooldridge have reviewed[26] their mercury corrosion data obtained in reflux type capsule experiments operating at temperatures from 600 to 1000°F. The test materials included austenitic and ferritic steels, Haynes 25 alloy, beryllium, chromium, and silicon. A principal theme is the consistency with which the large quantity of data obtained can be resolved into two familiar patterns: (1) a time dependency characterized by an initial linear corrosion rate followed by a steady-state parabolic rate, indicative of a diffusion-rate-controlling mechanism, and (2) a straight-line relation between parabolic corrosion-rate constants and reciprocal temperature (Arrhenius plot).

Compatibility experiments at Los Alamos have demonstrated[27] that approximately 10 ppm yttrium in tantalum–0.1 wt.% tungsten adds greatly to the ability of this alloy to withstand corrosive attack by a molten plutonium-iron alloy at 650 and 700°C. For example, at 700°C, 700-hr exposures with the nonyttrium-bearing alloy invariably result in failure. With the addition of yttrium, it has been possible to complete 2800-hr runs at 700°C successfully. Yttrium additions to tantalum alone do not bring about such a marked benefit, and failures after 1400 hr at 650°C are typical. A second experimental fuel system, plutonium-cobalt-cesium, is apparently less aggressive than the plutonium-iron system. For example, the former can be contained by unalloyed tantalum at 750°C for at least 2100 hr.

Mechanical-property and corrosion specimens of the following materials were exposed for 26 months (accumulating a total fast-flux dose of approximately 5×10^{19} neutrons/cm^2) in the core of the OMRE: types 304 and 347 stainless steel, ASTM-A-7 carbon steel, SAE 4130 alloy steel, 1100 aluminum, and magnesium.[28] The reactor fluid, Santowax OM, nominally about 18% diphenyl in terphenyls, operated in the 500 to 700°F range. The posttest observations indicated good correlation with out-of-pile corrosion exposures in that all the materials, except the magnesium, were essentially inert to attack. The alterations in tensile and impact strengths were apparently unrelated to the fluid environment since they were similar to those expected as a result of the radiation levels alone.

Argonne[29] is investigating the compatibility of vanadium–20 wt.% titanium with sodium circulating in a 650°C loop provided with a low-temperature bypass cold trap. After about 100 hr of exposure, insert samples show weight gains that do not change rapidly with additional time (to approximately 0.6 mg/cm^2 after 550 hr). The data have led to the belief that corrosion inhibition through a protective-film mechanism may be involved.

Solubility studies at the Naval Research Laboratory (NRL)[30] with niobium–1 wt.% zirconium alloy in 800 to 1380°C vacuum-distilled and filtered sodium indicate solubility ranges of 0.25 to 250 ppm (by weight) for niobium and 0.08 to 4 ppm for zirconium.

Investigators at Vallecitos, during the course of experiments with a sodium flow loop constructed of austenitic and ferritic materials, have observed that corrosion in isothermal regions decreases as the fluid moves downstream. They have labeled this the "downstream" effect. Such behavior is characteristic of a corrosion process in which the rate-controlling step is the rate of diffusion of material removed from the wall into the bulk stream. Mottley[31] has suggested that, in the case of the Vallecitos systems, the material-removal process involves a chemical reaction at the wall

by which Na_2O, which has diffused from the bulk stream, is reduced to form an iron-containing compound. The subsequent diffusion of this compound after dissolution in the sodium is apparently the rate-controlling step. It is stated that the compound may be FeO or some $Na_2O \cdot FeO$ complex. The likelihood that FeO is the product is debatable since, thermodynamically, Na_2O is more stable than FeO up to about 2150°F.

The free energies of solution of 15 elements in liquid sodium have been calculated by computer, on the basis of mathematical models from solubility data.[32] The results are expressed as a function of temperature and solute concentration. A plot based on a temperature of 1200°F gives free-energy values that range from 0 for approximately 17 ppm iron to −36 kcal/mole for approximately 0.1 ppm tin. In an illustrative application of the free-energy values, an analysis is made relating parts per million carbon in sodium and carbon activity at 1200 and 1500°F. The values are plotted, along with known carbon activities in gamma iron and type 304 stainless steel. The combined curves show that sodium containing 30 ppm carbon would be in equilibrium with 1.6 wt.% carbon in the steel at 1200°F or with 0.4 wt.% carbon in the iron at 1500°F.

Experiments in which zirconium, niobium, and niobium−1 wt.% zirconium were exposed to cesium at 1600, 1800, and 2500°F were conducted at Rocketdyne.[33] In the case of these particular combinations, the alkali metal will not reduce the refractory-metal oxides. Results showed (1) no appreciable dissolution of the zirconium or attack of the niobium or the niobium−1 wt.% zirconium at 1600°F, (2) broad-front dissolution of the niobium at 1800°F, and (3) limited intergranular attack of the niobium−1 wt.% zirconium at 1800°F but not at 2500°F.

Attention is called to the fact that the several papers on materials for sodium-cooled reactors presented at the 1963 ANS Winter Meeting have been compiled into a single volume.[34] (J. H. Stang)

Metal-Water Reactions

Argonne has reported additional studies[5] of metal-water reactions for molybdenum and aluminum. Of the high-melting-point metals studied previously, the oxides resulting from the metal-water reaction have not been volatile. Among the high-melting metals, however, are some which form at least one oxide whose melting and boiling points lie below those of the parent metal. The study of the reaction of such metals with steam is expected to shed new light on the mechanism and rate laws of metal-water reactions. Molybdenum was chosen for the initial study since information is available about the stability and volatility of molybdenum trioxide (MoO_3).

Molybdenum samples 1 cm in length were prepared from rods 5 or 13 mm in diameter. Holes $^1/_{16}$ or $^3/_{32}$ in. in diameter were drilled in one face of the rods to a depth of 6 mm for mounting the weighed specimens on an alumina tube containing the thermocouple. To carry out an experiment, workers weighed the specimen and mounted it on the alumina tube, and the volume of hydrogen evolved was recorded at suitable time intervals. The volume of hydrogen collected varied from 100 to 500 ml, depending on the rate of evolution which, in turn, varied with temperature and sample size from less than 1 to 200 ml/min. When an experiment was completed, the metal sample was washed in acetone and weighed.

The stoichiometry of the reaction was determined from the ratio of the gram moles of hydrogen produced to the gram atoms of molybdenum reacted. The average value of this ratio for 41 experiments was 2.96, indicating that the overall equation is

$$Mo + 3H_2O = MoO_3 + 3H_2$$

A value somewhat less than 3 is consistent with the observation that, although the oxide vapor is white with a yellow tinge, the aqueous condensate formed a colloidal blue solution characteristic of "moly blue" oxide, which has an oxygen-to-molybdenum ratio somewhat less than 3.

Experiments conducted in the range 1100 to 1700°C show that the reaction followed a linear rate law and that the experiments are quite reproducible, especially with the larger samples. The velocity constant (k) expressed in gram atoms of molybdenum per square centimeter per minute varied from 6×10^{-4} at 1700°C to 2×10^{-6} at 1130°C.

Some discrepancy was noted between the thermocouple and pyrometer temperatures, but

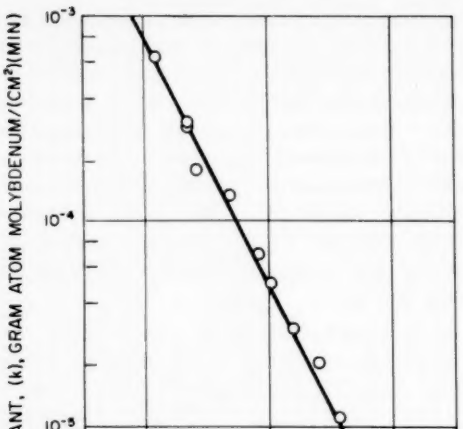

Fig. IV-1 Linear rate constants for the molybdenum-steam reaction.[5]

this was considered to be caused by the light absorption of the slightly yellow volatile oxide. The logarithm of the velocity constant is presented as a function of the reciprocal temperature in Fig. IV-1. The rapidity of the reaction [0.2 mg of molybdenum/(cm^2)(min)], even at the lowest temperature studied, precludes the use of molybdenum in an environment of high-temperature steam.

Previous observation of a self-sustained vapor-phase combustion process for aluminum prompted a study in which the rate of metal consumption was determined as a function of pellet size. This study was undertaken to provide a basis for estimating the rate of the aluminum-water reaction in the burning regime (metal temperature greater than 1750°C).

Samples of high-purity aluminum ranging in weight from 150 to 1000 mg were levitated, heated in air until they ignited, and then dropped into room-temperature water. The time that elapsed from the moment of dropping until burning ceased was measured. The results of these measurements are plotted in Fig. IV-2. The data points were fitted to a straight line by the method of least squares. The equation of the line was as follows:

$$D_0 = 0.160t_c + 3.36$$

where D_0 is the original diameter of the particle in millimeters and t_c is the consumption time in seconds.

Initially, a drop of burning aluminum would sink below the water surface, then rise and sink alternately as the hydrogen bubble surrounding it grew and broke off. As the drop became smaller, it would break the water surface, releasing the hydrogen, and then sink, form a bubble, and rise again. Eventually, when the size of the drop had become small enough, it would rise to the surface and float while continuing to burn. Once burning ended, the residual metal, enclosed in an irregular oxide coating, would sink to the bottom of the water container. While the drops were burning under water, they decreased in size, and the condensation of fine alumina particles was evident as a particle spray from the burning surface of the drop. (A. W. Lemmon, Jr.)

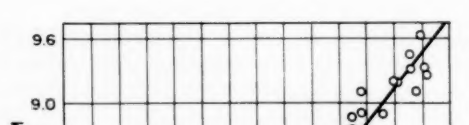

Fig. IV-2 Consumption of aluminum pellets burning in water.[5] *Water temperature, 25°C; metal temperature, 2050°C.*

Radiation Effects in Nonfuel Materials

Low-Alloy Steels

Numerous studies have demonstrated that radiation can produce large increases (as much as 450°F) in the brittle-to-ductile transition temperature of carbon and low-alloy steels. The mechanical properties of two reactor-vessel steels were determined by the French[35] on specimens that had been exposed to a fast-neutron dose of about 10^{19} neutrons/cm^2. Maximum irradiation hardening in the manganese-molybdenum steel (AMMO2, grade S) occurred at an irradiation temperature of 130 to 140°C. A 10-hr anneal at 250°C was sufficient to restore the yield point, regardless of the temperature at which the specimen had been irradiated. The results were more scattered for the weldable, high-yield-strength steel (DFOV 4S, grade V), but it appears that a hardening plateau occurred at an irradiation temperature of about 250°C.

Workers at NRL[36] conducted in-pile fatigue experiments on A-302B steel at 500°F in a flux of about 3.2×10^{12} neutrons/(cm^2)(sec), >1 Mev. No effect of the irradiation was observed in low-cycle tests, but the fatigue life of the specimens in the high-cycle (>50,000) range appeared to be increased by the exposure.

From tests on a weldable molybdenum steel under fast-neutron irradiation, the French[37] found that the degree of embrittlement was quite sensitive to the extent and location of a dispersed second phase. When this phase was finely dispersed throughout the grains, radiation caused less embrittlement than when the second phase was located preferentially along the grain boundaries.

Stainless Steels

Many of the current irradiation studies on stainless steels are being done at elevated temperatures. Workers at Oak Ridge[38] have found that the mechanical properties of AISI type 347 stainless steel are not affected appreciably by irradiation at temperatures above 1100°F. Their investigation included determinations of 0.2% offset yield strength, ultimate tensile strength, uniform elongation, and total elongation, after irradiation to 7×10^{20} neutrons/cm^2 ($E > 1$ Mev) from room temperature to 1500°F.

The effect of thermal neutrons on the creep properties of A-286, a precipitation-hardening stainless steel, has been investigated[39,40] by workers at General Electric. Stress-rupture specimens were irradiated with and without cadmium shielding, and the unshielded samples received about five times the thermal-neutron exposure of the shielded samples. Thermal neutrons lowered the creep-rupture life for a given stress by a factor of about 5 at 650°C and about 1.4 at 732°C. However, at any given stress the ratio of the rupture life of the unirradiated control specimens to that of either type of irradiated specimen was greater at 732°C than at 650°C. These effects are illustrated in Figs. IV-3 and IV-4. The ductilities of both the shielded and unshielded specimens were reduced drastically by the irradiations, as can be seen in Table IV-1. Figure IV-4 indicates that annealing an irradiated, unshielded specimen for 9.1 hr at 732°C produced very little recovery in creep-rupture strength. When a similar series of experiments was done on Hastelloy X, annealing resulted in complete recovery. This demonstrates the difference in the effects of neutron irradiation on precipitation-hardening alloys (A-286) and solution-strengthened alloys (Hastelloy X).

Refractory Metals and Zircaloy-2

Tube burst tests have been made on irradiated Zircaloy-2 tubes at Savannah River.[41] The

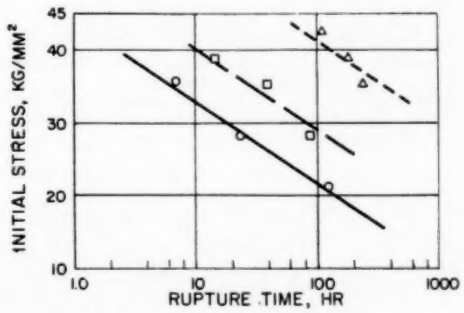

Fig. IV-3 Creep-rupture strength of A-286 shielded and unshielded specimens[39] tested at 650°C. △, control, heat C-2527, unirradiated. □, irradiated, shielded with 0.5 cm of cadmium, 3.5×10^{19} neutrons/cm^2 ($E_n \geq 1$ Mev), 2.3×10^{19} thermal neutrons/cm^2. ○, irradiated, unshielded, 3.6×10^{19} neutrons/cm^2 ($E_n \geq 1$ Mev), 11.0×10^{19} thermal neutrons/cm^2.

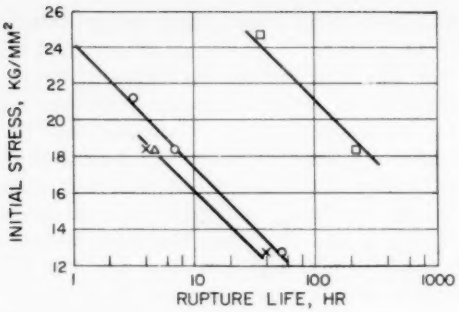

Fig. IV-4 Creep-rupture strength of A-286 shielded and unshielded specimens tested[40] at 732°C. □, control, heat C-2527. ○, irradiated, shielded with 0.5 mm of cadmium; 3.5×10^{19} neutrons/cm² ($E_n \geq 1$ Mev), 2.3×10^{19} thermal neutrons/cm². ×, irradiated, unshielded, 3.6×10^{19} neutrons/cm² ($E_n \geq 1$ Mev), 11.0×10^{19} thermal neutrons/cm². △, irradiated, unshielded plus annealed at 732°C in air for 9.1 hr.

Table IV-1 STRESS-RUPTURE TEST RESULTS OF SHIELDED AND UNSHIELDED A-286 ALLOY SPECIMENS[39] AT 650°C

Specimen*	Stress, kg/mm²	Rupture time, hr	Elongation in 3.81 cm, %	Reduction in area, %
Controls				
191 AS	42.2	111.7	11.9	15.0
36 ACS	38.7	181.2	13.5	20.2
185 AS	35.2	237.5	13.6	17.0
Unshielded†				
186 AS	35.2	6.8	1.1	3.3
187 AS	28.1	28.8	2.8	8.6
188 AS	21.1	125.6	1.4	8.2
Shielded‡				
29 ANS	38.7	14.5	1.2	2.3
28 ANS	35.2	39.5	1.2	2.0
33 ACS	28.1	89.8	3.2	1.2

*Smooth bar specimens from heat C-2527 heat-treated as follows: 900°C, 2 hr, water cooled; 720°C, 16 hr, air cooled; 650°C, 16 hr, air cooled.

†Irradiated in capsule 33MT-104A; 3.6×10^{19} neutrons/cm² ($E_n > 1$ Mev), 11.0×10^{19} thermal neutrons/cm².

‡Irradiated in capsule 33MT-104B shielded with a 0.5-cm cadmium-coated steel jacket; 3.5×10^{19} neutrons/cm² ($E_n \geq 1$ Mev), 2.3×10^{19} thermal neutrons/cm².

work was performed on sheathing tubes containing UO_2 pellets exposed to 10^{20} fast neutrons/cm² and irradiated in cooling water below 100°C. A slight increase in weld shear strength was noted; strength and ductility of the tubing were not affected.

Aluminum

An investigation to determine radiation-induced property changes in 6061 aluminum in the fully annealed, 20% cold-worked, and in the aged (T-6) condition was carried out at Oak Ridge.[42] The specimens were irradiated at 120 and 485°C to a total dose of 10^{19} neutrons/cm² (>2.9 Mev) and 10^{20} thermal neutrons/cm². Tensile tests run at 2.5%/min strain rate at room temperature and at the irradiation temperatures showed that irradiation did not influence the strength or fracture ductility for the conditions studied. (F. R. Shober)

Selected Mechanical Properties of Cladding and Structural Materials

A compilation[43] of the mechanical and physical properties of three superalloys has been issued by the Defense Metals Information Center. The alloys covered include MAR-M-200 (nickel base), MAR-M-302 (cobalt base), and MAR-M-322 (cobalt base).

The stress-rupture properties of three separate heats of INOR-8 at 1100, 1300, and 1500°F are illustrated[44] in Fig. IV-5. Heats NI-5055 and NI-5081 are comparable, whereas heat NI-5075 appears to be weaker and less ductile than the other two.

Zirconium

Hanford[45] has concluded a study of the fracture characteristics of Zircaloy-2 and reached the following conclusions:

1. Zircaloy-2 containing a crack or stress raiser undergoes a ductile-to-brittle transition with decreasing temperature. This ductile-to-brittle transition is characterized by a sudden change from relatively high nominal bonding strength and ductility to low nominal strength and undetectable ductility.

2. The ductile-to-brittle transition temperature is increased by increasing the loading rate, by increasing the amount of cold work, and by increasing the sharpness of the stress raiser.

3. Crack propagation occurs with nearly the same ease in both the rolling and transverse directions. However, crack propagation in annealed Zircaloy-2 at 45° to the rolling direction is much more difficult.

4. The fracture appearance is nearly the same both above and below the ductile-to-

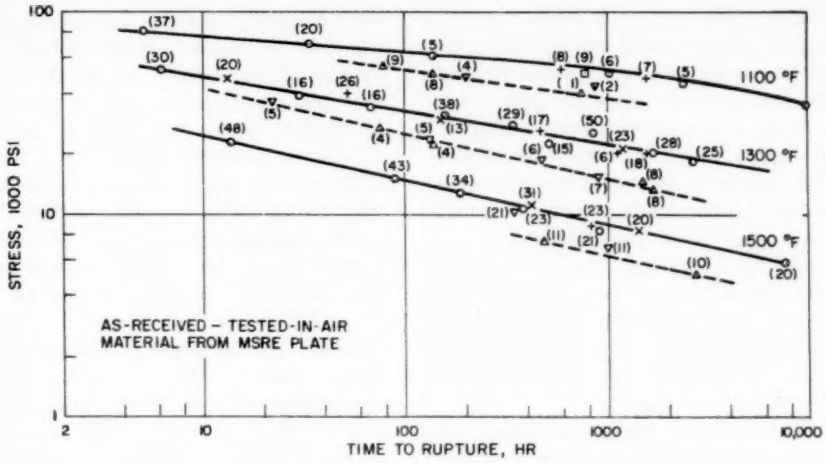

Fig. IV-5 Stress-rupture properties[44] of INOR-8. ○ and □, heat 5055. △ and ▽, heat 5075. + and ×, heat 5081; +, ○, and △, parallel to rolling direction. □, ×, and ▽, transverse to rolling direction. Numbers in parentheses are total elongation in percent.

brittle transition temperature and consists of mixed cleavage and tearing. On the basis of anisotropic behavior and interplanar spacings, it is inferred that the major cleavage plane is the $(1\,0\,\bar{1}\,0)$. (J. A. DeMastry)

Selected Metallurgical Aspects of Cladding and Structural Materials

Light Metals

Walford at Cambridge University[46] has proposed some changes in the aluminum-rich end of the aluminum-molybdenum phase diagram. The results of several workers indicate that two new phases, $MoAl_4$ and $MoAl_6$, have to be introduced and that one phase, $MoAl_2$, should be omitted from the existing diagram.

The Russians have been investigating magnesium-base alloys by determining the effects of alloy additions on the mechanical properties of magnesium-neodymium alloys[47] and by studying the recrystallization behavior and stress-rupture resistance of magnesium-cerium alloys.[48] They have also been studying the vanadium-magnesium and niobium-magnesium systems[49] and have constructed phase diagrams on the basis of microstructural, X-ray, and thermal analyses, as well as hardness and microhardness measurements.

Nickel and Steel

Although heat-treatments of Hastelloy N produce small variations in strength, their influence on ductility is of much importance. In a study at Oak Ridge,[50] four heats of air-melted material exhibited quite low fracture strains in the 1400 to 1800°F range, after they were annealed at temperatures above 2200°F. Aging at 1600°F, very slow cooling rates, and slow working were effective in restoring the ductility. The high-temperature ductility of Hastelloy N annealed at 2150°F was reduced by aging in the 1100 to 1200°F range. These effects are considered to be the result of the formation of a brittle grain-boundary layer along which a crack can propagate easily at elevated temperatures. Disrupting the continuity of this layer by aging or cold working restores good fracture ductility. The formation of this layer is associated with the presence of trace alloying elements. A vacuum-melted heat exhibited good ductility under all conditions studied.

A study at the Case Institute of Technology[51] on the solute-induced embrittlement in steel and several face-centered cubic alloys showed that a hydrogenated alloy of 66 wt.% nickel–20 wt.% copper–3 wt.% aluminum was subject to brittle delayed failure. The static fatigue curve

and discontinuous crack propagation were almost exactly the same as the effects observed in high-strength steel. The study also revealed that hydrogen produced an expansion of the lattice. An analysis of the flow behavior showed that hydrogen gave rise to a lattice frictional stress, which suggested an increased susceptibility to brittle fracture. The phenomenon of delayed failure has been correlated with microstructure in two alloy steels at three moderate strength levels. The sensitivity to delayed failure may persist, even though conventional tensile results indicate full ductility. Observed reductions in ductility are a function of microstructure at a given strength level.

Workers at Oak Ridge[52] report the results of a study directed toward an evaluation of the effects of hydrogen or argon environments on high-temperature creep-rupture properties of Inconel, Nickel 200, Nickel 270, electron-beam zone-refined nickel, high-purity copper, Armco iron, electrolytic iron, and type 304 stainless steel. All the nickel-base materials and the copper exhibited inferior creep resistance in hydrogen, and the iron-base materials were not influenced by environment.

Researchers in the United Kingdom[53] have investigated the metallurgical stability of four vacuum-melted stainless steels and air-melted Inconel. The stainless-steel compositions included the following: 18 wt.% chromium–8 wt.% nickel, 19 wt.% chromium–14 wt.% nickel, 20 wt.% chromium–25 wt.% nickel, and 25 wt.% chromium–20 wt.% nickel; all four contained 1 wt.% niobium. The stability of the materials after aging for periods up to 10,000 hr at temperatures of 600 to 800°C was assessed by means of hardness, Charpy impact, and Hounsfield tensile tests. All materials examined exhibited some degree of structural instability in this temperature range. The changes in mechanical properties are due to precipitation of carbides and the formation of sigma phase; the size, type, and distribution of these precipitated phases govern the degree of influence on the mechanical properties. The impact strength of all materials deteriorated after the aging treatment.

Refractory Metals

MOLYBDENUM AND TUNGSTEN

A study of dislocation structures in annealed and strained sheet of molybdenum and molybdenum alloys containing 18 and 35 at.% rhenium has been completed at the University of Pennsylvania.[54] No change in dislocation structures was observed in the deformed, low-rhenium-content alloys; dislocations started to tangle at an early stage of deformation (0.1% strain). Deformation seems to disturb subboundaries, and precipitates (possibly carbon) were found to be surrounded by dislocations in the deformed specimens. A profuse amount of twins was observed in the alloys containing 35 and 18 at.% rhenium deformed at room and liquid-nitrogen temperatures, respectively. A dislocation reaction between a slip dislocation and three twinning dislocations was frequently noted; this reaction appeared to be related to the nucleation of twins. It was concluded that (1) solution hardening observed in molybdenum-rhenium alloys must not be strongly related to stacking faults, (2) stacking-fault energy has little to do with twinning, and (3) nucleation of twinning is related to the dislocation of reaction between a slip dislocation and three twinning dislocations.

The internal friction of samples of molybdenum and molybdenum alloys containing zirconium or rhenium, annealed and deformed at room temperature, was measured[55] by Russian investigators in the temperature range 20 to 700°C. The temperature dependence of internal friction in deformed samples of molybdenum and molybdenum-zirconium had a peak that disappeared after annealing below the recrystallization temperature. For a fixed degree of plastic deformation, the temperature at which this peak occurred depended on the grain size.

An investigator at General Electric has made a study[56] of the intereffects of chemistry, processing, and heat-treatment on the microstructure and tensile properties of five molybdenum-base alloys containing 1.6 to 6.0 wt.% titanium, 0 to 0.6 wt.% zirconium, and 0.09 to 0.25 wt.% carbon. The nature and stability ranges of the carbides, aging kinetics, and morphology of carbide dispersion are shown to depend strongly on the concentration of titanium and/or zirconium and the resulting (Ti + Zr)/C ratio, with zirconium being much more influential than titanium. The effect of processing and heat-treatment on the tensile properties from 78 to 3500°F was determined, and their interdependency with the solution and aging characteristics is discussed in the publication.

The properties of molybdenum tubing in relation to its uses for missile and nuclear applications are discussed[57] by the Superior Tube Co. For all practical purposes the problems of notch sensitivity, limited size range, difficulty in holding tolerances and concentricity, and comparative brittleness no longer exist. The catastrophic oxidation above 1500°F and weld brittleness are still somewhat a problem, but these can be alleviated to a large extent by the use of silicide coatings and brazing, respectively.

The vapor pressure of molybdenum over the temperature range 1867 to 2262°C was determined by investigators[58] at Pratt & Whitney.

An experimental program[59] was carried out by researchers at Battelle to improve the low-temperature ductility of tungsten through the combined use of dispersed oxides for grain-size control and groups VII and VIII metal additions for matrix softening. Separate binary-alloy studies showed that increasing amounts of finely dispersed thoria or zirconia and critical amounts of rhenium, osmium, and iridium were effective in reducing significantly the ductile-to-brittle bend-transition temperature of tungsten, as well as in increasing its recrystallization temperature and decreasing the recrystallized grain size. The beneficial effects of each of these additions in binary combinations appeared to be additive in ternary combinations. Thus combined additions of 2 to 8 vol.% thoria with 5 wt.% rhenium, 0.87 wt.% osmium, or 0.30 wt.% iridium were effective in lowering the transition temperature of tungsten from 200 to 75°C, increasing its recrystallization temperature from 1600 to 1800°C, and decreasing its recrystallized grain size from 1175 to 6800 grains/mm^2.

The Lewis Research Center has conducted a study[60] to determine the effects of the interstitial impurities oxygen and carbon on the mechanical properties of polycrystalline and high-purity single-crystal tungsten. Additions of both oxygen and carbon to the polycrystalline material produced a marked increase in the ductile-to-brittle transition temperature; a smaller increase was noted in the single-crystal tungsten, as shown by tensile tests. Addition of oxygen to the polycrystalline tungsten lowered both the ultimate and yield strengths but had no measurable effect on the strength properties of the single-crystal specimens. Carbon additions to both single-crystal and polycrystalline material did not affect the ultimate strength but did result in a large increase in the yield strength. The results suggest that oxygen embrittlement in tungsten is caused by grain-boundary segregation, whereas carbon embrittlement is the consequence of an interaction between the carbon atoms and the dislocations within the tungsten lattice.

The strength properties of tungsten-base alloys containing TaC, Ta_2O_5, ThO_2, and carbon (carburized) were investigated[61] up to 1650°C at Westinghouse. Carbides and oxides stabilize the worked (stress relieved) structure to higher temperatures, and strengthening appears to be due primarily to work hardening. In the recrystallized condition, the alloys, in general, are not stronger than unalloyed tungsten.

Researchers at the Massachusetts Institute of Technology (MIT) have determined[62] the tungsten-palladium phase diagram by X-ray and metallographic techniques at temperatures above 1100°C. Tungsten dissolves a maximum of 5 wt.% palladium at the peritectic temperature of 1815°C, and the solubility decreases to 1.5 wt.% at 1100°C. The palladium solid solution forms by the peritectic reaction of the tungsten and liquid phases at 1815°C and 22 wt.% tungsten. At 1100°C the solubility of tungsten in palladium is reduced to 2.15 wt.%. No intermediate phases were observed at temperatures above 1100°C.

Nuclear Metals has conducted a survey[63] of tungsten alloys containing approximately 25 wt.% rhenium. Physical and mechanical properties, phase relations, consolidation and fabrication, and the softening and recrystallization behavior are included.

NIOBIUM AND TANTALUM

Investigators[64] at Nuclear Metals have used the techniques of metallography, X-ray powder patterns, electrical resistance, and electron-microprobe analysis to obtain data on six binary and four ternary constitution diagrams of some refractory metals. The systems studied are niobium-ruthenium, niobium-iridium, niobium-rhodium, niobium-hafnium, molybdenum-iridium, tungsten-palladium, molybdenum-zirconium-titanium, tantalum-tungsten-zirconium, tungsten-molybdenum-osmium, and tungsten-rhenium-hafnium.

Workers[65] at MIT have uncovered new intermediate phases and characterized their cell

structure in systems of niobium or tantalum with rhodium, iridium, palladium, or platinum. On comparing the mean atomic volumes for each phase with those calculated from Vegard's straight-line rule, a strong contraction for AB and AB_3 type phases was found, especially $TaPt_2$ and $TaRh_2$, and Nb_3Rh_5 was intermediate. The results support the concept that the determining factor in the stability of a given layer structure is the valence electron-to-atom ratio, resulting in two- or three-layer structures, but that small changes of this quantity and of the size factor, especially by off-stoichiometry or impurities, influence the layer type and produce more complex close-packed intermediate structures.

A homogeneous phase transformation from body-centered cubic niobium to a face-centered cubic lattice, probably NbO but also containing carbon and nitrogen, was observed[66] by researchers at the University of California. They utilized transmission electron microscopy both in thin foils and in bulk specimens containing about 0.5 at.% interstitials, after suitable aging treatments. The transformation proceeds in the following sequence: (1) ordering in niobium, (2) formation of a precipitate in alternate prisms of niobium and NbO, (3) growth to perfect NbO structure, and (4) recrystallization of NbO above 1000°C. The habit planes are four variants of {1 0 1}, but only those inclined at less than 90° to the foil surface operate. In bulk specimens the habit planes are observed to be {0 2 1}, which is in accord with the crystallographic theory for martensitic transformations. The difference between bulk and thin-film behavior is attributed to the lack of constraints in the latter, where the strains appear to be accommodated elastically.

Cellular precipitation of $NbCr_2$ in niobium-chromium alloys was studied at Pratt & Whitney[67] by optical and electron metallography and by microhardness measurements. Observation of precipitation along the cell-matrix interface supports a new extension to the original theory of cellular precipitation; i.e., when the process occurs at high temperatures (≥0.6 of the absolute liquidus temperature), cell growth is controlled by lattice diffusion instead of by short-circuit boundary diffusion. Cell growth is not found to be inhibited by small amounts of general precipitation or large amounts of Widmanstätten precipitation of $NbCr_2$ within grains, but subboundaries on which precipitation has occurred can stop all growth. Cell hardness was higher in water-quenched than in argon-quenched specimens.

German investigators[68] have measured the specific heat, the Debye temperature, the paramagnetic susceptibility, and the superconducting transition temperature in the niobium-rich region of the niobium-ruthenium system. Structural investigations proved that the single-phase region extends up to at least 45 at.% ruthenium at low temperatures, with a gradually increasing tetragonal deformation above 37 at.% ruthenium. The results revealed a flat minimum in the density of states near a concentration of 5.7 valence electrons per atom. Comparison of specific heat and susceptibility data lent support to the suggestion that a van Vleck paramagnetic contribution might be important in this and related alloy systems. The superconducting transition temperature for pure niobium was 9.49°K.

The isothermal section of the tantalum-titanium-zirconium-oxygen system at 1500°C was investigated[69] at the University of Cincinnati, using X-ray diffraction and metallographic techniques. Up to 71.4 at.% oxygen, the system contains nine four-phase regions. Isopleths were constructed at a number of oxygen concentrations.

The residual gases in a high-vacuum system at pressures between 10^{-6} and 10^{-8} torr are mainly H_2O, CO, CH_4, CO_2, hydrogen, and nitrogen. Investigators at Oak Ridge have found[70] that, when refractory-metal alloys are heated to between 600 and 1200°C for periods up to 1000 hr, the alloys suffer significant oxygen contamination. Although some carburization was also observed, a competing carbon-oxygen reaction became significant at the higher temperatures and caused severe decarburization in alloys depending on carbon for strength. Hydrogen contamination was not encountered, and nitrogen contamination was negligible. Alloying elements such as titanium, zirconium, and hafnium, which form oxides thermodynamically more stable than the base metals niobium, tantalum, and molybdenum, promote oxygen contamination. Wrapping an alloy with refractory-metal envelopes was effective in stabilizing the carbon content of the alloy as well as in reducing the oxygen contamination. Intentional low-pressure gas additions of CH_4 at 6×10^{-7} torr effectively lowered the oxygen contamination of TZM and niobium. The studies indicated

that higher pressures of CH_4 may also be effective in preventing decarburization.

Miscellaneous

One of the current problems in the theory of annealing of metals concerns the origin and nature of nuclei for recrystallization of cold-worked metals. A study[71] is under way at Oak Ridge concerning the annealing behavior of niobium single crystals containing deformation twins induced by mechanical working. These twins are thin lamellae that are related in structure to the bulk crystal by a plane of symmetry called the coherent twin boundary. At 1000°C the noncoherent twin boundaries were mobile, and the twins could expand or contract through the migration of these boundaries. The coherent twin boundaries were much less mobile and did not move in 30 days at 1000°C. The niobium recrystallized at this temperature but only at twin intersections. The new grains had fixed orientation relations to the intersecting twins and the matrix. The growth rates of these grains were very anisotropic, and the direction of fastest growth was parallel to the primary twin system.

Plenum Press has recently published a handbook[72] on high-temperature materials as an authorized translation from the Russian original. Information is included on stoichiometry and crystal chemistry and on thermal, thermodynamic, electrical, magnetic, optical, mechanical, chemical, and refractory properties.

(N. M. Griesenauer)

Diffusion Studies

Additional work on refractory-metal systems has been completed by Textron, Inc.,[73] in a study of interdiffusion coefficients for W-Ru, W-Ir, W-Rh, W-Pt, Nb-Cr, and Mo-$MoSi_2$. A detailed analysis was made on composition-penetration data in the temperature range 900 to 2100°C, and interdiffusion coefficients were computed.

As an additional contribution to the diffusion data of body-centered cubic metals, Oak Ridge has completed studies[42] of the self-diffusion of niobium. The surfaces of cylindrical specimens were coated with radioactive ^{95}Nb by vapor deposition, and penetration was measured by gamma spectroscopy. Diffusion coefficients varied by 9 orders of magnitude over the temperature range 950 to 2400°C. For diffusion anneals at temperatures above 500°C, standard sectioning techniques were used. For lower temperature work an anodizing method was developed which permitted the measurement of diffusion coefficients as low as 10^{-20} cm^2/sec. The Arrhenius type representation of self-diffusion coefficient was given as $D_{Nb} = 1.7 \exp(-97{,}600/RT)$ cm^2/sec.

Diffusion of intermetallic compounds was studied[74] by use of the diffusion-anneal reaction of molybdenum in beryllium vapors at 900 and 1250°C. Beryllide phases were observed on the molybdenum faces as layers of lower-to-higher beryllides, and the $MoBe_{22}$ layer was the predominant diffusing layer in continuous molybdenum beryllization.

A Ukranian paper[75] reports on the temperature dependence of the diffusion of iron in high-purity zirconium. The Arrhenius type equations for diffusion were $D_{\alpha Zr} = 2.5 \times 10^{-2} \exp(-48{,}000/RT)$ cm^2/sec, and $D_{\beta Zr} = 4 \times 10^{-2} \exp(-30{,}000/RT)$ cm^2/sec. The author also observed that iron-atom mobility in the zirconium lattice was greater than in tantalum or tin.

Workers at Lawrence Radiation Laboratory[76] have determined the diffusion coefficients and corresponding activation energies for silver, nickel, uranium, thorium, and radium in various types of graphite as a function of temperature. They suggest that discrepancies with previously reported values stem from the relative insolubilities of metals in graphite. Experimental evidence is presented indicating that interstitial diffusion, substitutional diffusion, and pore diffusion are negligible, and it is concluded that the predominant mechanism is grain-boundary and subgrain-boundary diffusion. Arrhenius parameters determined are listed in Table IV-2. (A. N. Ashurst)

Table IV-2 ARRHENIUS PARAMETERS FOR DIFFUSION OF SEVERAL METALS IN GRAPHITES[76]

Metal	Graphite	Direction	D_0, cm^2/sec	Q, kcal/mole
Silver	Pyrolytic	⟨a⟩	9.28×10^3	64,300
Nickel	Pyrolytic	⟨a⟩	1.02×10^2	47,200
Nickel	Pyrolytic	⟨c⟩	2.2	53,300
Uranium	Pyrolytic	⟨a⟩	6.67×10^3	115,000
Uranium	Pyrolytic	⟨c⟩	3.85×10^2	129,500
Uranium	ZTA		6.22×10^5	135,100
Uranium	S-700		9.29×10^5	136,600
Thorium	Pyrolytic	⟨a⟩	1.33×10^5	145,400
Thorium	Pyrolytic	⟨c⟩	2.48	114,700
Radium	Pyrolytic	⟨a⟩	1.18×10^4	99,400

Ceramic Technology

Table IV-3 shows thermal-expansion coefficients obtained by Carborundum workers[77] for the monocarbides of niobium, tantalum, and zirconium and for several binary carbides. Plots of total elongation vs. temperature for the monocarbides show distinct local inflections (decrease in slope, followed by an increase) in the neighborhood of 2000°C. These, and analogous inversions observed for the binary carbides, agree with similar anomalies reported from observations of other properties.

From measurements of heat content of niobium carbide, workers at the Bureau of Mines[78] derived the following relations:

For NbC (α), in the temperature range 298 to 670°K,

$$H - H_{298.15} = 10.98T + 0.69 \times 10^{-3}T^2 + 2.32 \times 10^{5}T^{-1} - 4113 \text{ cal/mole}$$

from which

$$C_p = 10.98 + 1.38 \times 10^{-3}T - 2.32 \times 10^{5}T^{-2} \text{ cal/(mole)(°K)}$$

For NbC (β), in the temperature range 670 to 2000°K,

$$H - H_{298.15} = 11.28T + 0.59 \times 10^{-3}T^2 + 2.50 \times 10^{5}T^{-1} - 4256 \text{ cal/mole}$$

from which

$$C_p = 11.28 + 1.18 \times 10^{-3}T - 2.50 \times 10^{5}T^{-2} \text{ cal/(mole)(°K)}$$

The above data can be used to compute the enthalpy and free energy of formation of NbC from niobium metal and graphite. These turn out to be quite insensitive to temperature over the range 298 to 2000°K, being

$$\Delta H \approx \Delta F \approx -33 \text{ kcal/mole}$$

A comprehensive program of thermodynamic and kinetic studies of zirconium and hafnium carbides and borides exposed to high-temperature (to 3000°K) oxygen or halogen-containing atmospheres has been completed by A. D. Little.

Table IV-3 MEAN THERMAL-EXPANSION COEFFICIENTS FOR MONOCARBIDES[77]

Material	Density, % of theoretical	Sample axis relative to hot-pressing direction	Peak temp., °C	Mean α, from 30°C to peak temp., 10^{-6}/°C
NbC	91.6	Perpendicular	1000	7.11
			1500	8.10
			2000	8.27
			2500	8.75
			2843	8.99
TaC	87.4	Perpendicular	1000	5.75
			1500	6.52
			2000	6.68
			2500	6.81
ZrC	89.3	Parallel	1000	6.91
			1500	9.15
			2000	9.77
			2390	10.34
8TaC·ZrC	95.9	Perpendicular	1000	6.03
			1500	6.63
			2000	6.75
			2330	7.02
4TaC·ZrC	89.9	Perpendicular	1000	5.57
			1500	6.19
			2000	6.50
			2475	6.59
TaC·ZrC	89.2	Parallel	1000	5.98
			1500	7.14
			2000	7.26
			2550	7.46
TaC·4ZrC	85.5	Parallel	1000	6.91
			1500	9.15
			2000	9.77
			2390	10.34

The final report[79] gives data obtained in 1963 and a review of the program from mid-1960. This program included preparation of borides and carbides; low-temperature heat-capacity measurements of HfB_2, HfC, and hafnium metal; estimation of entropies at 298°K for refractory diborides, nitrides, carbides, and oxides from high-temperature heat-content data; current status of heats of formation of the borides and carbides from oxygen and fluorine bomb calorimetry; and studies proving the feasibility of the "matrix isolation technique" for spectroscopy of high-temperature molecules through studies of the lithium halides. Status of electron-diffraction, equilibria, and heat-of-solution studies of the hafnium and zirconium halides is presented. Kinetic studies completed on the oxidation and fluorination of the hafnium and zirconium carbides and diborides are presented in detail. From a-c and d-c electrical-conductivity studies on tetragonal ZrO_2, a model of the defect structure is devised and oxygen diffusion in ZrO_2 is calculated.

The literature of group 4a, 5a, and 6a carbides and nitrides and the nitrides of thorium, uranium, and plutonium has been reviewed critically by Los Alamos.[80] The properties discussed include preparation, phase relation, lattice parameter and structure, appearance, chemical stability, hardness, resistivity, superconductivity, thermodynamic properties, and vaporization. Particular attention has been paid to methods by which the materials can be made oxygen-free and (for the carbides) nitrogen-free.

On the basis of X-ray diffraction and differential-thermal-analysis results, the A. O. Smith Corporation has proposed[81] a phase diagram for the Nb_2O_5-WO_3 system. Up to 33 mole % WO_3 dissolves in Nb_2O_5, but only a slight amount of Nb_2O_5 will dissolve in WO_3. The existence of the $Nb_2O_5 \cdot 3WO_3$ compound with a tetragonal unit cell was confirmed. In addition, two new compounds, $3Nb_2O_5 \cdot 2WO_3$ above 1100°C and $Nb_2O_5 \cdot WO_3$ at 1100°C and below, were postulated.

Two mechanisms were used by Ames and Gregor[82] to prepare thin films of molybdenum oxide: (1) direct thermal evaporation of solid MoO_3 pellets and (2) sublimation from a hot molybdenum tube through which oxygen was passed. The films formed were 30 to 10,000 A thick and had electrical resistivities ranging from 10^6 to 10^8 ohms-cm.

Marquardt[83] has developed metal-reinforced ceramic-coating systems that withstand temperatures in excess of 4000°F while providing thermal insulation for the supporting substructure. The coatings are applied by a vibratory casting technique in thicknesses ranging from 0.3 to 0.75 in. The report of this work includes an extensive bibliography of reinforced refractory ceramic systems and allied subjects.

Electrohydraulic crushing of refractory materials, of particular interest for remote crushing of radioactive material, has been improved by Harwell.[84] The energy consumption, still 5 to 10 times higher than for mechanical crushing, is many times lower than previously quoted for electrohydraulic crushers. The comminution is accomplished by high-intensity shock waves generated by underwater spark discharge. Materials such as marble, sintered urania, glass, high-density alumina, and silicon carbide have been effectively crushed.

Tensile-strength testing of ceramics, a troublesome technical area, has been accomplished at Stanford Research[85] with coefficients of variation of less than 7.6%, and in the majority of sets of data, of less than 5%. These tests were made using alumina as the test material, in an apparatus in which hydrostatic pressure is applied internally to a cylindrical test specimen. The method seems sensitive enough to be used as a more reliable measure of process variations in a materials-development program than are other test techniques. (D. J. Bowers)

References

1. Westinghouse Electric Corp., Bettis Atomic Power Laboratory, Pressurized Water Reactor (PWR) Project. Technical Progress Report, April 24–July 23, 1964, USAEC Report WAPD-MRP-109.
2. Hanford Atomic Products Operation, Metallurgy Research Operation. Quarterly Progress Report, March 1964, USAEC Report HW-81269, Apr. 15, 1964.
3. D. L. Douglass, Oxidation Mechanism of Zirconium and Its Alloys. II. Oxide Plasticity, USAEC Report GEAP-4473 (EURAEC-1078), General Electric Company, Vallecitos Atomic Laboratory, Feb. 20, 1964.
4. M. E. Bergstresser, Aluminum Corrosion in Subcritical and Zero Power Critical Reactors, USAEC Report DP-911, Savannah River Laboratory, July 1964.
5. Argonne National Laboratory, Chemical Engineering Division Semiannual Report, July–December 1963, USAEC Report ANL-6800, May 1964.
6. M. Warzee, J. Hennaut, M. Maurice, J. Waty, and P. Berge, Influence of Surface Treatment on the Corrosion of Carbon and Stainless Steels in High-Temperature Water and Steam. Part 1, USAEC Report EURAEC-1038, Société d'Études, de Recherches et d'Applications pour l'Industrie, and European Atomic Energy Community, Apr. 10, 1964.
7. Société d'Études, de Recherches et d'Applications pour l'Industrie, Studies of Steel Corrosion in High-Temperature Water and Steam, Quarterly Report No. 7, January 1–March 31, 1964, USAEC Report EURAEC-1047, Apr. 30, 1964.
8. L. D. Perrigo, Oxide Tenacity on Alloys Exposed to Reactor Coolants, USAEC Report HW-79811, Hanford Atomic Products Operation, December 1963.
9. S. P. Rideout, Effects of pH on Stress Corrosion Cracking of 18-8 Stainless Steel in Low-Chloride Water, USAEC Report CONF-492-2, Savannah River Laboratory, Mar. 5, 1964.
10. D. D. Whyte, A Long Term Corrosion Test of Reactor Structural Materials in a Chemical Shim Solution, USAEC Report WCAP-3737, Westinghouse Electric Corp., Atomic Power Division, March 1964.
11. H. M. Busey and R. H. Perkins, Corrosion of Stainless Steels by Water Boiler Reactor Fuels, USAEC Report LA-3101, Los Alamos Scientific Laboratory, June 16, 1964.

12. R. J. Sullivan, R. B. Cassidy, H. Mandel, and R. T. Keen, Postirradiation Examination of Surface Film Formation on OMRE Driver Element No. 219, USAEC Report NAA-SR-9637, Atomics International, Aug. 1, 1964.
13. Hanford Atomic Products Operation, Metallurgy Development Operation. Quarterly Progress Report, October–December 1963, USAEC Report HW-80112, Jan. 20, 1964. (Classified)
14. The Compatibility of Chromium-Alumimum Steels With High-Pressure CO_2 at Intermediate Temperatures, French Report CEA-R-2423, April 1964.
15. J. Morel and W. W. Bradley, Effect of Nuclear Irradiation on Oxidation of Iron and Copper, USAEC Report TID-20541, Massachusetts Institute of Technology, Mar. 27, 1964.
16. W. L. Pearl, E. G. Brush, G. G. Gaul, and G. P. Wozadlo, General Corrosion of Incoloy-800 in Simulated Superheat Reactor Environment, USAEC Report GEAP-4495, General Electric Company, Vallecitos Atomic Laboratory, March 1964.
17. F. W. Albaugh, Reactor and Fuels Laboratory Monthly Report, July 1964, USAEC Report HW-83445A, Hanford Atomic Products Operation, Aug. 14, 1964. (Classified)
18. S. T. Wlodek, Vanadium-Niobium Alloys, U. S. Patent 3,136,631 (to Union Carbide Corp.), June 9, 1964.
19. R. F. Voitovich and V. A. Lavrenko, Oxidation of Tungsten-Rhenium Alloys, *Metalloved. i Term. Obrabotka Metal.*, 4: 50-51 (1964).
20. D. E. Rosner and H. D. Allendorf, Kinetics and Aerodynamic Aspects of the Oxidation of Metals by Partially Dissociated Oxygen, Report TN-61, Aerochem Research Laboratories, Inc., May 1964.
21. W. E. Berry and J. A. DeMastry, Corrosion of Niobium-Base Alloys in Steam at 540 and 650°C, USAEC Report BMI-X-286, Battelle Memorial Institute, May 1964.
22. M. Marnoch, Research on High-Temperature Oxidation Resistant Hafnium-Tantalum Systems, First Quarterly Report Covering Period May 1–July 31, 1964, Report 24,142, The Marquardt Corp., August 1964.
23. National Aeronautics and Space Administration, Proceedings of the NASA-AEC Liquid-Metals Corrosion Meeting Held at Lewis Research Center, Cleveland, Ohio, October 2–3, 1963, Volume I, USAEC Report NASA-SP-41, April 1964.
24. National Aeronautics and Space Administration, Proceedings of the NASA-AEC Liquid-Metals Corrosion Meeting Held at Lewis Research Center, Cleveland, Ohio, October 2–3, 1963, Volume II, USAEC Report NASA-SP-42, April 1964. (Classified)
25. R. C. Andrews and K. R. Barker, Effect of High-Temperature Sodium on Austenitic and Ferritic Steels. Physical Properties of Materials. Topical Report No. 3. Results of Physical Property Tests of 2¼ Cr–1 Mo Steel Specimens in Sodium with High and Low Oxygen, Air and Helium Environments at 1100 F, USAEC Report MSAR-64-81, MSA Research Corp., July 1964.
26. J. F. Nejedlik and E. J. Vargo, Kinetics of Corrosion in a Two-Phase Mercury System, Report ER-5694 (CONF-492-3), Thompson Ramo Wooldridge, Inc., Jan. 1, 1964.
27. Los Alamos Scientific Laboratory, Plutonium Reactor Fuel Development. Quarterly Status Report for Period Ending May 20, 1964, USAEC Report LAMS-3096, June 24, 1964.
28. R. S. Neymark, Performance of Structural Materials Exposed to the Coolant in the OMRE, USAEC Report NAA-SR-9796, Atomics International, Aug. 1, 1964.
29. Argonne National Laboratory, Reactor Development Program. Progress Report, June 1964, USAEC Report ANL-6912, July 21, 1964.
30. T. A. Kovacina and R. R. Miller, The Solubility of Columbium–1 Wt.% Zirconium in Sodium by Activation Analyses, Report NRL-6051, Naval Research Laboratory, Mar. 20, 1964.
31. J. D. Mottley, Sodium Mass Transfer. VIII. Corrosion of Stainless Steel in Isothermal Regions of a Flowing Sodium System, USAEC Report GEAP-4313, General Electric Company, Vallecitos Atomic Laboratory, Febryary 1964.
32. D. L. Johnson, Phase Equilibria-Free Energy Relationships in Liquid Sodium Systems, USAEC Report NAA-SR-8381, Atomics International, Apr. 15, 1964.
33. W. T. Chandler and N. J. Hoffman, The Role of Oxygen on Attack of Refractory Metals by Alkali Metals, Report CONF-373-5, paper presented at National Refractory Metals Symposium, Los Angeles, California, December 9–10, 1963.
34. L. R. Kelman and S. Greenberg (Eds.), *Nuclear Metallurgy*, Volume IX of *IMD Special Report Series No. 12, Materials for Sodium-Cooled Reactors*, papers presented at ANS 1963 Winter Meeting, Nov. 19, 1963, The Metallurgical Society, American Institute of Mining, Metallurgical, and Petroleum Engineers, New York, 1963.
35. Commissariat à l'Énergie Atomique, Reactor Casing Steels. Irradiation of Steel Specimens in EL3 at Different Temperatures, and Post-Irradiation Tests, Special Report No. 2, USAEC Report EURAEC-816 (translated from the French), June 30, 1963.
36. J. R. Hawthorne and L. E. Steele, In-Reactor Studies of Low-Cycle Fatigue Properties of a Nuclear Pressure Vessel Steel, USAEC Report NRL-6127, Naval Research Laboratory, June 2, 1964.
37. E. Cibois, J. Lemaire, and M. Weisz, Contribution to the Study of Fast Neutron Irradiation Damage to Materials, *6e Colloq. Met.*, pp. 199-217, 1962.
38. Oak Ridge National Laboratory, Apr. 6, 1964. (Unpublished)
39. General Electric Company, Advanced Technology Services, High-Temperature Materials Program, Progress Report No. 37, Part A, USAEC Report GEMP-37A, July 31, 1964.
40. General Electric Company, Advanced Technology Services, High-Temperature Materials Program, Progress Report No. 39, Part A, USAEC Report GEMP-39A, Sept. 30, 1964.
41. M. R. Louthan, Jr., Destructive Evaluation of Irradiated Zircaloy Sheathing, USAEC Report DP-888, Savannah River Laboratory, May 1964.
42. Oak Ridge National Laboratory, Aug. 6, 1964. (Unpublished)
43. J. A. VanEcho and W. F. Simmons, Mechanical and Physical Properties of Three Superalloys—MAR-M200, MAR-M302, and MAR-M322, Report

DMIC-Memo-193, Battelle Memorial Institute, Defense Metals Information Center, May 6, 1964.
44. Oak Ridge National Laboratory, Molten-Salt Reactor Program. Semiannual Progress Report for Period Ending January 31, 1964, USAEC Report ORNL-3626, July 1964.
45. R. G. Hoagland and A. L. Bement, Jr., Fracture Studies of Zircaloy-2, USAEC Report HW-82631, Hanford Atomic Products Operation, June 4, 1964.
46. L. K. Walford, The Phase Diagram of the Aluminum-Molybdenum System, *Phil. Mag.*, 8(9): 513-516 (March 1964).
47. M. E. Drits, Z. A. Sviderskaya, and L. L. Rokhlin, Influence of Additional Alloying on the Properties of Alloys of the Mg-Nd System, *Fiz. Khim. Metody Issled. Vozdushn. Sredy, Vses. Tsentr. Nauchn.-Issled. Inst. Okhrany Truda*, 14: 120-129 1963.
48. E. S. Kadaner and A. A. Oreshkina, Investigation of the Recrystallization of Mg-Ce Alloys, *Fiz. Khim. Metody Issled. Vozdushn. Sredy, Vses. Tsentr. Nauchn.-Issled. Inst. Okhrany Truda*, 14: 130-138 (1963).
49. E. M. Savitskii, V. V. Baron, Yu. V. Efimov, and M. I. Bychkova, Interaction of Niobium and Vanadium with Magnesium, *Fiz. Khim. Metody Issled. Vozdushn. Sredy, Vses. Tsentr. Nauchn.-Issled. Inst. Okhrany Truda*, 14: 139-146 (1963).
50. H. E. McCoy, Jr., Influence of Several Metallurgical Variables on the Tensile Properties of Hastelloy N, USAEC Report ORNL-3661, Oak Ridge National Laboratory, August 1964.
51. W. M. Cain, C. C. Koch, J. L. Mihelich, and A. R. Troiano, Solute-Induced Embrittlement in Steel and Several Face-Centered Cubic Alloys, Report ARL-64-101, Case Institute of Technology, June 1964.
52. H. E. McCoy, Jr., Effects of Hydrogen on the High-Temperature Flow and Fracture Characteristics of Metals, USAEC Report ORNL-3600, Oak Ridge National Laboratory, June 1964.
53. M. Farrow, J. R. Caley, and J. A. Bardsley, The Metallurgical Stability of Four Vacuum-Melted Stainless Steels and Inconel, British Report TRG-Report-565, May 22, 1963.
54. K. Ogawa, Dislocation Structures in Molybdenum and Molybdenum-Rhenium Alloys, Thesis, University of Pennsylvania, 1963.
55. S. Z. Bakshtein, M. B. Bronfin, S. T. Kishkin, and V. A. Marichev, Internal Friction in Deformed Molybdenum and Its Alloys with Zirconium and Rhenium, *Soviet Phys.-Solid State (English Transl.)*, 5: 2253-2256 (May 1964).
56. W. H. Chang, Effect of Titanium and Zirconium on Microstructure and Tensile Properties of Carbide Strengthened Molybdenum Alloys, *Am. Soc. Metals, Trans. Quart.*, 57: 527-553 (June 1964).
57. L. C. Shakeen, Properties of Molybdenum. How Ductile is Molybdenum Tubing? *Metal Progr.*, 85(5): 112-114 (May 1964).
58. P. A. Vozzella, A. D. Miller, and M. A. DeCrescente, Vapor Pressure of Molybdenum, *J. Chem. Phys.*, 41: 589-590 (July 15, 1964).
59. J. L. Ratliff, D. J. Maykuth, H. R. Ogden, and R. I. Jaffee, Tungsten Sheet Alloys with Improved Low-Temperature Ductility, *Trans. Met. Soc. AIME*, 230: 490-500 (April 1964).
60. J. R. Stephens, Effects of Interstitial Impurities on the Low-Temperature Tensile Properties of Tungsten, Report NASA-TN-D-2287, National Aeronautics and Space Administration, Lewis Research Center, June 1964.
61. H. G. Sell, G. H. Keith, R. H. Schnitzel, and N. F. Cerulli, Physical Metallurgy of Tungsten and Tungsten-Base Alloys, Report WADD-TR-60-37 (Pt. IV), Westinghouse Electric Corp., May 1963.
62. W. K. Goetz and J. H. Brophy, A Constitution Diagram for the Tungsten-Palladium System, *J. Less-Common Metals*, 6: 345-353 (May 1964).
63. A. L. Geary, Fundamental and Applied Research and Development in Metallurgy. Survey of Tungsten Alloys Containing Approximately 25% Rhenium, USAEC Report NMI-1261, Nuclear Metals Division, Textron Inc., May 29, 1964.
64. V. Nerses, L. F. Pease, A. Taylor, et al., Refractory Metal Constitution Diagrams, Report WADD-TR-60-132(Pt. III), Nuclear Metals Division, Textron Inc., Massachusetts Institute of Technology, and Westinghouse Electric Corp., October 1963.
65. B. C. Giessen and N. J. Grant, New Intermediate Phases in Systems of Niobium or Tantalum with Rhodium, Iridium, Palladium, or Platinum, *Acta Cryst.*, 17: 615-616 (May 10, 1964).
66. L. I. Van Torne and G. Thomas, Phase Transformation in Niobium Involving Interstitials, *Acta Met.*, 12: 601-615 (May 1964).
67. J. S. Hirschhorn and R. A. Gregg, Cellular Precipitation in Niobium-Chromium Alloys, *J. Less-Common Metals*, 6: 333-344 (May 1964).
68. D. Bender, E. Bucher, and J. Mueller, Structure and Electronic Properties of Niobium-Ruthenium Alloys, *Physik Kondensierten Materie*, 1: 225-231 (1963).
69. M. Hoch and O. B. Butrymowicz, The Systems Tantalum-Titanium-Zirconium-Oxygen at 1500°C, *Trans. Met. Soc. AIME*, 230: 186-192 (February 1964).
70. H. Inouye, Contamination of Refractory Metals by Residual Gases in Vacuums Below 10^{-8} Torr, USAEC Report ORNL-3674, Oak Ridge National Laboratory, September 1964.
71. Oak Ridge National Laboratory, July 7, 1964. (Unpublished)
72. G. V. Samsonov, *Plenum Press Handbook of High Temperature Materials, No. 2 Properties Index*, Plenum Press, New York, 1964.
73. E. J. Rapperport, V. Nerses, and M. F. Smith, Diffusion in Refractory Metals, Report ML-TDR-64-61, Nuclear Metals Division of Textron Inc., March 1964.
74. N. N. Matyushenko, Diffusion Reaction in the Mo-Be System, *Izv. Akad. Nauk SSSR, Met. i Gorn. Delo*, 2: 167-171 (March–April 1964).
75. A. M. Blinkin and V. V. Vorobev, Diffusion of Iron in Zirconium, *Fiz. Zh.*, 9: 91-95 (January 1964).
76. J. R. Wolf, D. R. McKenzie, and R. J. Borg, The Diffusion of Nonvolatile Metallic Elements in Graphite, USAEC Report UCRL-7324, University of California Lawrence Radiation Laboratory, Apr. 29, 1964.
77. B. R. Miccioli and P. T. B. Shaffer, High Temperature Thermal Expansion Behavior of Refractory Materials. I. Selected Monocarbides and Binary Carbides, *J. Am. Ceram. Soc.*, 47: 351 356 (July 21, 1964).
78. L. B. Pankratz, W. W. Weller, and K. K. Kelley,

Thermodynamic Data for Columbium (Niobium) Carbide, Report BM-RI-6446, Bureau of Mines, Berkeley Thermodynamics Laboratory, September 1963.

79. L. A. McClaine (Ed.), Thermodynamic and Kinetic Studies for a Refractory Materials Program, Report ASD-TDR-62-204(Pt. III), Arthur D. Little, Inc., April 1964.
80. E. K. Storms, A Critical Review of Refractories, USAEC Report LA-2942, Los Alamos Scientific Laboratory, March 1964.
81. L. J. Fiegel, G. P. Mohanty, and J. H. Healy, Equilibrium Diagram of the System Nb_2O_5–WO_3, *J. Chem. Eng. Data*, 9: 365-369 (July 1964).
82. I. Ames and L. V. Gregor, Preparation and Properties of Thin Films of Molybdenum Oxide, *Electrochem. Technol.*, 2: 97-101 (March–April 1964).
83. C. Kalleys, Jr., S. Sklarew, and S. V. Castner, Application and Evaluation of Reinforced Refractory Ceramic Coatings, Report ML-TDR-64-81, Marquardt Corp., June 1964.
84. N. G. Maroudas and R. F. Taylor, Interim Report on the Electrohydraulic Crushing of Refractory Materials, British Report AERE-M-1261, August 1963.
85. R. Sedlacek, Tensile Strength of Brittle Materials, Report ML-TDR-64-49, Stanford Research Institute, March 1964.

Section V

Reactor Materials

Special Fabrication Techniques

Melting, Casting, and Fabrication

Fabrication techniques for more economical production of uranium and uranium-base fuel elements continue to be investigated at National Lead Co. of Ohio, Reactive Metals, Inc., and Nuclear Metals, Inc. National Lead reported[1] the results of studies conducted at Battelle Memorial Institute on the effects of small alloying additions on the rolling properties of uranium rods. These studies indicate that no rolling problems exist when 150 ppm of iron and 150 ppm of silicon are present in the uranium. Also, beta heat-treatments are effective in reducing the roll-separating forces when working these iron and silicon alloys, but are not beneficial when the uranium alloys contain aluminum and higher iron and silicon levels. Other studies conducted by National Lead have concerned themselves with improving operations for cleaning up the cast billets prior to extrusion. The latest technique investigated for scalping is a process known as "flo-peeling." If a machine made by Lodge and Shipley for flo-peeling at feed rates as high as 30 in./min Utilizing a machine made by The Lodge & Shipley Co. for flo-peeling at feed rates as high as 30 in./min. workers can produce billets with acceptable size variations and good surface finishes. As a result of tool-wheel rotation during processing, excellent tool life is achieved.

By electrochemical machining,[2] workers broached a 2-in.-diameter hole in a $7\frac{3}{8}$-in.-OD by $20\frac{5}{8}$-in.-long solid-uranium extrusion billet with an electrode penetration rate of $\frac{1}{10}$ in./min and a metal loss of only 3%. The surface of the hole was extremely smooth, and it had a diameter variation of only 0.002 to 0.005 in. Recent extrusion studies on billets of this size were directed toward reducing the grain coarsening and high extrusion pressures that were encountered as a consequence of the large billet diameter and length. It was found that finer grains can be obtained by extruding at lower temperatures, but this, in turn, limits the reduction ratio. It was also concluded that the ram speed has a greater effect on the extrusion pressure than does the temperature, but ram speed has little effect on coarseness of grains.

Nuclear Metals workers[3,4] found that at 800°C a splat-cooled uranium–0.2 wt.% beryllium alloy is about 10 times as hard as unalloyed uranium and that the hardness of the material does not change appreciably after it is heat-treated at 400, 500, or 600°C for times up to 100 hr. Uranium-base alloys containing beryllium, beryllium-carbon, or carbon and Zircaloy-2–1.14 wt.% beryllium have been produced and extruded to bar stock.

Experiments were made at Argonne[5,6] to ascertain the feasibility of centrifugally casting the uranium–25 wt.% plutonium–1.5 wt.% iron alloy into stainless-steel jackets. Silver foil was placed around the stainless steel, and split copper molds were employed as heat sinks surrounding the jackets.

An examination of the cast alloy revealed no reaction between the stainless-steel jackets and the cast core. The core had a density of approximately 95% of theoretical. Other casting studies, with the use of a uranium–20 wt.% plutonium-base alloy and with additions of 1.25, 1.87, or 2.5 wt.% molybdenum, 1.33 wt.% vanadium, or 1.27 wt.% titanium, are in progress. These alloys were cast into multiple-cavity graphite molds washed with yttria. The surface quality of the castings appeared to be a function of the mold temperature. The alloys exhibited shrinkage coefficients on the order of 1.7 to 2.2%, and they were easily machined.

Vanadium-titanium alloys containing 10 to 20 wt.% titanium are promising materials for fast reactor fuel jackets. Consumable-electrode arc melting of electrodes formed by electron-beam melting is being used to produce the materials for further evaluation. Electron-beam evaporation is being employed at Hanford[7] to produce gold-coated copper to be used in diffusion and irradiation experiments. At a power level of 7.5 kw for 45 min, uniform films 0.0003 in. thick were deposited on copper samples in a vacuum of 1×10^{-6} torr with the substrate 10 in. from the source.

At Nuclear Metals (Refs. 3, 4, 8, and 9), the successful extrusion of a tungsten sleeve with a 2.50-in. outside diameter and a 0.25-in. wall thickness to a $\frac{5}{8}$-in.-OD tube has been accomplished. The extrusion of tungsten tube shells to the stock size of 0.375 in. in outside diameter by 0.030 in. in wall thickness has been improved considerably by using more reliable heating techniques. Drawing and sinking studies on the extruded materials showed that problems of cracking in the swaged points can be decreased by the use of TZM alloy instead of steel for the auxiliary points inserted into the swaged ends. A drawing temperature of 580°C was found to be superior to the 510°C temperature for drawing tungsten. Tungsten–25 wt.% rhenium tubing coextruded at temperatures of 1500 to 2000°C has been drawn by multiple small reductions per pass to a cumulative reduction approaching 40%. The force required to sink the tungsten–25 wt.% rhenium alloy appears to be two to three times greater than that required to sink pure tungsten.

The Bureau of Mines[10] is also investigating the preparation of tungsten–25 wt.% rhenium alloys. Initial studies were conducted with the use of small button melts. These studies indicated that an overcharge of 10 wt.% rhenium would be required to obtain the desired composition in the final alloy. However, buttons made by consumable melting of electrodes prepared by compacting and sintering powder blends show the correct rhenium content without overcharge. Recent efforts were directed toward the production of hollow cylindrical tubes by vertical-axis spin casting. Two spun castings were extruded at Nuclear Metals at a ratio of 16:1 at 1600°C. Microstructures of these castings show a quantity of second-phase material, and chemical analyses indicate a high carbon content. It is believed that the second phase is carbide rather than sigma phase.

Tungsten-base alloys containing 2 wt.% thoria or 15 wt.% molybdenum are being processed at Westinghouse.[11] The alloys containing thoria were produced by General Electric and exhibited a density of 93.9 to 94.3% of theoretical prior to extrusion. Extrusion was accomplished at 4000°F, and it resulted in a completely cold-worked structure with no evidence of recrystallization. The tungsten–15 wt.% molybdenum ingots were produced by centrifugal-casting techniques at Oremet. The 2.940- and 2.970-in.-diameter by 4.48- to 5.05-in.-long castings exhibited centerline shrinkage believed due to inadequate mold feeding. Preliminary examinations indicate that this porosity healed during extrusion. (N. E. Daniel)

Cladding

Rolling, Swaging, and Coextrusion

Investigators at Du Pont[12] have studied the fabrication of powder-compacted slugs containing 40 wt.% UO_2 or ThO_2 dispersed in a matrix of aluminum. The assembled billets were coextruded at 450°C at a ram speed of 3.5 in./min. An aluminum sheath was employed to produce the clad slug. The extrusion container was swabbed with a mixture of powdered lead and oil prior to loading each billet. After extrusion these lubricants were removed by an etch, followed by rinses in dilute nitric acid and water. Evaluation of the cores revealed a consistently high density and a uniform cladding thickness. A strong, continuous bond was obtained between the core and the cladding. Adequate blending of the powders before compacting gave a uniform dispersion of the oxide throughout the aluminum matrix.

In the U.K.[13] investigators have studied the fabrication by roll bonding of uranium-aluminum fuel plates clad with aluminum and dispersions of UO_2 in stainless steel clad with stainless steel. The "picture-frame" technique was employed in which separately prepared fuel cores are placed into frames, and these are then sandwiched between cover plates to form "fuel packs." The uranium-aluminum fuel plates were soaked at 580 to 600°C and hot rolled to a 60% total deformation. The UO_2–stainless steel was heated to 1200°C and then hot rolled to a 70% total reduction in thickness. Rolling speeds

were 90 to 100 ft/min for the aluminum-uranium and 60 to 70 ft/min for the UO_2–stainless steel. Optimum bond quality was obtained at these rolling speeds, temperatures, and reductions. The quality of the bonds was evaluated by metallurgical examination, by tensile testing, by thermal cycling, and by a shear test. The authors concluded that, to obtain optimum bonding, it is necessary to roll bond at temperatures above the recrystallization temperature of the material being bonded.

A U. S. patent[14] has been issued for roll bonding of uranium or zirconium or their alloys to ferrous metals by using an interposed molybdenum barrier. The assembly is encased in an evacuated and sealed container, forged at 600 to 1000°C to half the original thickness, and soaked at the same temperature for 2 hr. The heated assembly is then cross rolled to 20% of the original thickness, again soaked at temperature, and cooled. The container is then removed from the bonded product.

(R. J. Diersing)

Pressure Bonding

The solid-state bonding of refractory metals by use of a vacuum hot-pressing technique was investigated.[15] Major emphasis was placed on the joining of sheet materials of a molybdenum–0.5 wt.% titanium alloy and tungsten sheet with 0.001-in. foils of nickel, titanium, niobium, and tantalum. A brief study of the effects of pressure demonstrated that 10,000 psi yielded the desired results. With this pressure and with bonding times of 20 min, the following temperatures were established for the various couples studied:

Sheet material	Foil	Temp., °F
Molybdenum–0.5 wt.% titanium	Titanium	1680
Molybdenum–0.5 wt.% titanium	Nickel	1700
Molybdenum	Niobium	1840
Tungsten	Nickel	1700
Tungsten	Titanium	1700
Tungsten	Niobium	1700

The effects of postbonding heat-treatments were also investigated to provide data on diffusion and potential for high-temperature service. Molybdenum couples were heat-treated for 30, 50, and 78 hr at 2050°F, resulting in the formation of new phases and thermal cracking on cooling. Tungsten couples were heated for 24 and 48 hr at 2100°F with no apparent recrystallization or grain growth. On the basis of these results, titanium and niobium were recommended as interface materials for bonding tungsten and molybdenum assemblies.

The use of pressure at elevated temperature has been presented[16] as a method for joining ceramics to metals. This approach, which can eliminate the need for intermediate joining aids, produces an infiltrated interface. Under the combined action of temperature and pressure, the metal is extruded into the surface irregularities of the ceramic, and the joint may be further enhanced by diffusion bonding or chemical bonding. Bonding of alumina directly to chromium under conditions of 10,000-psi pressure and 2200°F is described. The use of pressure bonding to consolidate graded cermet structures in joining ceramics to metals is also noted, with a thoria-tungsten joint cited as an example.

(S. W. Porembka)

Nonelectrolytic Chemical-Plating Techniques

The use of chemical vapor deposition to prepare both metallic and nonmetallic materials in quantity and in useful shapes is reviewed here. Overlay and diffusion coatings for protective applications also are discussed below.

A research project is under way[17] to evaluate chemical vapor deposition for use in commercial plating applications. Evidence of further interest in chemical vapor deposition, based on metal-organic source materials, was contained in a paper[18] presented before the New York Academy of Science. A Russian patent[19] describes the design of equipment for the refining of metals by the iodide process.

Methods of depositing niobium and tantalum from the vapor phase were reviewed.[20] Vapor forming of useful shapes continues to hold the interest of many workers. The metal tungsten[21,22] and its alloys with rhenium[23] are currently under investigation. Free standing shapes, such as rocket nozzles and tubing, formed by chemical vapor deposition are being evaluated. The vapor-deposited, bulk nonmetallic material of greatest interest[24] is pyrolytic graphite. As in the case of tungsten, vapor-formed shapes of pyrolytic graphite are feasible and are of considerable commercial potential.[25–27] Fluidized-bed chemical vapor

deposition is employed as a means of preparing high-purity titanium dioxide.[28]

Overlay coatings of tungsten are of interest as high-temperature claddings for nuclear fuel elements.[29] A successful procedure was developed for the deposition of a coherent electroless nickel coating on an aluminum (6061 alloy) surface.[30] Pyrolytic carbon coatings can be used for sealing[31,32] and joining[31] objects made of carbon. The results were reported[33] of a Russian study on the deposition of titanium carbide coatings formed on self-resistance-heated refractory-metal substrates.

As has been the case for a number of years, much effort is still going into the development of diffusion coatings, for the most part applied by pack-cementation methods, for the protection of various refractory metals and alloys against high-temperature oxidation. New insight on the mechanism of silicide-coating formation and the thermodynamics of the coating systems employed is being developed.[34] Work on the development of protective coatings for the following refractory-metal substrates was reported: niobium–10 wt.% tungsten–1 wt.% zirconium,[35] molybdenum-base alloys,[36] 90 wt.% tantalum–10 wt.% tungsten and tantalum–30 wt.% niobium–7.5 wt.% vanadium alloys,[37] and vanadium–60 wt.% niobium–1 wt.% titanium alloy.[38] Fluidized-bed chemical vapor deposition has been used to successfully repair damaged silicide-coated parts.[39] Russian investigators[40] have studied the pack boronizing of tungsten, molybdenum, niobium, tantalum, and titanium substrates. (E. M. Sherwood)

Metals Joining

Welding

The gas tungsten-arc electron-beam spot-welding characteristics, the postweld aging treatment, and the effect of protective coatings on niobium alloy D-43 were the subjects of a recent report by Gerken.[41] The bend ductility (45° transition temperature) was reduced significantly by the fusion processes. Gas tungsten-arc and electron-beam welding raised the transition temperature from −320°F to −140°F and to −200°F, respectively. The application of a protective coating increased this temperature further. Normal aging treatments for D-43 also raised the transition temperature, but it was lowered again by overaging.

General Electric[42] investigators have published the results of a study of the weld stability in niobium alloys D-43 and B-66. Variables such as welding speed, voltage, and current were studied to determine their effects on interdendritic spacing because of its relation to bend ductility and aging kinetics. It was found that, as the interdendritic spacing increased with decreased welding speed, the metallurgical reactions occurring between 1400 and 2600°F became sluggish, and the ductile-to-brittle transition temperature increased. The interstitial elements, nitrogen and oxygen, had a similar effect. Increased nitrogen content drastically increased the bend ductile-to-brittle transition temperature and the sluggishness of aging reactions. Oxygen-content increases had a like, but lesser, effect.

Brazing

Investigators at Northrop[43] have reported some success in the development of brazing alloys for molybdenum which can be used at relatively low temperatures but which have high remelt temperatures. They are using the diffusion-sink (addition of pure metal powders to basic brazing alloy) technique. Molybdenum alloy, TZM, tee and lap joints brazed at 2300°F with a titanium–25 wt.% chromium–13 wt.% nickel alloy remelted above 3100°F. Lap-joint strengths were about 300 psi at 3000°F, and the molybdenum retained its ductility. The tantalum–10 wt.% tungsten alloy is being brazed by the same technique, but with less success. Pure titanium and titanium–30 wt.% vanadium offer the most promise for use on the tantalum-tungsten alloy. There are indications in this study that no advantage is gained by the diffusion-sink technique. The base metal alone acts to furnish the material that raises the remelt temperature. (R. M. Evans)

Nondestructive Testing

Ultrasonic Techniques

Workers at Hanford[44] claim to measure accurately, by means of an ultrasonic tester designated UT-2C, the grain size of uranium cores for use as reactor fuel elements. The tester works on the familiar ultrasonic attenuation principle; so the readout voltage is inversely proportional to the grain size. Measurements

are made before cladding. The instrument is calibrated by means of a set of standard fuel cores. The accuracy of the UT-2C is good if certain normal precautions are observed. For instance, the positioning of the transmitting and receiving transducers with respect to each other and to the specimen is critical. Also, best results are obtained when the diameter of the calibration standard is the same as the diameter of the fuel cores being tested.

A transistorized capacitive microphone for use in ultrasonic measurements has been developed at Oak Ridge[45] which employs the pulse-echo technique. The response of the electronic system is flat from 10 to 100 Mc/sec, with no more than 1% deviation in sensitivity over this range. No data are reported which show actual ultrasonic measurements at these frequencies and at nondestructive-testing amplitudes.

The discrete incidence angles on thin metallic inspection objects at which optimum ultrasonic imaging occurs can be correlated with the generation of Lamb waves, according to researchers at Argonne.[6] Tests with thin plates of aluminum, stainless steel, and brass in various thicknesses have shown that first-order modes are always preferred for imaging. There is often a preferred choice between first-order modes. For instance, if the velocity of the asymmetrical mode approaches that of surface waves, the symmetrical mode is preferred.

(D. Ensminger)

NDT Methods Other Than Ultrasonic

A two-color infrared radiometer approach is under study at Oak Ridge[46] to detect nonbond areas between the fueled and unfueled sections of fueled-graphite spheres. The two-color approach is being used to reduce the effect of variations in thermal emissivity. When optical filters are arranged over some of the openings in a chopper wheel, two-color sensitivity is realized with one detector, and a different signal frequency is obtained for each color. After amplification the two signal frequencies are separated by electrical filtering, are rectified, and are divided one by the other to produce a quotient that is a function of temperature only. The fueled spheres are heated to 178°C and then cooled locally by a jet of cool air during the inspection to detect nonbond. The two-color method is expected to provide sensitivities greater than were realized with a one-channel method in which nonbond areas having a diameter-to-shell thickness ratio of less than 4:1 were obscured by emissivity variations.

An X-ray-sensitive television system is being used to measure and record the position of a specimen subjected to transient thermal conditions at Oak Ridge.[47] Conventional measuring techniques have not been useful owing to the lack of thermal equilibrium in the specimen. By observing the television image, the operator can maintain the position of a marker signal supplied by an oscilloscope at a given distinctive feature of the specimen image. By dissecting the television video information by means of the oscilloscope, the operator can derive the position of the distinctive feature from known reference signals to within 0.002 in.

A theoretical and experimental study of the internal diffusion of eddy currents induced in flat, thick metal has been completed at Hanford.[48] The cases for an impinging plane electromagnetic wave and for an isolated cylindrical coil were considered mathematically. Experiments were then conducted using a cylindrical drive coil to induce step-function currents into a container of liquid Wood's metal. Current pickup loops located inside the Wood's metal were used to measure the intensities and rates of diffusion of the internal currents. It was found that the currents decay and redistribute much more rapidly than calculated for the plane-wave case. This rate of decay of the eddy currents was found to be a function of the distance from the axis of the drive coil, with the decay rate decreasing as the distance from the coil axis increases. Analog studies revealed that an array of inductively coupled loops could be made to represent the actual case more nearly than could a ladder network. Curves and wave forms of current diffusion are presented as functions of time and geometry.

A statistical method for evaluating the homogeneity of radioactive fuel distribution by means of counting techniques has been described by investigators at Atomics International.[49] The effects of practical factors, such as instability in the counting system, are included. The application of the method to SNAP fuel rods showed that the instrument used was capable of determining the ^{235}U content for each rod within 0.1%, and changes in homogeneity of 0.3% for a 4-cm^2 surface area at a 99% level of likelihood.

(A. F. Leatherman)

References

1. R. Burgett (Ed.), Summary Technical Report (on Feed Materials) for the Period April 1–June 30, 1964, USAEC Report NLCO-920, National Lead Co. of Ohio, Aug. 19, 1964.
2. D. R. Jefferson, Quarterly Progress Summary (on Uranium Fabrication), January–March 1964, USAEC Report BRB-81, Reactive Metals, Inc., June 3, 1964.
3. Nuclear Metals, Inc., Fundamental and Applied Research and Development in Metallurgy, Progress Report, March 1964, USAEC Report NMI-2127, May 13, 1964.
4. Nuclear Metals, Inc., Fundamental and Applied Research and Development in Metallurgy, Progress Report, April 1964, USAEC Report NMI-2128, June 12, 1964.
5. R. L. Lesser and J. E. Ayer, The Feasibility of Centrifugal Casting for Manufacturing Masurca Elements, USAEC Report ANL-6876, Argonne National Laboratory, May 1964.
6. Argonne National Laboratory, Reactor Development Program Progress Report, May 1964, USAEC Report ANL-6904, June 15, 1964.
7. Hanford Atomic Products Operation, Metallurgy Development Operation, Quarterly Progress Report, October–December 1963, USAEC Report HW-80112, Jan. 20, 1964. (Classified)
8. Nuclear Metals, Inc., Fundamental and Applied Research and Development in Metallurgy, Progress Report, February 1964, USAEC Report NMI-2126, Apr. 10, 1964.
9. Nuclear Metals, Inc., Fundamental and Applied Research and Development in Metallurgy, Progress Report, May 1964, USAEC Report NMI-2129, July 17, 1964.
10. Bureau of Mines, Albany Research Center, Quarterly Metallurgical Progress Report No. 23, April 1–June 30, 1964, USAEC Report USBM-RC-1122.
11. G. A. Reimann and D. R. Carnahan, The Extrusion, Forging, Rolling, and Evaluation of Refractory Alloys, Interim Technical Progress Report No. 1, August 1–November 29, 1963, Report AD-426705, Westinghouse Electric Corp., June 4, 1964.
12. H. G. Marsh, Coextrusion of Powder-Compact Slugs, USAEC Report DP-443, Savannah River Laboratory, April 1960.
13. H. Lloyd and J. M. Davies, Roll Bonding of Nuclear Fuel Plates, British Report AERE-R-4634, June 1964.
14. F. B. Quinlan and R. G. Wheeler, Cladding of Nuclear Fuel Elements, U. S. Patent 3,136,051 (to USAEC), June 9, 1964.
15. A. T. D'Annessa, Solid-State Bonding of Refractory Metals, *Welding J. (N. Y.)*, 43(5): 232s-240s (May 1964).
16. S. W. Porembka, Jr., Joining Ceramics to Metals for High-Temperature Service, *Battelle Tech. Rev.*, 13(9): 2-7 (September 1964).
17. R. Hoyle, Project No. 20—Plating by Thermal Decomposition. A Progress Report on Plating System Design and Evaluation, paper presented at 1964 Annual Meeting, American Electroplaters' Society, St. Louis, Mo., June 15–18, 1964.
18. H. Podall and M. M. Mitchell, Jr., The Use of Organometallic Compounds in Chemical Vapor Deposition, paper presented at Conference on Industrial Synthesis and Application of Organometallics, New York Academy of Science, June 9–11, 1964.
19. V. Yelyutin, B. Ly'sov, and C. Tyurin, Device for Repeated Iodide Refining of Metals, *Byul. Izobr. i Tovar Znakov* (Russian Patent No. 162968, Class 4), No. 11: 48-49 (1964).
20. Ya. Polyakov, L. Nisel'son, and A. Krestnovikov, Preparation of Niobium and Tantalum from the Vapor Phase, *Tsvetn. Metal.*, (1): 131-138 (1964).
21. V. A. Nieberlein, Vapor-Plating of Tungsten for Rocket Applications, Report RR-TR-64-6, Army Missile Command, July 1, 1964.
22. R. Heestand, J. I. Federer, and C. F. Leitten, Jr., Preparation and Evaluation of Vapor-Deposited Tungsten, USAEC Report ORNL-3662, Oak Ridge National Laboratory, August 1964.
23. Oak Ridge National Laboratory, Sept. 4, 1964. (Unpublished)
24. P. Higgs, R. Finicle, R. Bobka, E. Seldin, and J. Zeitsch, Research and Development on Advanced Graphite Materials. Volume XXXVII. Studies of Graphite Deposited by Pyrolytic Processes, Report WADD-TR-61-72(Vol. XXXVII), Advanced Materials Laboratory and Research Laboratories of National Carbon Co., May 1964.
25. E. Stover, Pyrolytic Graphite Article, British Patent 956,342, Apr. 22, 1964.
26. R. Diefendorf, Deposition Method of Forming a Pyrolytic Graphite Article, U. S. Patent 3,138,434 (to General Electric Company), June 23, 1964.
27. R. Diefendorf, Deposition Apparatus and Method for Forming a Pyrolytic Graphite Article, U. S. Patent 3,138,435 (to General Electric Company), June 23, 1964.
28. J. Richmond, Vapor Phase Process for Producing Metal Oxides, U. S. Patent 3,148,027 (to Laporte Titanium, Ltd.), Sept. 8, 1964.
29. R. Holzl, Structural and Containment Properties of Vapor Deposited Tungsten Cladding on Nuclear Fuel Elements at Very High Temperatures, *Symposium Proceedings of Materials Science and Technology for Advanced Applications*, 2: 658-666 (1964).
30. W. H. Roberts, Electroless Nickel Plating on Aluminum, USAEC Report RFP-367, Dow Chemical Co., Rocky Flats Division, Jan. 10, 1964.
31. R. Blanchard, C. Moreau, and J. Philippot, Sealing and Welding of Carbon Materials by Means of Hydrocarbon Cracking, British Translation NP-tr-1120 (from report presented at 19th International Congress of Pure and Applied Chemistry, London, July 10–17, 1963).
32. R. L. Bickerdike, A. R. G. Brown, G. Hughes, W. Johnson, and W. Watt, Process of Making an Impermeable Composite Carbon Tube, U. S. Patent 3,132,979 (to UKAEA), May 12, 1964.
33. V. Yelyutin, G. Pepekin, and B. Ly'sov, Formation of Titanium Carbide Precipitated from the Vapor Phase, *Izv. Vysshikh Uchebn. Zavedenii, Chernaya Met.*, No. 3: 124-130 (1964).
34. R. Bartlett and P. Gage, Investigation of Mechanisms for Oxidation Protection and Failure of Intermetallic Coatings for Refractory Metals, Eighth Quarterly Progress Report, Philco Research Laboratories, July 15, 1964.
35. J. Zupan, E. Pike, and J. Whitney, Investigation of Practical Techniques for Coating Refractory

Metals, Quarterly Progress Report No. 4 on Contract AF33(657)-8920, Suppl. 1, The Pfaudler Co., May 15, 1964.

36. H. Blumenthal and N. Rothman, Development of a Powder and/or Gas Cementation Process for Coating Molybdenum Alloys for High Temperature Protection, Report ML-TDR-64-74, Chromalloy Corp., June 1964.
37. A. Stetson and J. Long, Development of Protective Coatings for Tantalum-Base Alloys, Quarterly Progress Report No. 4, Mar. 1–May 31, 1964, on Contract AF33(657)-11259, Solar, Division of International Harvester, June 19, 1964.
38. Illinois Institute of Technology Research Institute, High-Temperature Oxidation Protective Coatings for Vanadium-Base Alloys, Report IITRI-B-6019-4, July 1, 1964.
39. L. Wyckoff, Refractory Coating Repair Processes, Report D2-81116, The Boeing Company, Dec. 27, 1963.
40. A. Epik, Boronizing of High-Melting Transition Metals, *Poroshkovaya Met., Akad. Nauk Ukr. SSR*, 3(5): 21-27 (1963).
41. J. M. Gerken, A Study of Welds in Columbium Alloy D-43, Report NP-13940 (TM-3865-67), Thompson Ramo Wooldridge, Inc., Mar. 25, 1964.
42. R. E. Yount and D. L. Keller, The Structural Stability of Welds in Columbium Alloys, Report ML-TDR-64-210, General Electric Co., June 1964.
43. A. H. Freedman and E. B. Mikus, Research on Tantalum and Molybdenum Brazing Techniques, Quarterly Progress Report, January–March 1964, Report NOR-64-86, Northrop Corp., Norair Division, April 1964.
44. R. D. Spice, Standardization and Evaluation of a Grain Size Test for Uranium Fuel, USAEC Report HW-81752, Hanford Atomic Products Operation, Apr. 21, 1964.
45. Oak Ridge National Laboratory, July 7, 1964. (Unpublished)
46. Oak Ridge National Laboratory, Gas-Cooled Reactor Program. Semiannual Progress Report for Period Ending March 31, 1964, USAEC Report ORNL-3619, July 1964.
47. Oak Ridge National Laboratory, Aug. 6, 1964. (Unpublished)
48. K. W. Atwood and H. L. Libby, Diffusion of Eddy Current, USAEC Report HW-79844, Hanford Atomic Products Operation, December 1963.
49. M. A. Greenfield, C. T. Nelson, and R. L. Koontz, Nondestructive Determination of Uranium-235 Content of SNAP Fuel Rods. Volume II. Statistical Methods for Evaluating Data Obtained from Counting Experiments, USAEC Report NAA-SR-9600, Atomics International, July 15, 1964.

Section

VI

Reactor Materials

Materials Information Presented at the Third Geneva Conference

At the Third International Conference on the Peaceful Uses of Atomic Energy, held in Geneva starting on Aug. 31, 1964, there were six sessions devoted to topics specifically within the scope of *Reactor Materials:*

Session	Topic	No. of papers
2.1	Metallic and Various Fuels	19
2.2	Ceramic Fuels	29
2.3	Fuel Element Fabrication and Experience	21
2.4	Corrosion Studies; Non-Destructive Testing	18
2.8	Structural Materials	19
2.9	Moderators and Control Materials	24

Many of these 130 papers are up-to-date state-of-the-art reviews. For the most part, the significant developments described in these papers have been reviewed at one time or another in *Reactor Materials,* using regular progress reports and publications as reference sources. Since it is the policy of *Reactor Materials* to call attention to the existence and availability of new state-of-the-art summaries, with a minimum of editorial comment or review, the materials papers of the Conference are listed at the end of this section by session, number, author, and title.

Readers who are interested in a comprehensive technical review of these papers are referred to the October 1964 issues of *Nuclear News* (American Nuclear Society) and *Nucleonics* (McGraw-Hill). Those wishing copies of papers may purchase them for two Swiss francs (46¢) each, plus postage, from:

European Office of the United Nations
Palais des Nations
Geneva, Switzerland
Attn: R. Furstenberg, Chief
Distribution Service
Documents Division

When the supply at the United Nations is gone, the International Atomic Energy Agency, No. 1 Kaerntnerring, Vienna, will fill orders at a price of $1.50 per paper. Also, the American Nuclear Society, 244 E. Ogden Avenue, Hinsdale, Illinois 60521, will provide Xerox copies of any paper at 25¢ per page.

Reproduced copies of all U. S. papers (no foreign) may be purchased at a price of $1.00 per paper from the Clearinghouse for Federal Scientific and Technical Information (formerly OTS), by writing to:

National Bureau of Standards
U. S. Department of Commerce
5285 Port Royal Road
Springfield, Va. 22151

The USAEC Division of Technical Information Extension, Oak Ridge, Tenn., has prepared micronegatives of all Geneva papers. Complete sets of duplicated negatives were distributed to the AEC, to Government agencies, and to their contractors. Sets of the U. S. papers only were distributed to AEC Depository Libraries, the locations of which are listed on the inside covers of *Nuclear Science Abstracts.* The U. S. papers were abstracted and indexed in Vol. 18, No. 18, of *Nuclear Science Abstracts,* and the foreign papers, in Vol. 18, No. 21.

References*

Session 2.1 Metallic and Various Fuels

61. P. Nollet and P. Sarrat (France), Research on Processes for the Conversion of Uranium Compounds with High Isotope Enrichment: Design and Construction of a Treatment Plant.

*Numbers are the official paper numbers assigned by the Conference Secretariat.

62. Y. Adda, J.-P. Mustelier and Y. Quere (France), Behaviour of Uranium Under Irradiation.
97. M. Englander et al. (France), The Effect of Neutron Irradiation on Certain Fuels Used in Gas–Graphite Type Reactors.
145. R. S. Barnes, R. G. Bellamy, B. R. Butcher, and P. G. Mardon (United Kingdom), The Irradiation Behaviour of Uranium and Uranium Alloy Fuels.
152. F. S. Martin, F. J. P. Clarke, R. W. M. D'Eye, and D. T. Livey (United Kingdom), Preliminary Development of Dispersed Fuels in the UKAEA.
239. J. H. Kittel, T. K. Bierlein, B. R. Hayward, and W. C. Thurber (U. S.), Irradiation Behavior of Metallic Fuels.
241. W. R. Grimes, E. G. Bohlmann, and L. D. Kirkbride (U. S.), Irradiation Behavior of Fluid Fuels.
333. A. A. Bochvar, V. G. Kuznetsova, V. S. Sergeev, and F. P. Butra (USSR), Self-Diffusion in α- and β-Uranium.
336. G. A. Meerson, G. P. Kurbatov, Ya. D. Pakhomov, G. N. Kalinin, E. V. Ryabin, and G. L. Zverev (USSR), Uranium Prepared by Powder Metallurgy Techniques.
337. T. A. Badajeva, G. K. Alekseenko, and R. I. Kuznetsova (USSR), Structure and Properties of Ternary Alloys with Thorium.
338*a*. V. M. Agranovic, E. Y. Mikhlin, L. P. Seminov, V. I. Pupko, Y. I. Likhachev, and V. P. Zvonarev (USSR), Theory of Fissile Materials Swelling.
475. G. Petzow and S. Steeb (Germany, Federal Republic), Phase Equilibria Between Intermetallic Compounds in Uranium Alloys.
506. A. Bar-Or, G. Hirsch, I. Goldstein, and P. Wynblatt (Israel), Uranium Alloys.
526. V. Kraus (Czechoslovak SR), Diffusion Bonding of Uranium with Magnesium by Means of Intermediate Layers.
701. B. Djurić, Dj. Drobnjak, Dj. Lazarević, S. Malcić, A. Mihailović, Dj. Milosavljević, and S. Milošević, (Yugoslavia), Metallurgical Properties of Some Uranium Alloys.
702. B. S. Brčić, J. Slivnik, D. Kolar, B. Frlec, M. Komac, and P. Glavič (Yugoslavia), On the Uranium–Hydrazine System.
735. G. Colabianchi, C. Fizzotti, G. Traversi, J. J. Stobo, and F. Squadrelli-Saraceno (Italy), Irradiation Experiments on Uranium-Rich Alloys.
820. A. Ramamoorthy and A. K. Ganguly (India), Determination of Ratio of U-235 and U-238 in Uranium Samples.
864. M. R. Bastelli, C. D'Amato, G. C. Giacchetti, S. Granata, R. Renzoni, F. S. Saraceno, T. B. Wilson, S. Donato, G. Piatti, and R. Theisen (Italy), Fundamental Metallurgical Studies for the Improvement of Metallic Uranium Fuel Elements.

Session 2.2 Ceramic Fuels

17. J. A. L. Robertson, A. S. Bain, J. R. MacEwan, and M. J. F. Notley (Canada), UO_2 Performance: The Importance of Temperature Distribution.
19. W. B. Lewis, J. R. MacEwan, W. R. Stevens, and R. G. Hart (Canada), Fission-Gas Behaviour in UO_2 Fuel.
59. A. Accary and R. Delmas (France), Recent Developments in Refractory Fuels.
154. L. E. Russell, B. T. Bradbury, H. J. Hedger, N. Parkinson, R. G. Sowden, and M. B. Waldron (United Kingdom), Monocarbides as Reactor Fuels.
155. L. E. J. Roberts, P. Brock, J. R. Findlay, B. R. T. Frost, L. E. Russell, J. B. Sayers, and E. Wait (United Kingdom), The Behaviour of UO_2 and of $(U,Pu)O_2$ Fuel Materials Under Irradiation.
233. S. Naymark and C. N. Spalaris (U. S.), Oxide Fuel Fabrication and Performance.
234. H. Pearlman and R. F. Dickerson (U. S.), Carbide Fuel Fabrication and Performance.
235. R. W. Dayton, W. V. Goeddel, and W. O. Harms (U. S.), Ceramic-Coated-Particle Nuclear Fuels.
236. E. A. Evans, W. E. Roake, F. J. Leitz, and A. Strasser (U. S.), Uranium-Plutonium Ceramic Fuels.
240. T. J. Pashos, D. R. deHalas, D. L. Keller, and L. A. Neimark (U. S.), Irradiation Behavior of Ceramic Fuels.
338. V. M. Golyanov, and N. F. Pravdyuk (USSR), Behaviour of Nuclear Fuel Under Irradiation (Investigation of Thin Layers of Irradiated Uranium Dioxide).
338*b*. N. F. Pravdyuk, S. M. Astrakhantsev, K. P. Dubrovin, E. G. Ivanov, and V. I. Karpuhin (USSR), Behaviour of Nuclear Fuel Under Irradiation.
398. H. Bildstein, A. Burtscher, P. Koss, and F. P. Viehböck (Austria), Irradiation Behavior of Coated Fuel Particles.
444. P. Nagels, W. Van Lierde, R. Penninckx, J. Devreese, M. Denayer, L. De Jonghe, R. De Coninck, R. De Batist, H. Blank, R. Givers, and S. Amelinckx (Belgium), Preparation and Physical Properties of UO_2 Single Crystals.
469. R. Schwarzwälder, J. Höchel, and J. Fischer (Germany, Federal Republic), Examination of an In-Pile-Burnout Damage on a Boiling Water Fuel Rod.
472. F. Felix, T. Lagerwall, P. Schmeling, and K. E. Zimen (Germany, Federal Republic), Rare Gas Release From Solids with Special Attention to Nuclear Fuel Materials.
530. D. Jakeš and H. Landsperský (Czechoslovak SR), Development of Ceramic Nuclear Fuel in Czechoslovakia.
543. R. Smith (Australia), The Development of Beryllia-Based Fuels for H. T. G. C. Reactor Systems.
554. F. Barbesino, E. Brutto, R. Di Pietro, A. Gioia, G. Perona, and R. Sesini (Italy), UO_2 Fuel Elements Shaped as Small Spheres.
555. G. Cogliati, R. De Leone, G. R. Guidotti, R. Lanz, L. Lorenzini, E. Mezi, and G. Scibona (Italy), The Preparation of Dense Particles of Thorium and Uranium Oxide.
634. M. E. A. Hermans, H. S. G. Slooten, and N. V. Kema (Netherlands), Preparation of UO_2 and ThO_2 Powders in the Subsieve Range.
700. D. S. Jovanović, E. M. Kostić, I. G. Momčilović, V. J. Petrović, and M. M. Ristić (Yugoslavia), Ceramic Fuel Obtained by Metallic Grade UO_2 Powder.
703. V. Pravdič, M. Branica, and Z. Pučar (Yugoslavia), Uranium Dioxide Production. A Sur-

vey of Electrochemical Reduction and Precipitation From Carbonate Solutions.

726. R. G. Schölvinck, P. F. Sens, and E. Jensen (Netherlands), The Norwegian-Netherlands' Fuel Irradiation Experiment.

749. M. D. Karkhanavala, A. C. Momin, A. M. George, V. D. Damani, N. Singh, and V. Amirthalingam (India), Study of the High-Temperature Behaviour of Uranium Oxides and of the Kinetics and Mechanism of Formation of Urania-Thoria Solid Solutions.

750. V. K. Moorthy, A. K. Kulkarni, and S. V. K. Rao (India), Relation Between the Origin, Powder Characteristics and Sintering Treatments on the Densification and Microstructures of Compacts of Urania and Thoria.

751. S. Fareeduddin, R. K. Garg, U. C. Gupta, S. K. Kantan, R. Rajendran, N. K. Rao, K. K. Sinha, G. V. S. R. K. Somayajulu, and Subramanian (India), Fabrication of Uranium Oxide Fuel Elements at Trombay.

832. P. Himmelstein, W. Hoppe, B. Liebmann, L. Schäfer, L. Schikarski, and W. in der Schmitten (Germany, Federal Republic), Fabrication of Fused UO_2, UC Feed Material, and Cast UC Rods.

843. S. Takahashi, Y. Honda, T. Kubota, S. Fujinaga, C. Ito, A. Takashima, Y. Akimoto, T. Suzuki, and H. Doi (Japan), Development of Rod and Hollow-Type Swaged UO_2 Fuel Elements and Some Irradiation Behaviors.

Session 2.3 Fuel Element Fabrication and Experience

18. R. D. Page, D. G. Hardy, A. J. Mooradian, J. Howieson, G. R. Fanjoy, and D. B. Nazzer (Canada), Engineering and Performance of UO_2 Fuel Assemblies.

58. P. Bussy, J.-P. Mustelier, and R. Pascard (France), Study and Manufacture of Plutonium Fuels.

60. M. Salesse, J. Stohr, and G. Jeanpierre (France), Recent Developments Concerning French Fuel Elements for Natural Uranium–Graphite–CO_2 Reactors.

147. J. W. Hughes, G. H. Inglis, C. H. Jones, and J. Price (United Kingdom), The Development and Evaluation of Uranium Magnox Fuel Elements.

148. G. W. Greenwood and B. F. Sharpe (United Kingdom), Postirradiation Examination of C.E.G.B. Fuel Elements.

149. G. B. Greenough, J. S. Nairn, and J. D. Thorn (United Kingdom), Progress Towards the Design of A. G. R. Fuel Elements for Power Reactors.

150. S. A. Cottrell, E. Edmonds, P. Higginson, and W. Oldfield (United Kingdom), Development and Performance of Dounreay Fast Reactor Metal Fuel.

151. S. E. Smith, J. S. Broadley, F. Brown, and W. L. C. Kent (United Kingdom), Development of a Large-Scale Manufacturing Process and Plant for Plutonium Fast Reactor Fuel.

153. B. R. T. Frost, L. H. Cope, J. D. B. Lambert, H. Lloyd, W. Long, J. E. Manson, and P. G. Mardon (United Kingdom), Fabrication and Irradiation Studies of UO_2–Stainless Steel and $(U,Pu)O_2$–Stainless Steel Cermets.

238. R. E. Macherey, H. W. Alter, and A. A. Shoudy (U. S.), Fabrication of Solid Fuels for Fast Reactors.

426. R. Segane, T. Yoshioka, N. L. Franklin, B. E. Eltham, P. T. Fletcher, and B. C. Woodfine (Japan), The Design and Development of the Tokai Hollow Rod Fuel Element.

442. M. Huberlant, J. Wertz, A. de Streel, and J. van Mulders (Belgium), Design and Fabrication of PWR Fuel Elements in Belgium.

443. J. M. Leblanc (Belgium), Irradiation of Plutonium-Enriched Ceramic Fuel Rods in the BR 3 Power Reactor.

485. T. D. de Souza Santos, H. M. Haydt, and C. T. de Freitas (Brazil), Developments in Fuel Fabrication for Research Reactors in Brazil.

486. T. D. de Souza Santos, H. M. Haydt, and C. T. de Freitas (Brazil), Experimental Studies on the Fabrication of Thin Fuel Plates With U_3O_8-Al Cermets.

493. J. D. Pedregal, H. Bergua, J. Díaz, A. D. Beltrán, and E. Aparicio (Spain), Fuel Element Production at the JEN.

560. J. C. C. Stewart, V. W. Eldred, T. J. Heal, D. O. Pickman, and H. Rogan (United Kingdom), Review of Progress of Development, Manufacture, and Performance of Magnox Fuel Elements in the United Kingdom.

608. H. Mogard, S. Djurle, I. Multer, H. P. Myers, B. Nelson, and U. Runfors (Sweden), Fuel Development for Swedish Heavy Water Reactors.

635. J. J. Went (Netherlands), The Aqueous Homogeneous Suspension Reactor Project.

716. J. Planquart, M. Huberlant, F. Mathieu, D. Tytgat, and P. De Meester (Belgium), Fuel Elements in the Form of Concentric Cylindrical Plates (Concentric Tube Fuel Elements).

837. C. Araoz, C. A. Martínez Vidal, J. Mazza, R. Morando, and O. Wortman (Argentina), Fabrication of Fuel Elements for Research Reactors.

Session 2.4 Corrosion Studies, Non-Destructive Testing

63. R. Darras and H. Loriers (France), Compatibility of Cladding Materials With Carbon Dioxide at High Temperatures.

157. J. E. Antill, C. S. Campbell, D. Goodison, W. B. Jepson, and C. G. Stevens (United Kingdom), Corrosion Behaviour of Steels in CO_2/CO Atmospheres.

158. J. K. Dawson, R. C. Asher, J. Boulton, B. Watkins, and J. N. Wanklyn (United Kingdom), The Properties of Zirconium Alloys for Use in Water-Cooled Reactors.

243. J. E. Draley, J. A. Ayres, W. E. Berry, E. Hillner, and S. P. Rideout (U. S.), Corrosion in Aqueous Systems.

244. D. H. Gurinsky, J. R. Weeks, C. J. Klamut, L. Rosenblum, and J. H. DeVan (U. S.), Corrosion in Liquid Metal Systems.

245. W. J. McGonnagle (U. S.), Nondestructive Testing of Nuclear Reactor Components.

340. V. E. Ivanov, V. F. Zelenskii, S. I. Feifer, I. A. Petelguzov, and V. K. Khorenko (USSR), Devel-

opment of Heat-Resistant Mg-Be as a Cladding Material for Fuel Elements.

341. V. S. Emelyanov, A. I. Evstyukhin, G. B. Fedorov, G. G. Ryabova, N. V. Borkov, I. I. Korobkov, and P. L. Gruzin (USSR), Corrosion Resistance of Zirconium and Its Alloys in Water and Steam at High Temperatures.

342. A. D. Amaev, R. S. Ambartsumyan, I. A. Anisimova, A. M. Glukhov, V. V. Goncharov, E. G. Ivanov, A. A. Kiselev, S. T. Konobeevskiy, L. M. Lebedev, V. A. Myshkin, M. S. Orlov, P. F. Pravdyuk, E. P. Ryazantsev, and V. V. Skvortsov (USSR), Influence of Some Factors Upon Hydriding and Variation of Properties of Zirconium Alloy With 1% Nb Used for Fuel Element Cladding in Water-Moderated Water-Cooled Power Reactors.

343. B. A. Nevsorov, V. V. Zotov, G. P. Fedortsev-Lutikov, D. M. Skorov, N. M. Beskorovagynii, Ju. S. Belomytsev, M. D. Abramovitch, E. V. Umnyashkin, V. K. Ivanov, E. I. Yakovlev, S. A. Iodkovskii, S. M. Golubenkova, and N. M. Samarina (USSR), Corrosion Resistance of Constructional Materials in Alkali Metals.

399. M. J. Higatsberger, H. Hick, and P. Weinzierl (Austria), Burn-up Determination of Nuclear Fuel by High-Resolution Gamma Spectroscopy.

416. J. Rohlin, S. Nilsson, B. Lundqvist, and R. Hardell (Sweden), A Crystal Diffraction Spectrometer for Non-Destructive Burn-up Analysis.

429. N. Takagi, Y. Mishima, and Y. Imai (Japan), Development of Nuclear Fuel Inspection Techniques in Japan.

430. H. Kamogawa, H. Tomishima, H. Nagami, K. Ogawa, N. Oi, N. Wakabayashi, T. Ohno, and K. Naito (Japan), Irradiation Tests of UO_2 Fuel: Radiography With Betatron and Neutron; Relocation of Fission Products and Plutonium.

445. M. J. Brabers, G. Mestdagh, J. Meunier, G. Spaepen, and P. Weisgerber (Belgium), Corrosion of Reactor Materials (An Electrochemical Study of the Effect of Irradiation on the Corrosion of Some Reactor Materials).

566. R. Lind and J. Wright (United Kingdom), Factors Controlling Reaction Between Graphite and Radiolysed Carbon Dioxide.

574. F. Barbesino, E. Brutto, R. Di Pietro, G. Masini, G. Perona, and R. Sesini (Italy), Zircaloy-2 Pressure Tubes Corrosion.

785. K. Chandramoleshwar, M. P. Navalkar, D. V. S. Ramakrishna, R. Ramanna, and K. R. Subbaramu (India), A Feasibility Study of Non-Destructive Assay of Plutonium-239 in Irradiated Fuel Rods Using Slowing-Down Time Spectrometer.

Session 2.8 Structural Materials

21. W. R. Thomas, S. B. Dalgaard, W. Evans, V. Fidleris, G. W. Parry, and P. A. Ross-Ross (Canada), Irradiation Experience With Zircaloy-2.

22. C. E. Ells, S. B. Dalgaard, W. Evans, and W. R. Thomas (Canada), Development of Zirconium-Niobium Alloys.

23. D. G. Boxall, W. M. Brown, D. B. Nazzer, J. T. Rogers, R. G. Hart, and K. L. Smith (Canada), Development of Fuel and Coolant Tubes for a Reactor Cooled by Organic Liquid.

69. J. L. Bernard, H. Foulquier, and P. Thome (France), Core Structures of the Heavy Water–Gas Reactor EL 4.

146. P. Greenfield, R. G. Coffin, G. C. E. Olds, B. Pickles, and T. C. Wells (United Kingdom), Development of Magnesium Alloys for Fuel Elements in the United Kingdom.

156. A. T. Churchman, J. H. Buddery, B. Edmondson, G. W. Greenwood, R. V. Hesketh, and G. K. Williamson (United Kingdom), Long-Term Studies of Materials Problems in Gas-Cooled Reactors.

242. J. C. Tobin, M. S. Wechsler, and A. D. Rossin (U. S.), Radiation-Induced Changes in the Properties of Non-Fuel Reactor Materials.

255. W. P. Chernok, R. M. Mayfield, and J. R. Weir, Jr. (U. S.), Cladding Materials for Nuclear Fuels.

350. A. N. Ogarev, D. D. Frolov, N. G. Aksenov, A. I. Nedelyaev, S. V. Golovin, V. S. Yudin, and N. F. Muchortov (USSR), Studies of Electrolytic Preparation of Zirconium Metal.

419. G. Öestberg and H. P. Myers (Sweden), Aspects of Swedish Studies of Cladding Materials for Water-Cooled Reactors.

421. N. Hansen, P. Knudsen, A. C. Winther, and E. Adolph (Denmark), Sintered Aluminum Products for Organic-Reactor Application.

431. M. Kawasaki and M. Sasagawa (Japan), On the Thermal Fatigue Behavior of Fuel Sheath Material Subjected to Constrained Deformation Caused by Core Material.

456. M. Y. Farah and I. S. El-Yamani (United Arab Republic), Nuclear-Grade Zirconium From Egyptian Zircon Placers.

460. W. Siegfried and S. Zimering (Switzerland), On the Long-Term Mechanical Properties of Metals Used at Elevated Temperatures and Subjected to Neutron Irradiation.

471. J. Diehl and W. Schilling (Germany, Federal Republic), Hardening of Face-Centered Cubic Metals Due to Reactor Irradiation.

477. W. Jung-König, H. Richter, W. Spalthoff, and E. Starke (Germany, Federal Republic), Properties and Technology of Zirconium Alloys With Niobium and Tin.

591. S. Aas and K. Videm (Italy), Improved Aluminum Alloys as Fuel Cladding Material in Water-Cooled Power Reactors.

733. D. Gualandi and P. Jehenson (Italy), Contribution to the Studies of the Technology of Al-Al_2O_3 Compounds With Regard to Nuclear Application.

757. E. Bodmer, J. J. Chene, R. C. Eriksson, and R. Ferrarini (Switzerland), The Structure and the Mechanical Properties of Welded Zircaloy-2.

Session 2.9 Moderators and Control Materials

20. H. K. Rae, G. M. Allison, A. R. Bancrott, W. D. Mackintosh, J. F. Palmer, E. E. Winter, J. E. LeSurf, and S. R. Hatcher (Canada), Experience With the Chemistry of Water in Moderator and Coolant Systems.

68. P. Leveque, F. M. L. Lang, and J. Rappeneau (France), Special Graphites.
70. L. Dolle, D. Conan, and G. Dirian (France), Behaviour of Water and Heavy Water in Nuclear Reactors and Problems of Power Regulation by Physico-Chemical Methods.
71. G. Sainfort, G. Cabane, and M. Salesse (France), FeAl 40, A New Canning Material for Reactors Using Refractory Fuel.
101. M. Weisz and J. Mallen (France), The Use of Beryllium as a Canning Material. The Problems Arising From the Brittleness of the Metal, and Their Present Solutions.
162. D. R. Harries, K. Q. Bagley, J. P. Bell, W. S. Gibson, J. Gillies, P. C. L. Pfeil, and S. B. Wright (United Kingdom), Irradiation Behaviour of Steel as a Structural and Cladding Material.
163. J. H. W. Simmons, B. T. Kelley, P. T. Nettley, and W. N. Reynolds (United Kingdom), The Irradiation Behaviour of Graphite.
253. A. N. Holden, B. Weidenbaum, and C. F. Leitten, Jr. (U. S.), Control Rod Materials.
254. R. E. Nightingale, C. G. Collins, and J. A. McGurty (U. S.), Developments in Solid Moderator Materials.
339. A. D. Amaev, P. A. Platonov, and N. F. Pravdyuk (USSR), Study of Tendency to Brittleness of Ferrite-Pearlite Steels for Reactor Vessels During Neutron Irradiation.
339*a*. E. V. Gusev, P. A. Platonov, N. F. Pravdyuk, and N. M. Sklyarov (USSR), Effect of Reactor Irradiation on Stress-Rupture Strength of Austenitic Steels and Heat-Resistant Materials Based on Iron and Nickel.
351. B. G. Ignatiev, L. A. Ishvanov, N. I. Poltoratsky, V. N. Stepanov, A. K. Savenko, N. F. Mironov, P. L. Volodin, and M. I. Tumbakova (USSR), The Technology of Reactor Construction Fabrication of Metal Beryllium and Its Oxide.
412. N. Melašin (Yugoslavia), Microstructure and Grain-Size Effects on Irradiation Hardening of Low Carbon Steel for Reactor Tanks.
420. H. P. Myers, M. Grounes, and N. E. Hannerz (Sweden), Irradiation Behaviour of Swedish Steels for Reactor Pressure Vessels.
432. Y. Ando, T. Fujimura, M. Nomaguchi, and Y. Inoue (Japan), Development of Bonding Methods for Graphite Materials.
449. I. Kiss and F. Szabo (Hungary), Radiolytical and Heat Transfer Properties of Some Organic Coolant-Moderators.
470. M. Buetell and O. Vohler (Germany, Federal Republic), Influence of Various Parameters on the Behaviour of Graphite Under Neutron Irradiation.
476. F. Haessner, G. Petzow, and E. Preisler (Germany, Federal Republic), The Present State of Knowledge About Cadmium and Indium Tantalate as Possible Control Materials for High-Temperature Reactors.
490. R. Barrera Piñero and J. Manero Rodríguez (Spain), Investigation of Commercial Hydrocarbon Mixtures Suitable for the Moderation-Refrigeration of Nuclear Reactors.
573. B. Chinaglia, M. Domenici, F. Pieragostini, and H. Walther (Italy), Some Studies Concerning Structure, Radiation-Damage Annealing and Fission-Product Diffusion in Pyrolytic Carbon.
593. S. Aas, R. H. Soevik, K. Videm, and E. Brodahl (Norway), Thin-Walled Stainless Steel as Fuel Cladding Material in Water-Cooled Power Reactors.
595. L. Hammar, R. Rose, and G. M. Allison (Norway), Water Chemistry Research at HBWR.
727. H. C. van Elst, W. L. Korbee, E. C. J. Buys, and C. A. Verbraak (Netherlands), A New Method for Measuring the Tendency to Brittle Fracture in Reactor Vessel Steels.
799. K. Kida, S. Nishigaki, S. Ohashi, K. Kobayashi, and S. Mochida (Japan), Recent Development of Beryllium Study in Japan.

LEGAL NOTICE

This journal was prepared under the sponsorship of the U. S. Atomic Energy Commission. Neither the United States, nor the Commission, nor any person acting on behalf of the Commission:

A. Makes any warranty or representation, expressed or implied, with respect to the accuracy, completeness, or usefulness of the information contained in this journal, or that the use of any information, apparatus, method, or process disclosed in this journal may not infringe privately owned rights; or

B. Assumes any liabilities with respect to the use of, or for damages resulting from the use of any information, apparatus, method, or process disclosed in this journal.

As used in the above, "person acting on behalf of the Commission" includes any employee or contractor of the Commission, or employee of such contractor, to the extent that such employee or contractor of the Commission, or employee of such contractor prepares, disseminates, or provides access to, any information pursuant to his employment or contract with the Commission, or his employment with such contractor.

NUCLEAR SCIENCE ABSTRACTS

The U. S. Atomic Energy Commission, Division of Technical Information, publishes *Nuclear Science Abstracts (NSA)*, a semimonthly journal containing abstracts of the literature of nuclear science and engineering.

NSA covers (1) research reports of the U. S. Atomic Energy Commission and its contractors; (2) research reports of government agencies, universities, and industrial research organizations on a world-wide basis; and (3) translations, patents, books, and articles appearing in technical and scientific journals.

Complete indexes covering subject, author, source, and report number are included in each issue. These are cumulated quarterly, semiannually, and annually providing a detailed and convenient key to the literature.

Availability of *NSA*

SALE *NSA* is available on subscription from the Superintendent of Documents, U. S. Government Printing Office, Washington, D. C., 20402, at $30.00 per year for the semimonthly abstract issues and $22.00 per year for the four cumulated-index issues. Subscriptions are postpaid within the United States, Canada, Mexico, and all Central and South American countries, except Argentina, Brazil, British and French Guiana, Surinam, and British Honduras. Subscribers in these Central and South American countries, and in all other countries throughout the world, should remit $37.00 per year for subscriptions to semimonthly abstract issues and $25.00 per year for the four cumulated-index issues.

EXCHANGE *NSA* is also available on an exchange basis to universities, research institutions, industrial firms, and publishers of scientific information. Inquiries should be directed to the Division of Technical Information Extension, U. S. Atomic Energy Commission, P. O. Box 62, Oak Ridge, Tennessee, 37831.

TECHNICAL PROGRESS REVIEWS may be purchased from Superintendent of Documents, U. S. Government Printing Office, Washington, D. C., 20402. *Isotopes and Radiation Technology* at $2.00 per year for each subscription or $0.55 per issue; the other four journals at $2.50 per year and $0.70 per issue. The use of the coupon below will facilitate the handling of your order.

POSTAGE AND REMITTANCE: Postpaid within the United States, Canada, Mexico, and all Central and South American countries except as hereinafter noted. Add $0.50 per year, or $0.15 per single issue for the *Isotopes and Radiation Technology* journal and $0.75 per year or $0.20 per single issue for the other four journals for postage to all other countries, including Argentina, Brazil, British and French Guiana, Surinam, and British Honduras. Payment should be by check, money order, or document coupons, and MUST accompany order. Remittances from foreign countries should be made by international money order, or draft on an American bank, payable to the Superintendent of Documents, or by UNESCO book coupons.

order form

SUPERINTENDENT OF DOCUMENTS
U. S. GOVERNMENT PRINTING OFFICE
WASHINGTON , D. C., 20402

Enclosed:
document coupons ☐ check ☐ money order ☐

Charge to Superintendent of Documents No. _____

Please send a one-year subscription to

☐ NUCLEAR SAFETY

☐ POWER REACTOR TECHNOLOGY

☐ REACTOR FUEL PROCESSING

☐ REACTOR MATERIALS

(Each subscription $2.50 per year; $0.70 per issue.)

☐ ISOTOPES AND RADIATION TECHNOLOGY

(Each subscription $2.00 a year; $0.55 per issue.)

SUPERINTENDENT OF DOCUMENTS
U. S. GOVERNMENT PRINTING OFFICE
WASHINGTON, D. C., 20402

(Print clearly)

Name _____

Street _____

City _____ Zone ____ State _____